STATIONARY RANDOM RESPONSE

OF BILINEAR HYSTERETIC SYSTEMS

Thesis by

Loren Daniel Lutes

In Partial Fulfillment of the Requirements

For the Degree of

Doctor of Philosophy

California Institute of Technology

Pasadena, California

1967

(Submitted February 23, 1967)

ACKNOWLEDGMENTS

ABSTRACT

This study of the stationary random vibration of single degree of freedom bilinear hysteretic oscillators consists of both experimental investigations and approximate analytical investigations. The experimental results are obtained from a differential analyzer electrical analog computer excited by an approximately white, Gaussian source. Measurements of mean squared levels, power spectral density and probability distribution of oscillator response are reported. The applicability of certain approximate analytical techniques is investigated by comparing analytical predictions and experimental measurements of the statistics of the response.

The analog computer results indicate that for a system containing viscous damping, yielding may sometimes act to increase the rms level of displacement response. In addition, the experimental results show that yielding has a marked effect on the response power spectral density, and in some instances this statistic has the general character of that for a two mode linear system. The response probability distribution is also affected by yielding and is generally not Gaussian.

An extension of the Krylov-Bogoliubov method of equivalent linearization and a method based on defining an approximately equivalent nonlinear nonhysteretic system are considered. The Krylov-Bogoliubov method gives a reasonable estimate of the rms velocity

response for all cases considered but gives meaningful information about the rms displacement response only for cases of moderate non-linearity. The second approximate method is shown to be quite good for predicting rms levels of response for cases of high yield level where the Krylov-Bogoliubov method is less successful. The application of the second method to other cases and to the problem of predicting probability distributions is also discussed.

v

TABLE OF CONTENTS

SUMMARY OF NOMENCLATURE

Symbol	Explanation or Definition
A	amplitude of vibration
B	filter bandwidth, cps
C	capacitor
C(A)	see expression (3. 14) or (4. 6)
E. D.	energy dissipated during one cycle
E. D. Y.	energy dissipated due to yielding during one cycle
F(H)	$\int_0^H f(h)dh$
G(x)	$\int_0^x g(y)dy$
H(x, ẋ)	$\dot{x}^2/2 + G(x)$, energy
H(iω)	complex transfer function
$K_1, \ldots, K_4$	see expression (4. 31)
N(t)	white, Gaussian excitation
P	Prob. (x > X)
Q	transistor
R	resistor
S(A)	see expression (3. 14) or (4. 7)
S(ω)	power spectral density
T	sampling time
Y	yield level
b	half the distance between half-power points, rad/sec

Symbol	Explanation or Definition
c	constant dashpot coeffecient
f(H)	nonlinear dashpot coefficient
g(x)	nonlinear restoring force
i	$\sqrt{-1}$
k	constant spring coefficient
m	mass
n(t)	random excitation
p	probability density function
r_1, r_2	see expression (4.39)
t	time
u	$\sqrt{2H/\omega_o^2}$
v	voltage
x	displacement
Γ	gamma function
α	slope ratio in bilinear system
β	fraction of critical viscous damping
δ	Dirac delta function
ϵ	deficiency term in equivalent linearization, normalized standard error in error analysis
θ	phase angle
λ	$2\sigma_x^2/Y^2$
σ	rms level
$\varphi(x)$	normalized nonlinear restoring force

Symbol	Explanation or Definition
ω	circular frequency

Dots over variables denote derivatives with respect to time. A bar over a term denotes a time average.

I. INTRODUCTION

Problems of mechanical vibration induced by random excitation have received considerable study in recent years. One major motivation for such study has been the problems which arise in the fields of aircraft and space travel. Another problem which has also particularly motivated study of random vibrations is that of structural response to earthquakes. This latter problem is certainly ancient but only in fairly recent times has enough information about the nature of earthquakes been accumulated to allow any scientific analysis of the subject.

To describe a process as random simply means that insufficient information is available to allow one to completely describe its time history. Rather, various statistical measures are used to characterize a random process. Of course, records of actual excitation by jet noise or earthquake are available, but the randomness of the problem arises from the fact that future excitations by the same type of source cannot be expected to have the same time history. Analysis of a large number of individual records of a random process permits determination of the statistical measures which can be expected to also characterize future records. The earthquake problem is particularly complicated by the scarcity of time history records of past strong-motion earthquakes. To date the ground acceleration has been recorded for only about twenty strong-motion earthquakes.

The theory of the stationary response of linear systems to

random excitation is quite well developed and is available in common reference books[1-3]. In particular, given the power spectral density of the excitation one can compute the power spectral density and mean squared level of the linear system response. If the excitation has a Gaussian or normal probability distribution then the linear system response is also Gaussian. Other statistics such as number of zero crossings and peak distributions can also be obtained for a Gaussian process.

For systems subjected to random excitation of relatively short duration the statistics of the response may be strongly time dependent rather than stationary and appropriate measures of response must be used. In earthquake engineering the most commonly used measure of response is the maximum response of the system due to the transient excitation. Curves of these maxima for single-mass linear oscillators of various natural frequency and fraction of critical viscous damping are called response spectra and are available for past strong-motion earthquakes[4]. The probability distribution of the maximum response of a single mass linear oscillator excited by an earthquake-like random process has also been studied[5-7].

The response of nonlinear systems to random excitation is a much broader and more complicated subject than the response of linear systems. Virtually all real physical systems exhibit some form of non-linearity for sufficiently large motions, and various forms of nonlinearity result in greatly varied effects on system response.

One method of studying the random response of a nonlinear system is to find an approximate equivalence between the nonlinear system and some linear system so that the linear theory can be applied. Probably the most common such method is an extension of the well known Krylov-Bogoliubov technique to problems with random excitation[8]. Using a somewhat different approach other authors have characterized the effect of certain types of nonlinearities solely by an amount of equivalent viscous damping[9, 10]. Predictions of the response of nonlinear systems based on the results of linear theory can normally be expected to apply only to systems with small nonlinearities.

Perturbation techniques have also been used to investigate the random vibrations of nonlinear systems[11]. Here again it is required that the nonlinearity be small so that an initial approximation to the response of the nonlinear system can be found by neglecting the nonlinearity.

Solution of the general Fokker-Planck equation appropriate to a nonlinear system gives the exact transitional or conditional probability density function of stationary response to a Gaussian excitation with a white frequency spectrum[12]. From the transitional probability density one can obtain the common measures of a stationary random process, such as power spectral density, mean squared level and ordinary probability distribution. As yet, however, no one has succeeded in solving the general Fokker-Planck equation for any second-order nonlinear system such as a spring-mass oscillator.

The stationary probability density function for the response of a nonlinear system to white, Gaussian excitation is the solution of a reduced form of the Fokker-Planck equation for the system. The most general class of nonlinear second-order systems for which such a stationary solution has been obtained includes systems with nonlinear nonhysteretic springs and nonlinear damping which is a function of the amount of energy in the system[13]. This class of nonlinear systems contains all the particular examples for which stationary solutions have been obtained to date.

Exact analytical results from solution of the Fokker-Planck equation are thus limited to a class of nonlinear systems which excludes all hysteretic systems. Further the approximate results obtained by perturbation methods or methods using the results of linear theory are limited to problems with small nonlinearities, although the exact meaning of small is normally not specified. Particularly in earthquake engineering the nonlinearities of principal interest are hysteretic and not necessarily small. Many researchers have thus taken recourse to various experimental techniques wherein some mathematical or physical representation of the nonlinear system is subjected to the desired excitation and the resulting system response is analyzed. Digital and analog computers have been the primary tools in such investigations.

Bilinear hysteresis has been the most widely studied type of hysteretic nonlinearity. Figure 1 shows a plot of restoring force versus displacement (or restoring moment versus angle) for a bilinear hyster-
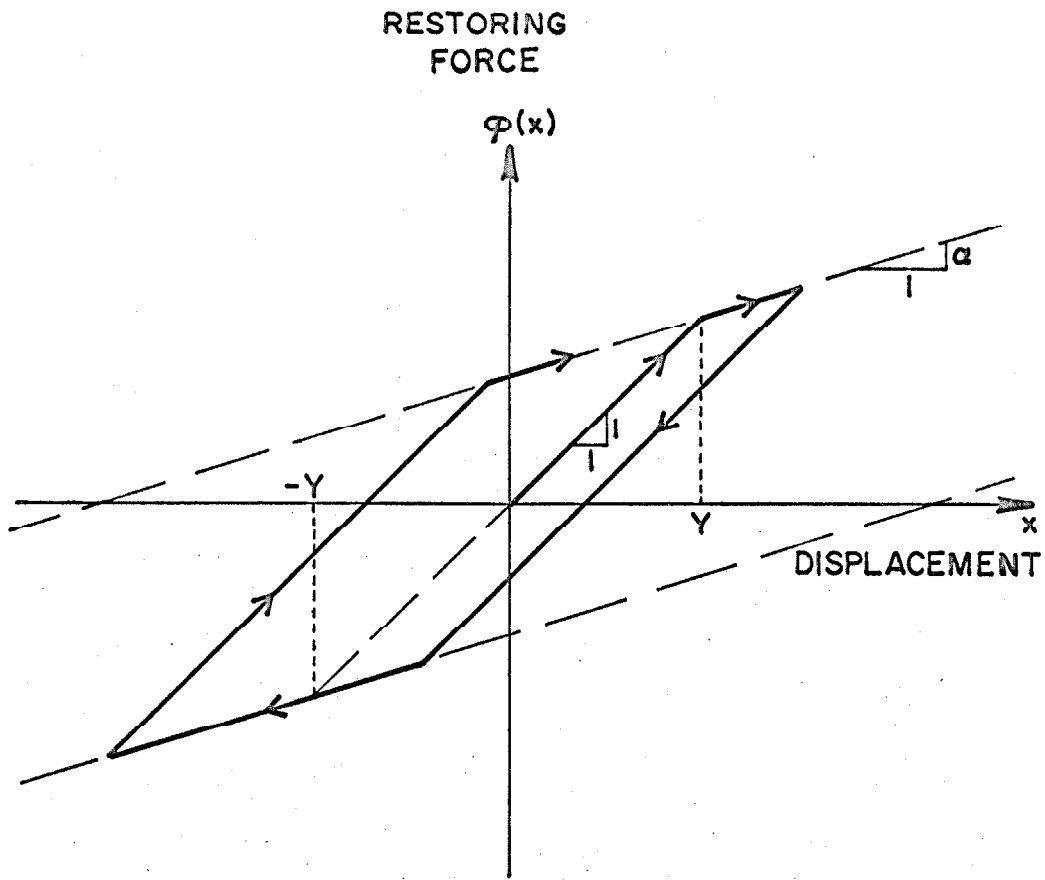
Figure 1. Bilinear Hysteretic Restoring Force.

etic spring. The steady state response to harmonic excitation of a single-mass oscillator with such a bilinear hysteretic spring has been thoroughly investigated by exact and approximate techniques[14, 15]. Also the stationary response of the system with white, Gaussian excitation has been investigated by the approximate method of equivalent linearization[16]. The applicability of these latter results is presumably limited to situations where the two slopes of the restoring force curve are nearly equal.

Analog and digital computers have been used to obtain response spectra for bilinear systems excited by the ground acceleration recorded for past earthquakes. Such response spectra are available for the elasto-plastic system excited by at least five different strong-motion earthquakes[17-21] and for some other bilinear systems for at least two strong-motion earthquakes[21]. The elasto-plastic system is, of course, simply the particular bilinear system with the second slope equal to zero. In addition to the studies of the single mass oscillator, several investigators have studied the earthquake response of buildings using multi-mass models with bilinear hysteretic springs[22-24].

The specific objectives of the present study are:

1. By use of an analog computer, to experimentally investigate the stationary response of bilinear hysteretic single-mass oscillators to random excitation, and

2. To investigate the applicability of some approximate analytical techniques to such nonlinear systems.

The results of such a study of stationary response will, of course, be directly applicable only to problems of stationary vibration. In addition, however, an investigation of the stationary response of a nonlinear system should also give some indication of how the non-linearity may effect transient vibrations of the system. In particular for problems where the excitation persists only for a set time interval and where the statistics of the excitation are stationary over that time interval the system response should approach stationary vibration as the time interval of excitation is increased. Further, the general effects of a particular type of nonlinearity on a system response to any random excitation should be somewhat similar to the effects on stationary response, provided that the excitation persists for several periods of vibration of the system. This condition can be seen to apply to many earthquake engineering problems since the strong motion of the ground due to an earthquake may persist for about thirty seconds whereas the longest natural period of vibration of a tall building may be about two seconds.

Chapter II describes an analog computer investigation of random vibration of a bilinear hysteretic system. The excitation used was approximately Gaussian and white. Mean squared levels of displacement and velocity response, power spectral density, and probability distribution determined for the system response are presented in graphical form. The two particular bilinear systems with the slope parameter α equal to 1/2 and 1/21 were investigated. Systems with and without viscous damping are both included.

Chapter III discusses the approximation of the bilinear hysteretic system by a linear system with both spring constant and damping constant chosen for equivalence. An application of the Krylov-Bogoliubov method to the problem of random vibration is discussed with particular emphasis on the assumptions involved. Basically, it is assumed that the effect of the nonlinearity is small. The response determined from the analog computer results of the second chapter is compared with that predicted by direct application of the Krylov-Bogoliubov method.

The approximation of a bilinear hysteretic system by a nonlinear nonhysteretic system is discussed in Chapter IV. A study is made of a particular nonhysteretic system which belongs to the class of systems for which the stationary solution of the Fokker-Planck equation is known. For the limiting case of a high yield level the results predicted by this approximation are evaluated and compared with the analog computer results. The amount of energy dissipated due to yielding is discussed and a comparison is made between the amounts predicted by two distinctly different nonhysteretic approximations of an elasto-plastic system with a high yield level.

Chapter V discusses the general characteristics experimentally determined for the stationary response of bilinear hysteretic oscillators with random excitation. A comparison of these characteristics with those for systems for which analytical solutions are available gives some indication of the advantages and limitations of various analytical techniques for approximating the response of bilinear hysteretic systems.

II. ANALOG COMPUTER INVESTIGATIONS

2.1. Description of System

A mechanical system which exhibits a bilinear hysteretic restoring force is shown in Fig. 2. The equation of motion can be written as:

$$m\ddot{x} + c\dot{x} + (k_1 + k_2)\varphi(x) = n(t)$$

or
$$\ddot{x} + 2\beta_o \omega_o \dot{x} + \omega_o^2 \varphi(x) = \frac{n(t)}{m} \qquad (2.1)$$

where $\omega_o = \sqrt{\dfrac{k_1 + k_2}{m}}$, small amplitude undamped natural circular frequency

$\beta_o = \dfrac{c}{2\omega_o m}$, small amplitude fraction of critical damping

$\varphi(x)$ is bilinear hysteretic restoring force as shown in Fig. 1 for $\alpha = k_2/(k_1 + k_2)$.

No exact solutions for the statistics of the response of such a hysteretic system to random excitation have yet been obtained by analytical techniques. Thus, it is necessary to use some form of experimental technique, wherein some system described by equation (2.1) is subjected to a forcing function, $n(t)$, of certain statistics and the statistics of the response are experimentally measured. Several such experimental techniques are:

1. mechanical model, as shown in Fig. 2,
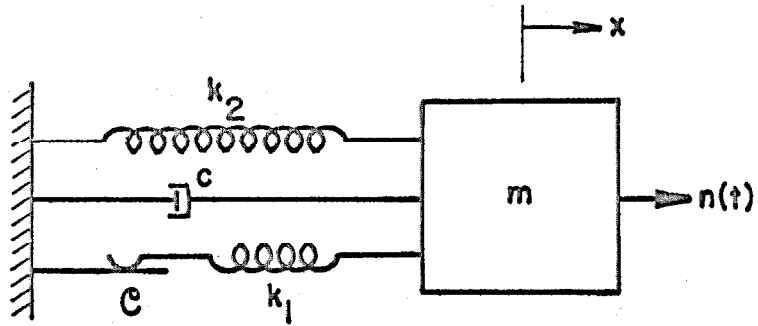
Figure 2.   Bilinear Hysteretic Mechanical Oscillator.

Figure 3.   Analog Computer Circuit for Hysteretic Oscillator.

Figure 4. Elasto-Plastic Function Generator.

2. passive electrical analog of the system shown in Fig. 2,

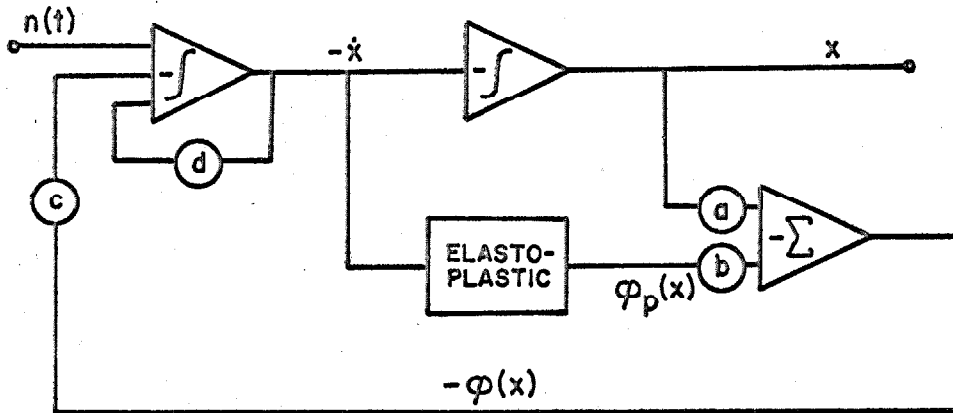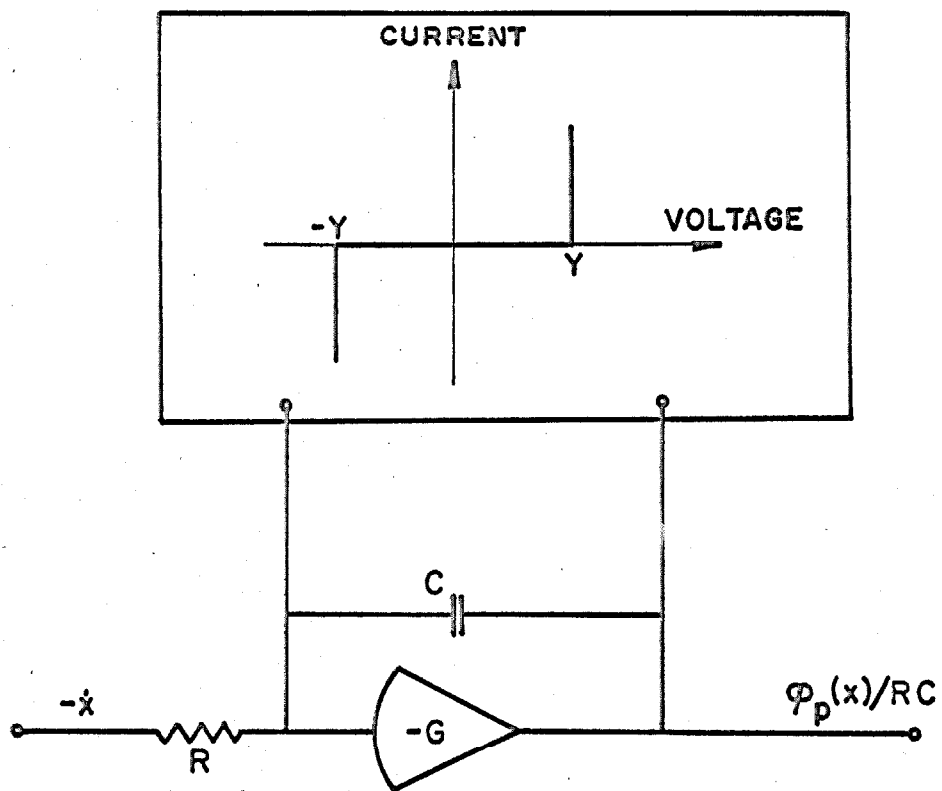3. differential analyzer electrical analog of equation (2.1),

4. numerical integration of equation (2.1).

Method 3, using a conventional electrical analog computer, was

chosen for this study because it is economical, has flexibility with

respect to choice of parameters, and allows an accurate description

of the bilinear hysteretic restoring force.

The basic analog circuit used is shown schematically in Fig. 3.

The bilinear restoring force was developed by adding a linear and an

elasto-plastic restoring force. Figure 4 illustrates the general tech-

nique used to obtain an elasto-plastic function by modifying a conven-

tional analog integrator. In this study the nonlinear function was

obtained by using flip-flop circuits to bias switching transistors. The

details of the analog circuit are included in Appendix A.1. The small-

amplitude, undamped natural circular frequency used was $\omega_o = 3,120$

radians per second.

Photographs of oscilloscope traces of the elasto-plastic func-

tion $\varphi_p(x)$ versus x for several frequencies of periodic motion are

reproduced in Fig. 5. These photographs show that the restoring

force function was essentially independent of frequency over the range

from 5 cps to 1000 cps and was, in fact, a good approximation to the

ideal elastoplastic function. Curvature of the sides of the hysteresis

loop is detectable at 1 cps and lower frequencies. The relative levels

of error introduced by this curvature at low frequencies and by the
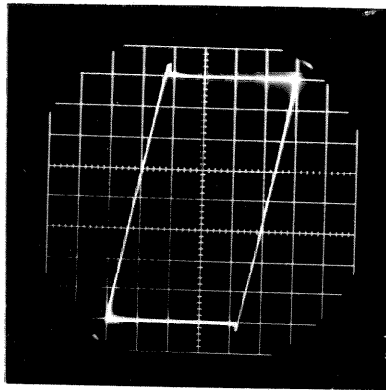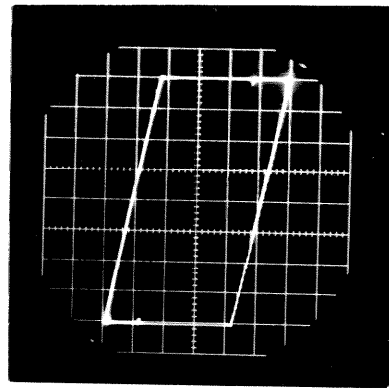
1000 cps   5 cps
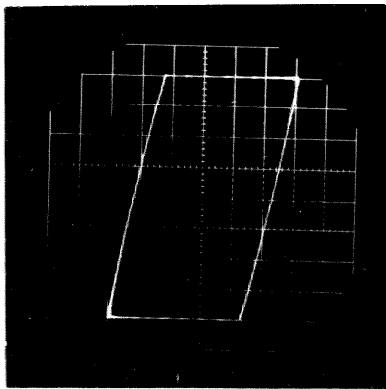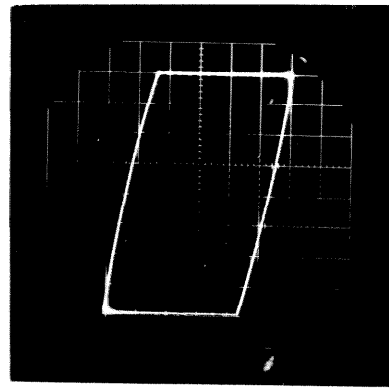
1 cps   0. 5 cps

Figure 5. Oscilloscope Traces of $5\varphi_p(x)$ versus x.

overshoot at initiation of yield apparent at 1000 cps are discussed in Appendix A. 1. Both of these errors were considered to be negligible in this study.

A General Radio Random Noise Generator, Type 1390-B was used to furnish the random exciting signal. The output from this equipment is an approximation to a white, Gaussian source. In the mode of operation which was used the power spectral density is essentially independent of frequency from about 20,000 cps down to near 100 cps. The gas discharge tube which provides the basic random signal in the noise generator failed during the course of the experiments, hence some results were obtained using a replacement tube. Figure 6 indicates experimental measurements of the spectral density of the random signal for both the original and the replacement tubes with σ_n, the rms value of the signal, at 5. 0 volts in both instances. The results are plotted as square root of power spectral density, i. e., rms voltage passing through a filter with a one radian/sec pass band. The results were actually obtained using a wave analyzer which has an effective bandwidth of 28. 4 rad/sec; thus the measured rms voltage was divided by $\sqrt{28.4}$, assuming the spectral density to be flat across the band.

The output from the noise generator was found to have a somewhat unsymmetric probability distribution. For example, Fig. 7 reveals that the unfiltered output using the original gas discharge tube had a probability of being more negative than -2. 5 σ_n of 1. 2%; but the
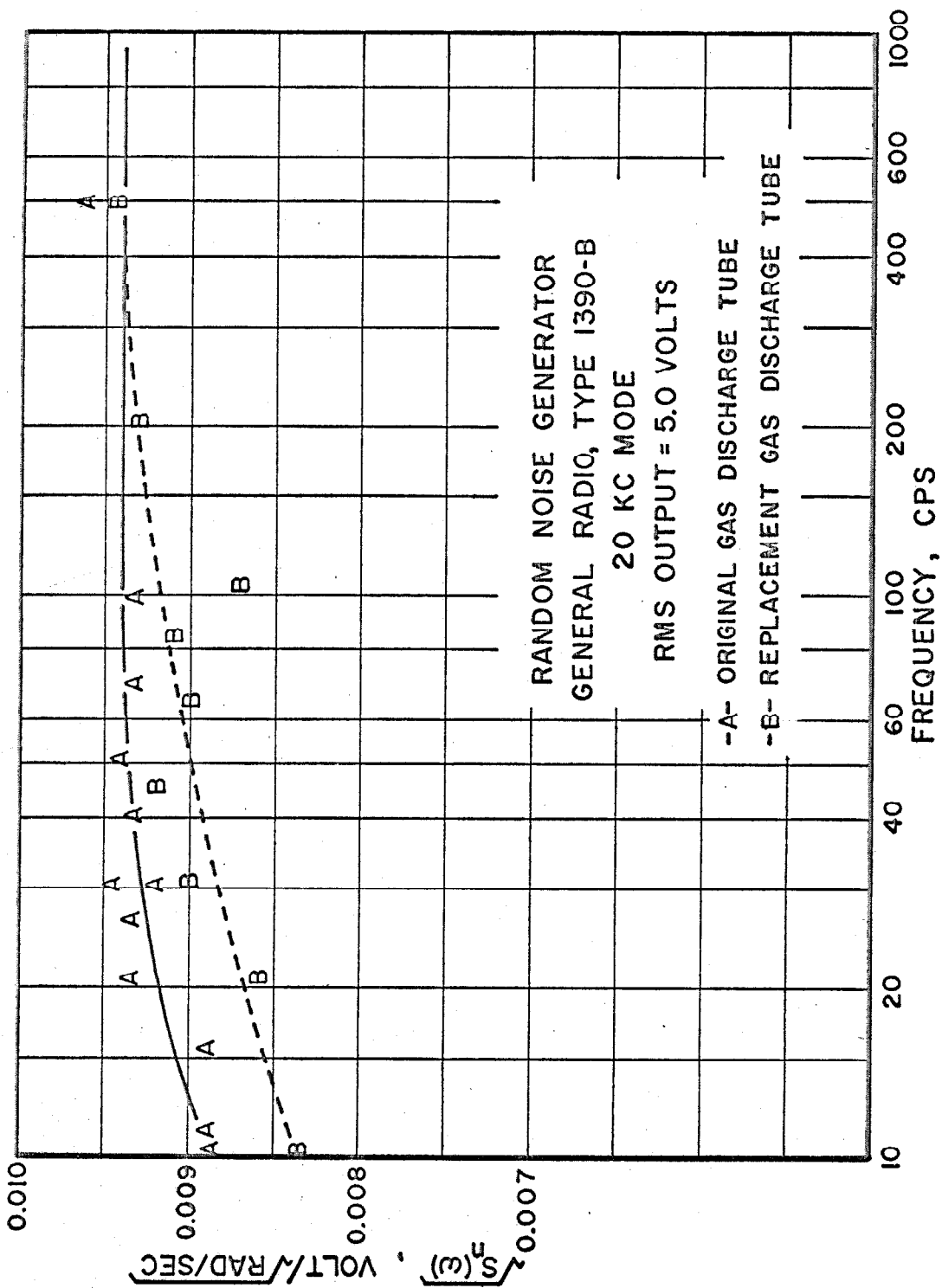
Figure 6.   Power Spectral Density of Random Noise Generator.
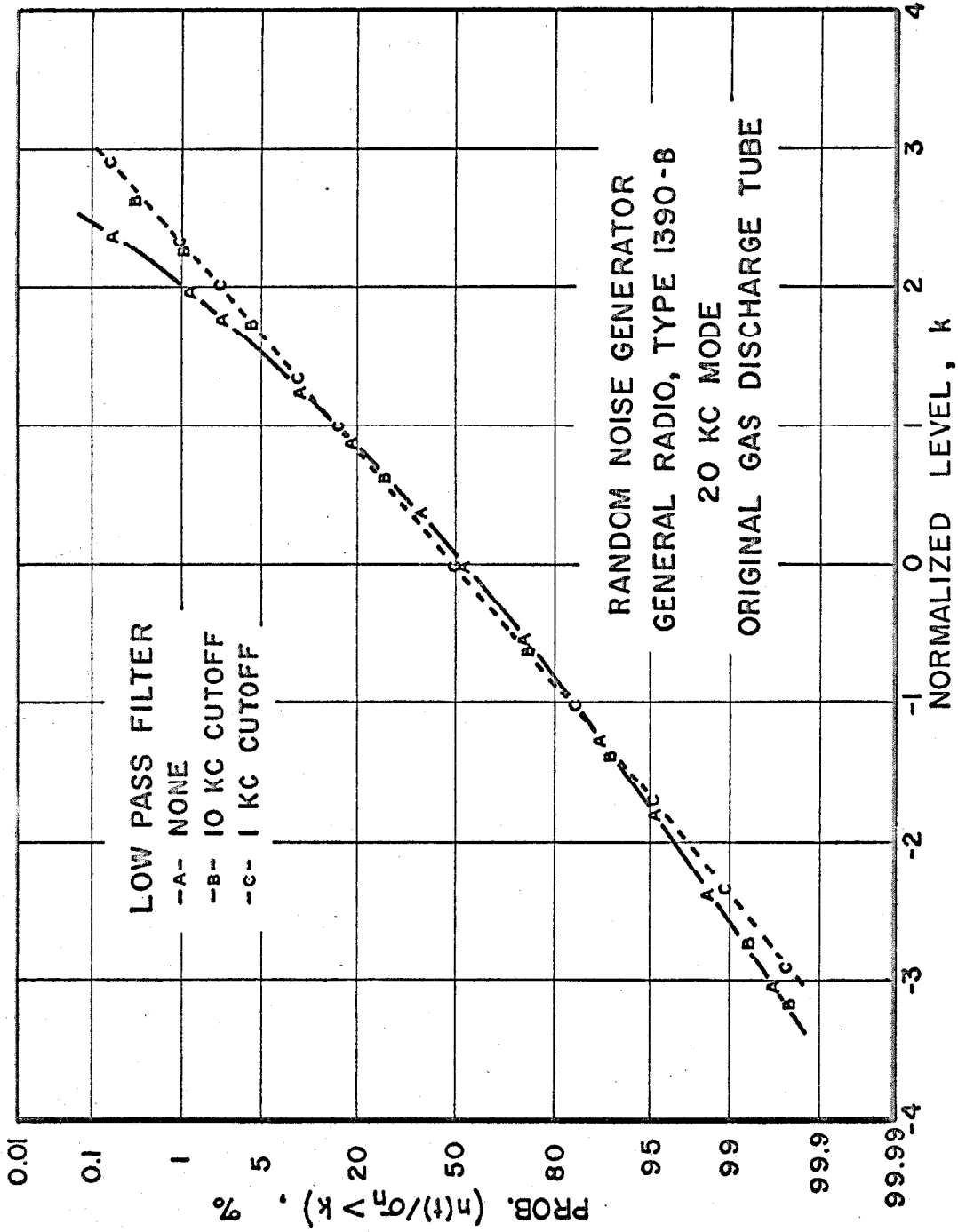
Figure 7.   Probability Distribution of Random Noise Generator.
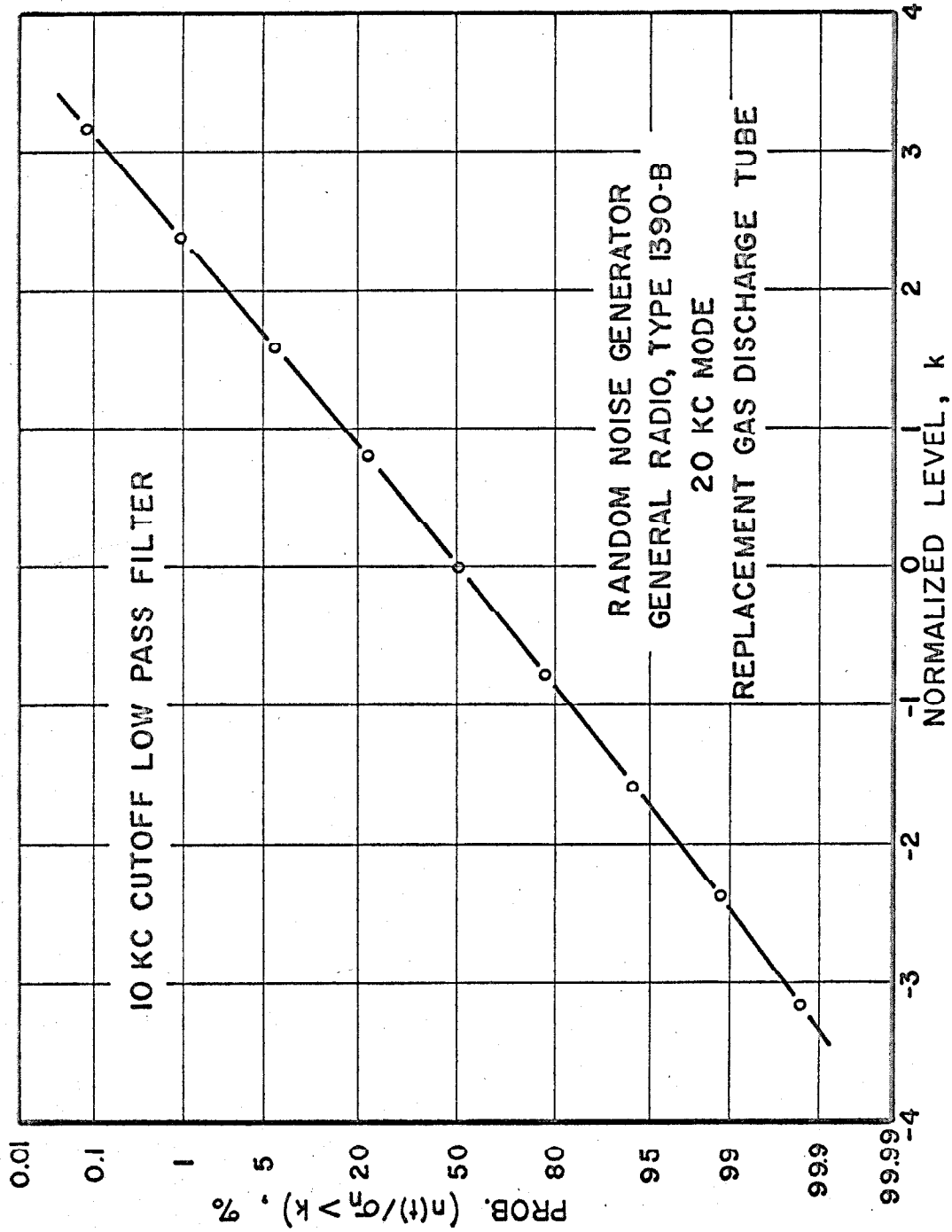
Figure 8. Probability Distribution of Random Noise Generator.

probability of being more positive than $+2.5\,\sigma_n$ was only 0.08%. Experimentation showed that passing the signal through a low pass filter greatly improved its probability distribution. This indicates that the lack of symmetry was due to the higher frequency components of the signal. When the cutoff frequency was set at 1,000 cps the probabilities of exceeding $\pm 2.5\,\sigma_n$ were 0.6% and 0.7%. The scales in Figures 7 and 8 are such that the probability distribution of a Gaussian signal plots as a straight line.

The resonant frequency of the analog system tested never exceeded 500 cps and thus the part of the excitation above 1000 cps contributed relatively little to system response to nearly white excitation. (This fact of small response above 1000 cps will be quite evident when power spectral density of response is examined in a later section.) Since the analog system itself acted to filter out high frequency components of the excitation. the output of the noise generator without filtering was used to excite the system in this study.

2.2. Mean Squared Level of Response

The mean level is the simplest measure of a random signal, but it tells nothing of the variability of the signal. In fact, in the present study the mean levels of both excitation and response were zero. One simple measure of how much a signal of zero mean value varies from that mean value is the mean squared level of the signal. For a Gaussian signal knowledge of mean level and mean squared

level is sufficient to completely determine all probability density functions of that signal.

In this study rms levels were measured using a Brüel and Kjaer Random Noise Voltmeter, Model 2417, which has an averaging time which is adjustable from 0.3 to 100 seconds. Due to the well known beat effect resulting from summing signals of nearly the same frequency, the amplitude of a narrow-band random signal tends to vary with a much lower frequency than the center frequency of the process. This low frequency variation necessitates using relatively long averaging times in order to measure the true rms level. This is illustrated in Appendix B.1, where it is shown that for a narrow-band random signal with mean zero and a bandwidth of 2b radians per second between half-power points the normalized standard error in measuring mean squared level is approximately $(bT)^{-1/2}$ when an averaging time of T seconds is used. It is shown that the equipment used was capable of determining the rms response levels reported in this chapter within an accuracy of about 2% except for two particular instances where the accuracy was limited to about 3.5%.

The rms levels of both the displacement, x, and the velocity of the response of the bilinear system were measured. For a linear oscillator the rms velocity is the product of the rms displacement and the undamped natural circular frequency, but this simple relationship does not hold true for the bilinear system.

The response of a linear system governed by the differential

equation

$$\ddot{x} + 2\beta_1\omega_1\dot{x} + \omega_1^2 x = \frac{n(t)}{m} \tag{2.2}$$

can be obtained by using the complex transfer function of the sytem:

$$H_x(i\omega) = \frac{1}{m\omega_1^2\left[\left(1 - \frac{\omega^2}{\omega_1^2}\right) + i\left(2\beta_1\frac{\omega}{\omega_1}\right)\right]} \tag{2.3}$$

This transfer function is merely the steady-state response, x, to a unit amplitude harmonic excitation. The real part of $H_x(i\omega)$ is the component of response which is in phase with the excitation, and the imaginary part is the component which leads the excitation by a 90° phase angle. The power spectral density of the response of such a linear system is given by

$$S_x(\omega) = |H_x(i\omega)|^2 S_n(\omega) \tag{2.4}$$

where $S_n(\omega)$ is the power spectral density of the excitation. For any signal the mean squared value is obtained by integrating the power spectral density:

$$\sigma^2 = \int_{-\infty}^{\infty} S(\omega)d\omega \quad . \tag{2.5}$$

For a system described by equation (2.2) and with a white excitation with power spectral density

$$S_n(\omega) = \begin{cases} 0 & \text{if } \omega < 0 \\ S_o & \text{if } \omega \geq 0 \end{cases} \tag{2.6}$$

performing the integration of the power spectral density of the

response yields

$$\sigma_x^2 = \frac{\pi S_o}{4m^2\beta_1\omega_1^3} .$$

(2. 7)

Similarly for the response velocity, the transfer function is given by

$$H_{\dot{x}}(i\omega) = \frac{i\omega}{m\omega_1^2\left[\left(1-\frac{\omega^2}{\omega_1^2}\right)+i\left(2\beta_1\frac{\omega}{\omega_1}\right)\right]} .$$

(2. 8)

and the mean squared response to white excitation is

$$\sigma_{\dot{x}}^2 = \frac{\pi S_o}{4m^2\beta_1\omega_1} .$$

(2. 9)

One notes from (2. 9) that the rms velocity response depends on the mass, m, and the dashpot coefficient, $2m\beta_1\omega_1$, but is independent of the stiffness, $m\omega_1^2$, of the linear oscillator.

In this study the yield level of the bilinear system is treated as the principal independent variable. Thus Figures 9-12 are presented in the form of rms response levels versus yield level for bilinear systems with a constant level of excitation. The terms σ_x, $\sigma_{\dot{x}}/\omega_o$ and Y are all normalized by dividing by $\sqrt{S_o\omega_o}/m\omega_o^2$. For a constant excitation power spectral density S_o, this normalization factor is like a measure of the effective amplitude of the excitation force divided by the small-displacement spring constant, $m\omega_o^2$. (Figure 6 shows that the experimental $S_n(\omega)$ closely approximated a constant value S_o, particularly above 100 cps.) Normalized in this

way the yield level and the response levels are nondimensional and the results presented can be used for any level of excitation of the bilinear system with the given value of α.

In some mechanical systems where yielding corresponds to straining of ductile members the ratio σ_x/Y may be an important factor in failure criteria, since it is a measure of how much yielding is taking place. Grid lines for σ_x/Y are presented in Figs. 9 and 11 for convenient reference.

As mentioned in Appendix A. 1 the system with nominally zero viscous damping actually acted as though it had about 0. 05% negative damping. Because of the small magnitude of this term the curves obtained under this condition are labeled $\beta_o = 0$. In a few instances, however, the effect of this negative damping can be detected. In particular, in Figs. 9 and 11 one can observe that the ratio σ_x/Y begins to increase when $Ym\omega_o^2 \big/ \sqrt{S_o\omega_o}$ is increased beyond about 30. This means that in this range a reduction of the level of excitation S_o while keeping Y constant resulted in an increase in the level of response. Such an effect must be due to negative damping. When S_o was reduced to zero the ratio σ_x/Y tended upward to 0. 707 since the system then oscillated with harmonic motion of amplitude Y.

The two limiting cases of the bilinear system for infinite and zero yield levels are linear systems governed by equation (2. 2) with $\omega_1^2 = \omega_o^2$ and $\omega_1^2 = \alpha\omega_o^2$ respectively, and with $\beta_1\omega_1 = \beta_o\omega_o$ in both cases. For the linear system described by equation (2. 2) and with white excitation, expressions (2. 7) and (2. 9) give

$$\sigma_x \frac{m\omega_1^2}{\sqrt{S_o\omega_1}} = \sigma_{\dot{x}} \frac{m\omega_1}{\sqrt{S_o\omega_1}} = \frac{1}{2}\sqrt{\frac{\pi}{\beta_1}} \quad . \tag{2.10}$$

The response to white noise for the linear limiting cases of the bilinear systems presented in Figs. 9-12 have been calculated from expression (2. 10), and are presented in the following table. The systems with no viscous damping are not included in the table since their response would be unbounded for infinite or zero yield level.

Response	$\alpha = \frac{1}{2}$ $\beta_o = 0.01$		$\alpha = \frac{1}{21}$ $\beta_o = 0.01$		$\alpha = \frac{1}{21}$ $\beta_o = 0.05$	
	$Y = \infty$	$Y = 0$	$Y = \infty$	$Y = 0$	$Y = \infty$	$Y = 0$
$\sigma_x \dfrac{m\omega_o^2}{\sqrt{S_o\omega_o}}$	8.88	12.6	8.88	40.6	3.96	18.2
$\sigma_{\dot{x}} \dfrac{m\omega_o}{\sqrt{S_o\omega_o}}$	8.88	8.88	8.88	8.88	3.96	3.96

The curves in Figs. 9-12 all approach relatively near the limiting values in the table for large and small yield values although the yield values are finite and the experimental excitation was not strictly white.

The elasto-plastic system has often been chosen for study by investigators of nonlinear systems, because of its simplicity and because many physical systems supposedly act in an approximately elasto-plastic manner. The elasto-plastic system cannot be used in the study of stationary response, however, since its response to
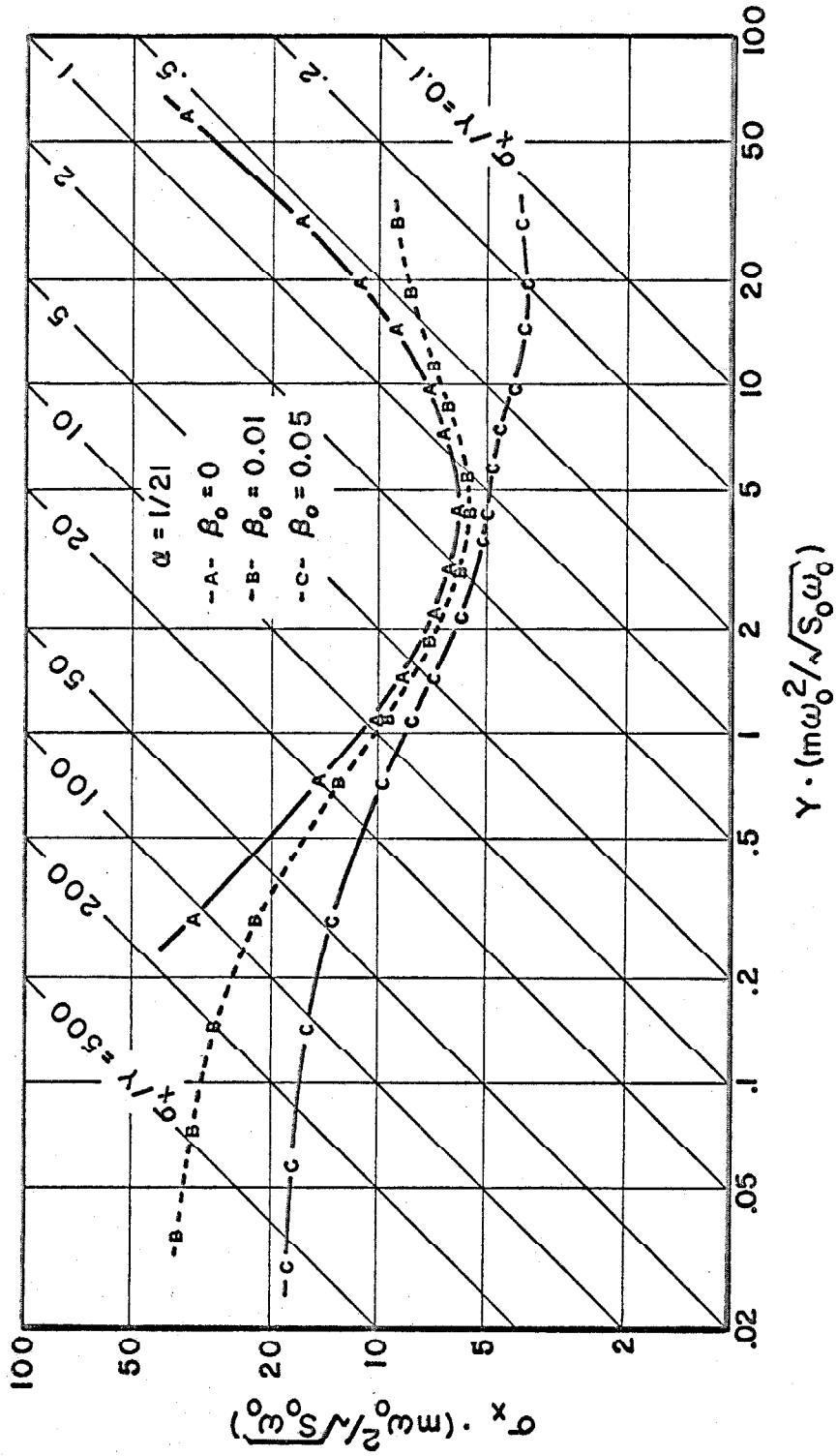
Figure 9. RMS Displacement Response.

-25-
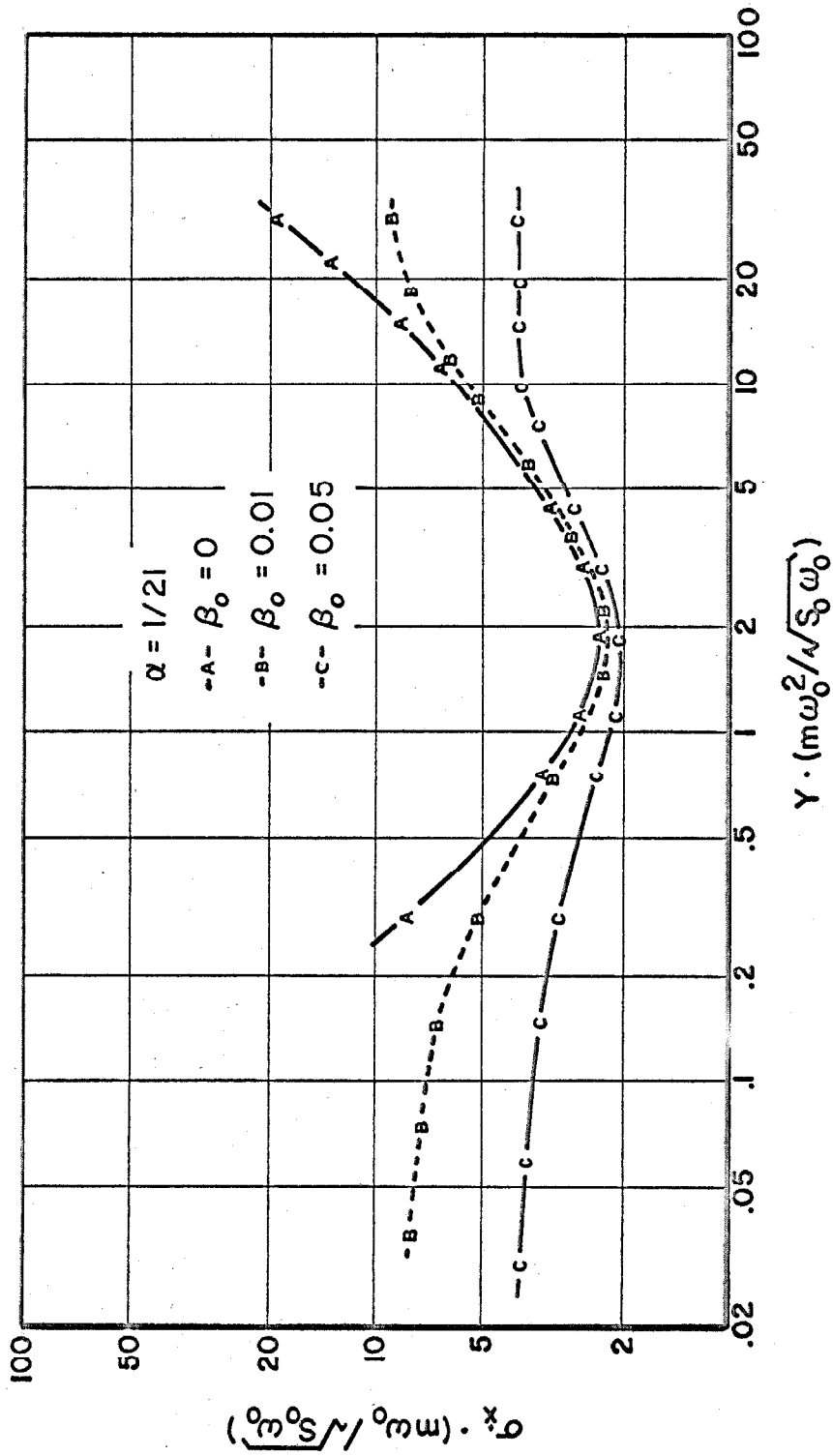
Figure 10. RMS Velocity Response.
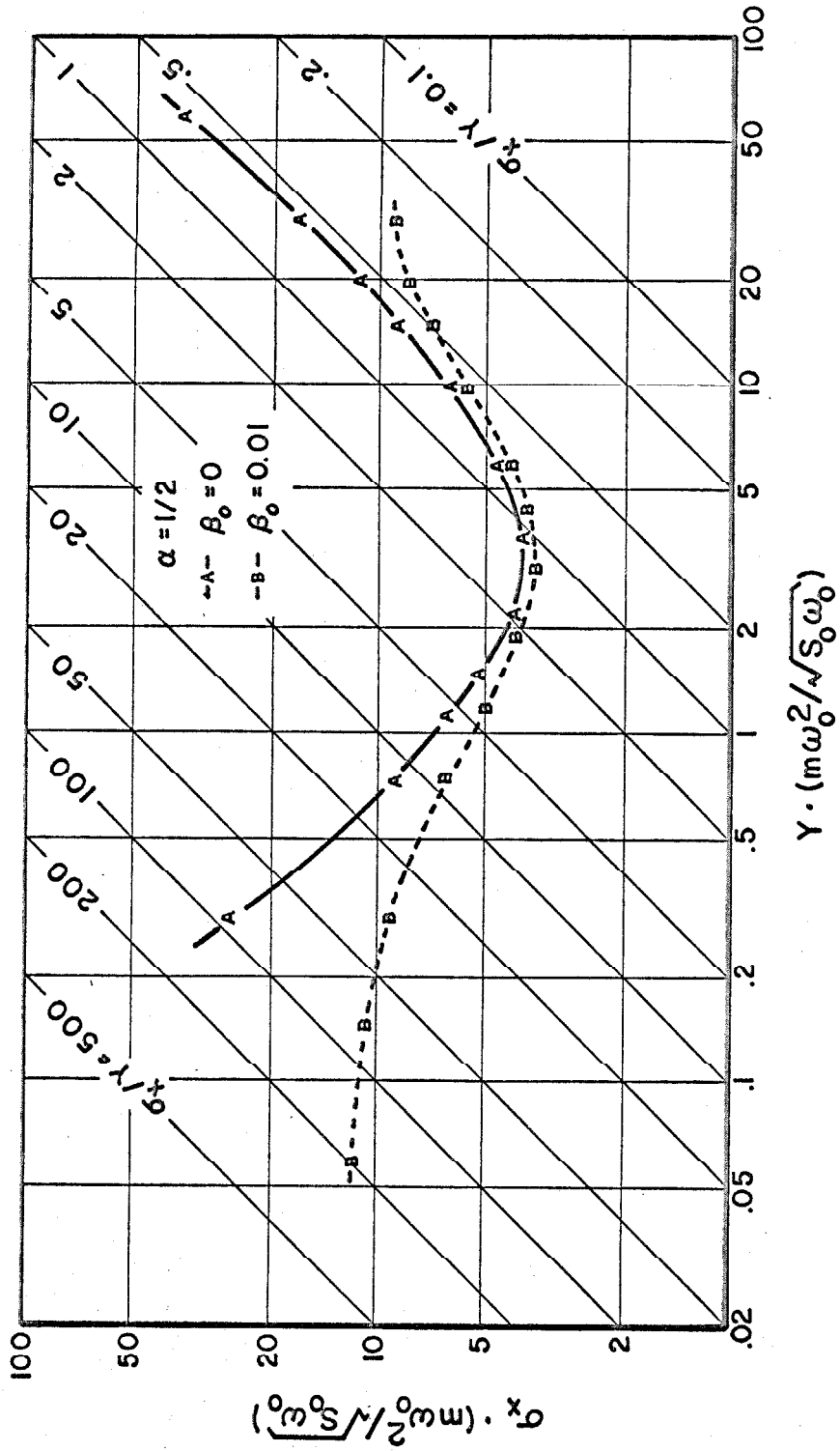
Figure 11. RMS Displacement Response.
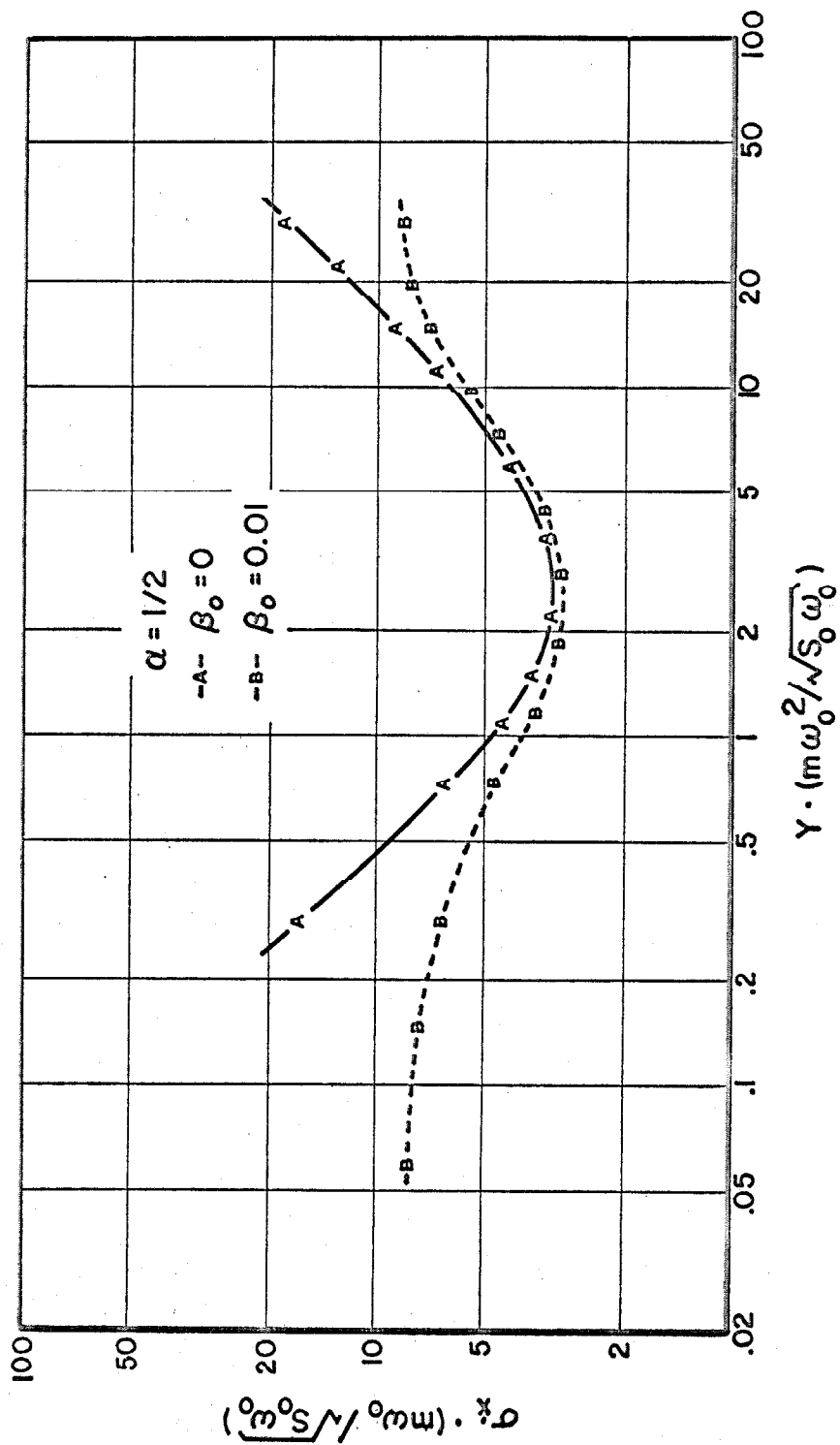
Figure 12. RMS Velocity Response.

stationary excitation is not a stationary process. Consideration of

Fig. 2 with $k_2 = 0$ demonstrates why this is true. With $k_2 = 0$ there is

no restoring force which is dependent on the total distance that the

system has departed from its initial position; hence, once the system

has yielded, it in essence forgets where it started. Thus, the re-

sponse of the elasto-plastic system is free to wander endlessly, and

is useful only for studies of transient motion. The system with

$\alpha = 1/21$ was chosen to represent nearly elasto-plastic systems in this

study, while eliminating the problem of wander.

Curve A in Fig. 9 reveals that for a given level of excitation

of the system with $\alpha = 1/21$ and no viscous damping the resulting dis-

placement response is minimized when the yield level is chosen such

that σ_x / Y falls in the range of one to two. Use of expression (2.10)

shows that this minimum response is approximately the same as that

for a linear system with resonance at ω_o and having about 2% of critical

viscous damping. Curve B for the bilinear system with $\beta_o = 0.01$ shows

that the response, σ_x, of this system is decreased by about 1/3 as the

yield level is reduced from infinity to the region where $\sigma_x / Y \approx 1.3$,

then σ_x increases again with further reduction in yield level. The re-

sponse σ_x for $\beta_o = 0.01$ is less than that for $Y = \infty$ whenever $\sigma_x / Y < 7.5$,

thus yielding reduces σ_x over quite a wide range of yield values. For

the system with $\beta_o = 0.05$, curve C reveals that the effect of yielding

is to increase σ_x above that for $Y = \infty$ for virtually all values of yield

level.

Figure 10 shows that the effect of yielding with $\alpha = 1/21$ on

rms velocity response, $\sigma_{\dot{x}}$, is quite different from the effect on dis-

placement. The effect of reducing the yield level from infinity to

where $\sigma_x / Y = 1.3$ is to limit the velocity by about the same amount as

it would be limited by the addition of 15% viscous damping while

keeping $Y = \infty$. For all values of yield level the velocity response is

reduced by yielding.

A less severely nonlinear system which was chosen for study

is the one with $\alpha = 1/2$. When this system has no viscous damping the

maximum reduction in σ_x, as shown in Fig. 11, occurs when $\sigma_x / Y \approx 1.2$

and is about like the addition of 5% viscous damping to the system with

infinite yield level. When viscous damping $\beta_0 = 0.01$ is introduced the

rms displacement is reduced below that for $Y = \infty$ whenever $\sigma_x / Y < 30$.

Figure 12 shows again that rms velocity is always decreased by yield-

ing and use of expression (2.10) shows that the maximum reduction in

$\sigma_{\dot{x}}$ due to yielding for $\alpha = 1/2$, is approximately like the addition of 7%

viscous damping with infinite yield level.

One can observe from the measured responses that while

$\alpha = 1/21$ results in considerably more reduction in $\sigma_{\dot{x}}$ than does $\alpha = 1/2$,

the less severely nonlinear of the two systems is more effective in re-

ducing the rms displacement, σ_x. The "softening" spring effect of the

nonlinearity tends to increase displacement response, in some cases

overpowering the damping effect of the hysteresis, but velocity response

reflects only the damping effect.

2.3. Power Spectral Density Measurements

The essential basic component of a system for direct measurement of power spectral density is a narrow band filter with variable center frequency. The filter is a linear device characterized by a continuous transfer function $H_F(i\omega)$. The mean squared value of the output from the filter is given by

$$\sigma_{out}^2 = \int_{-\infty}^{\infty} S_{in}(\omega) |H_F(i\omega)|^2 d\omega$$

where $S_{in}(\omega)$ is the spectral density of the input to the filter. Considering the case where $|H_F(i\omega)|$ is symmetric with respect to its center frequency ω_c and expanding $S_{in}(\omega)$ in a Taylor series about ω_c:

$$S_{in}(\omega) = S_{in}(\omega_c) + (\omega - \omega_c) \frac{dS_{in}}{d\omega}(\omega_c)$$

$$+ \frac{(\omega - \omega_c)^2}{2} \frac{d^2 S_{in}}{d\omega^2}(\omega_c) + \dots$$

one obtains

$$\sigma_{out}^2 = S_{in}(\omega_c) \int_{-\infty}^{\infty} |H_F(i\omega)|^2 d\omega$$

$$+ \frac{1}{2} \frac{d^2 S_{in}}{d\omega^2}(\omega_c) \int_{-\infty}^{\infty} (\omega - \omega_c)^2 |H_F(i\omega)|^2 d\omega + \dots \qquad (2.11)$$

Thus if $|H_F(i\omega)|$ is sufficiently sharply peaked as compared to the magnitude of the second and higher even derivatives of $S_{in}(\omega)$ at ω_c, the following approximate relationship is obtained:

$$\sigma_{out}^2 \approx S_{in}(\omega_c) \int_{-\infty}^{\infty} |H_F(i\omega)|^2 d\omega$$

or

$$S_{in}(\omega_c) \approx \frac{1}{B_e} \sigma_{out}^2 \qquad (2.12)$$

where

$$B_e = \int_{-\infty}^{\infty} |H_F(i\omega)|^2 d\omega \quad . \qquad (2.13)$$

The expression B_e can be considered the effective bandwidth of the

filter since an ideal "square-window" filter for which

$$|H(i\omega)| = \begin{cases} 1 & \text{for} \quad |\omega - \omega_c| \leq B_e/2 \\ 0 & \text{for} \quad |\omega - \omega_c| > B_e/2 \end{cases}$$

would result in the same relationship between input spectral density

and mean squared output, under the assumptions leading to expression

(2.12).

Expression (2.12) is used to determine the spectral density

of a process from a measurement of the rms of the output of the

narrow-band filter. In order to use expression (2.12), though, near

the peak frequency of a narrow-band input process it is necessary to

have an extremely narrow-band filter, since the second derivative of

$S_{in}(\omega)$ is large there. Appendix B.3 discusses the error inherent in

using (2.12) to determine power spectral densities with sharp peaks.

It is shown that the maximum error in plotted spectral density, due to

the bandwidth of the filter used, for the figures in this chapter is probably less than 1%.

Measurement of spectral density was accomplished in this study by using a Radiometer Wave Analyzer, Model FRA2. Experimental measurement of the characteristics of the nominal 2 cps band of the wave analyzer confirmed the shape of the transfer function used by P. Y. Hu[25] to evaluate the effective bandwidth as

$$B_e = 4.53 \text{ cps} = 28.4 \text{ rad/sec.}$$

The relative sharpness of the peak of this transfer function can be seen in Fig. 13. When the center frequency of the wave analyzer is set lower than about 100 cps the maximum transmissibility (i.e. the maximum value of $|H_F(i\omega)|$) is noticeably reduced. In order to determine spectral densities at low frequencies one must divide the measured rms value of the filter output by the factor plotted in Fig. 14.

As mentioned in Section 2.2 a normalized standard error of about $(bT)^{-1/2}$ in mean squared level can be expected when an averaging time of T seconds is used in measuring the level of a narrow-band signal with a width 2b radians per second between half-power points. Using Figure 13 to determine the bandwidth of the wave analyzer filter it appears that an averaging time of 100 seconds will result in an error of about 1.5% in determining the rms level of the output from the filter. In order to achieve such long averaging times the random noise voltmeter described in the previous section was used to measure the output of the wave analyzer.
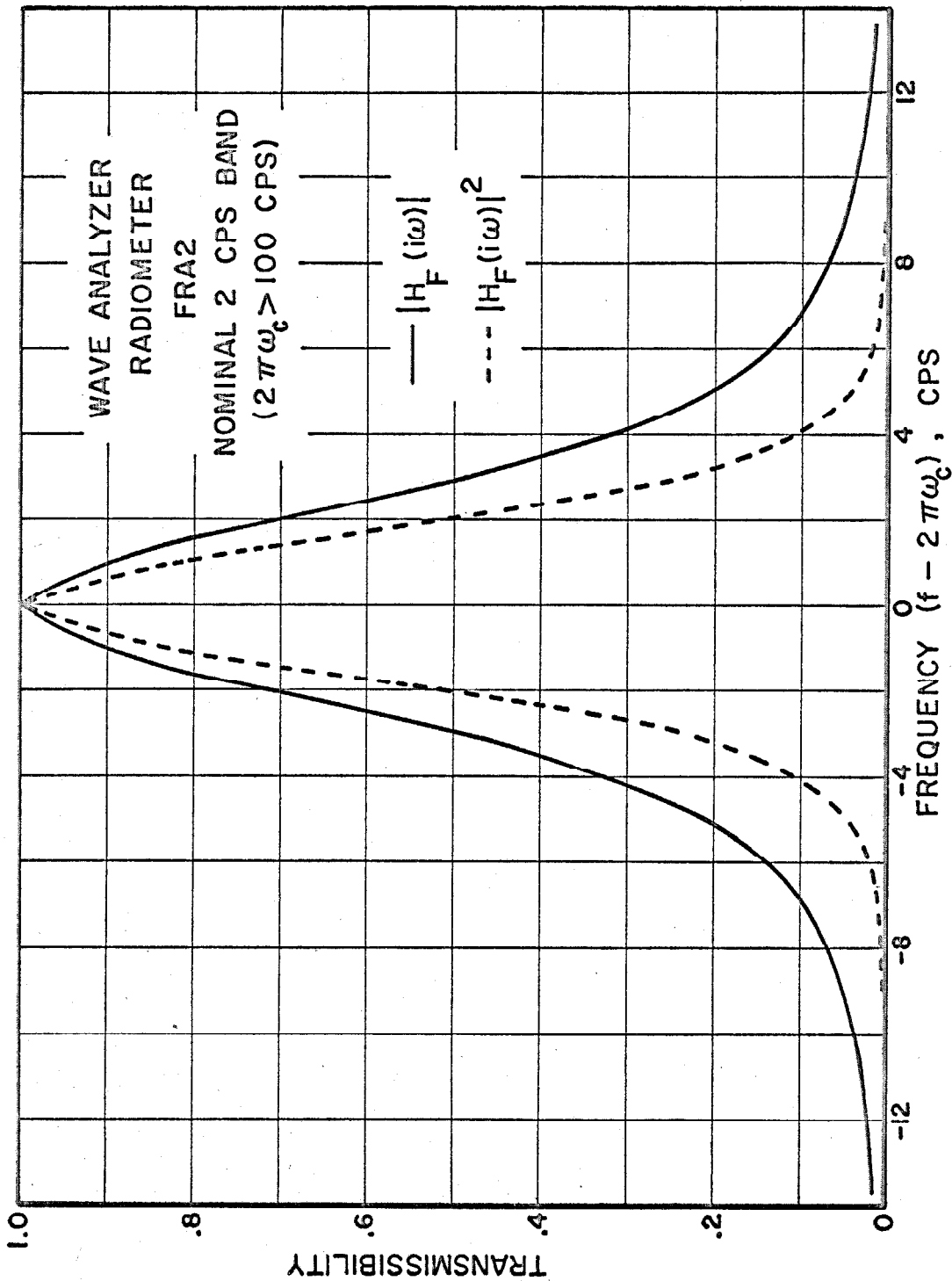
Figure 13. Pass-Band of Wave Analyzer.
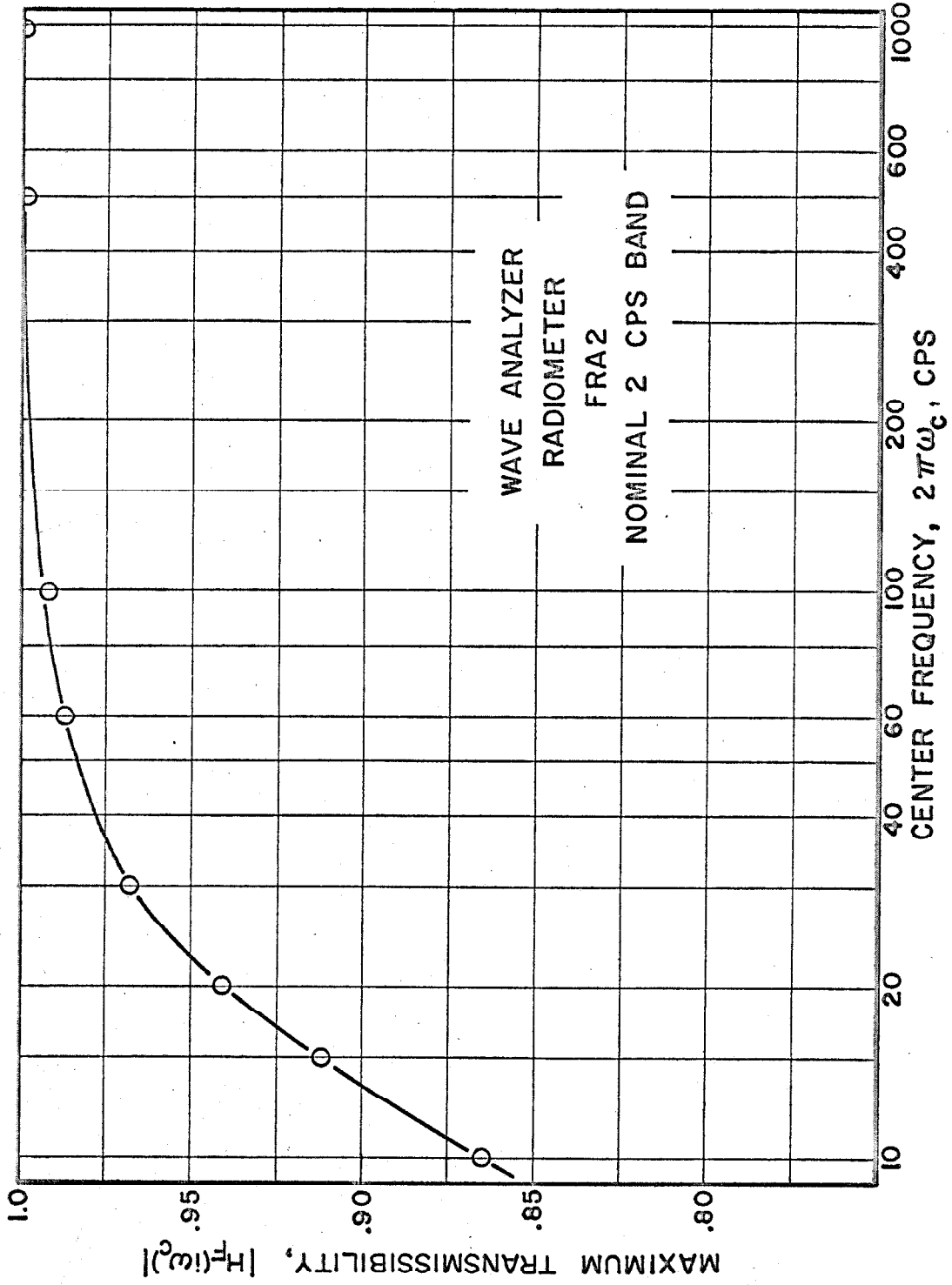
Figure 14. Attenuation of Wave Analyzer.

Tests were conducted to determine spectral densities for the displacement variable, x, of the bilinear system. The exciting force in these tests was the noise generator with the original gas discharge tube.

The system with $\alpha = 1/21$ and $\beta_o = 0$ was investigated rather extensively and the results for this nearly elasto-plastic system are presented in Figures 15, 16, and 17. Figure 15 presents an overall view of the general tendencies of the curves obtained, while Figs. 16 and 17 use expanded scales to better display the details of the data.

For a linear system, as mentioned in the previous section, the power spectral density of the response is directly related to the excitation power spectral density by the transfer function of the system (equation 2.4). Thus, one can experimentally obtain the absolute value of the transfer function of a linear system by measuring power spectral density when the system is excited by some random signal and using the relationship

$$|H_x(i\omega)| = \sqrt{S_x(\omega)/S_n(\omega)} \quad . \tag{2.14}$$

Equation (2.14) does not give the harmonic-excitation transfer function for a nonlinear system in general since separate solutions to a nonlinear problem do not superpose to form another solution. Nonetheless, the parameter $m\omega_o^2 \sqrt{S_x(\omega)/S_n(\omega)}$ was chosen to present the power spectral density of the response of the bilinear system in a manner which allows easy comparison with linear systems. The

steady-state response of bilinear systems to harmonic excitation has been accurately predicted by various techniques and experimentally verified by T. K. Caughey[14] and W. D. Iwan[15].

From expression (2.3) one notes the following limiting conditions for the transfer function of a linear oscillator:

$$H_x(0) = 1/m\omega_1^2$$

and

$$H_x(i\omega) \approx 1/m\omega^2 \quad \text{as} \quad \omega \to \infty \, .$$

Since the limiting cases of the bilinear system for infinite and zero yield levels are linear systems governed by equation (2.2) with $\omega_1^2 = \omega_0^2$ and $\omega_1^2 = \alpha\omega_0^2$ respectively, one might expect the following limiting conditions for the bilinear system:

1. When $\sigma_x/Y \to 0$ and $\omega \to 0$

    then $m\omega_0^2\sqrt{S_x(\omega)/S_n(\omega)} \to 1$

2. When $\sigma_x/Y \to \infty$ and $\omega \to 0$

    then $m\omega_0^2\sqrt{S_x(\omega)/S_n(\omega)} \to 1/\alpha$

3. When $\omega \to \infty$ and either $\sigma_x/Y \to 0$ or $\sigma_x/Y \to \infty$

    then $m\omega_0^2\sqrt{S_x(\omega)/S_n(\omega)} \to \omega_0^2/\omega^2 \, .$

From curve A in Figs. 15 and 16 one can observe that when the yield level was approximately one per cent of the rms level of displacement response, the system response was very similar to that of a linear system with a restoring spring constant $\alpha\omega_0^2$. However,
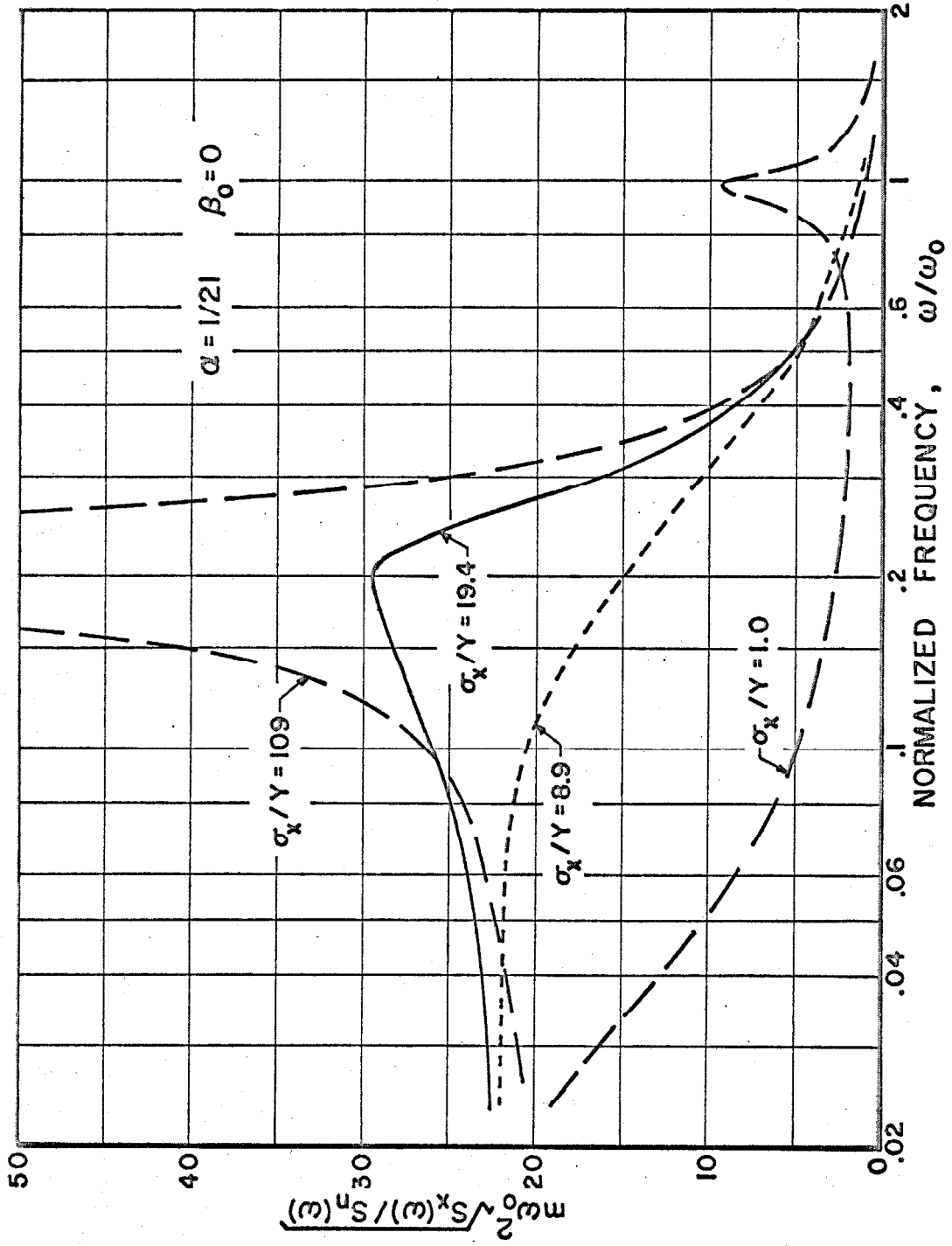
Figure 15. Response Power Spectral Density.

-38-
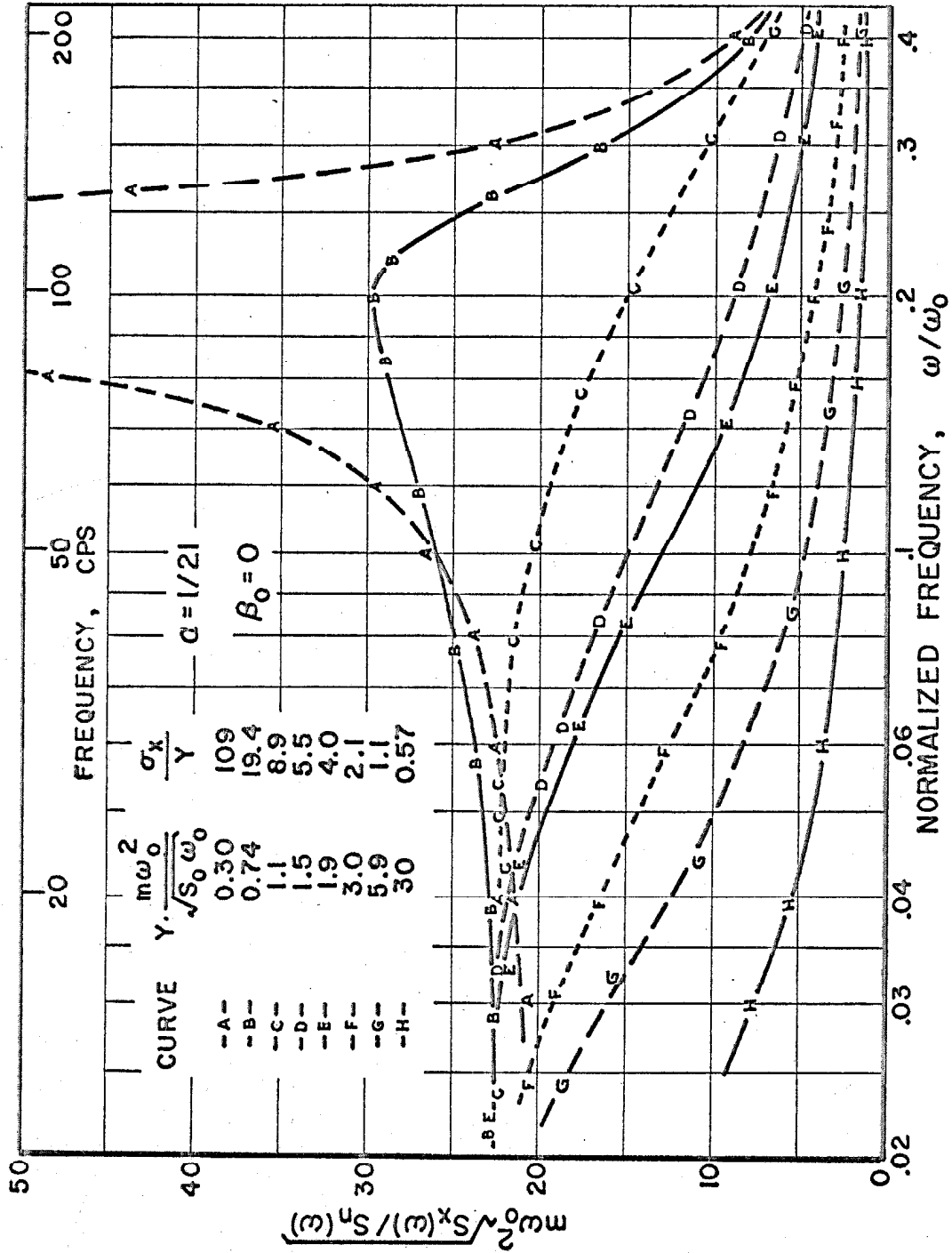
Figure 16. Response Power Spectral Density.
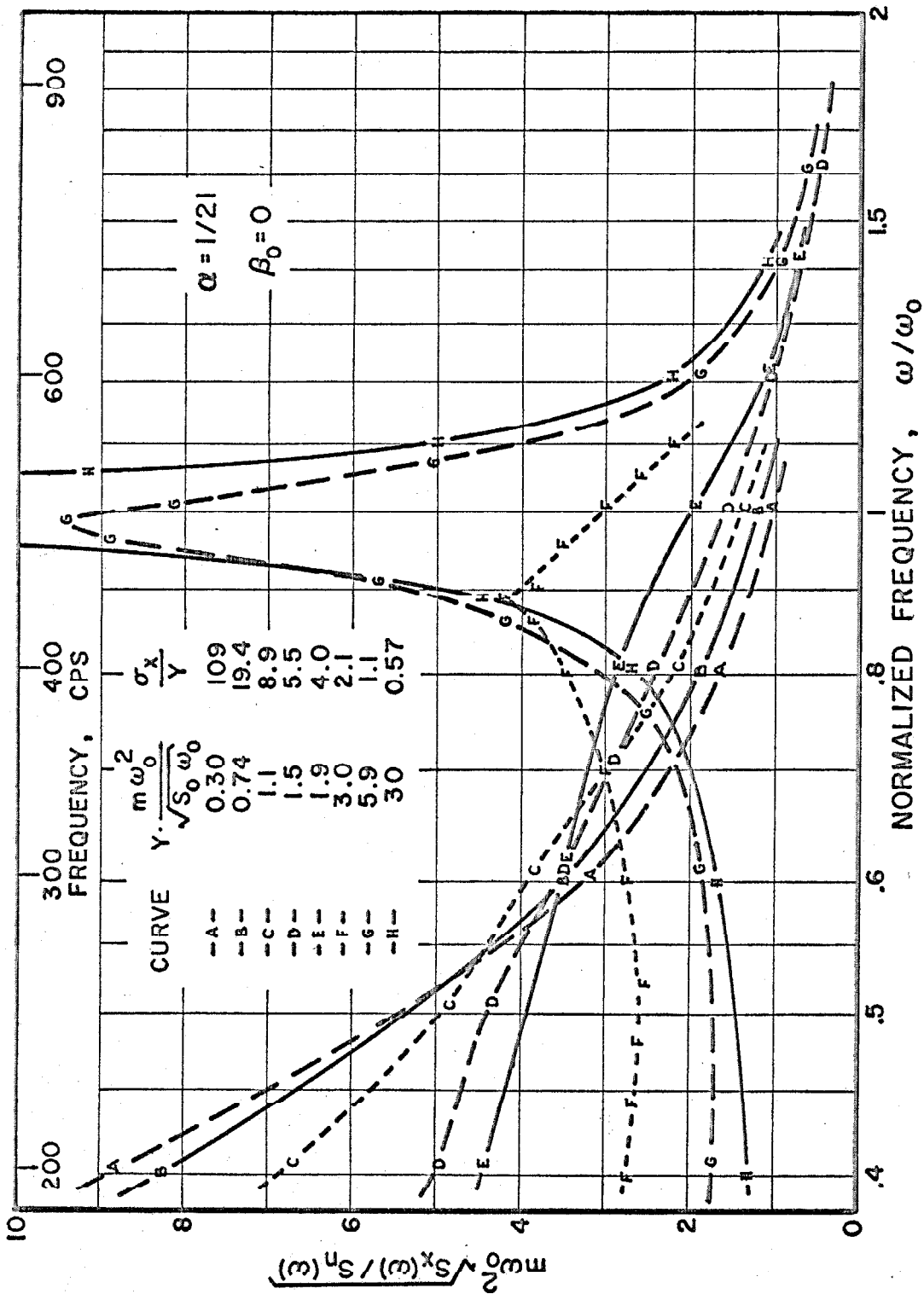
Figure 17. Response Power Spectral Density.
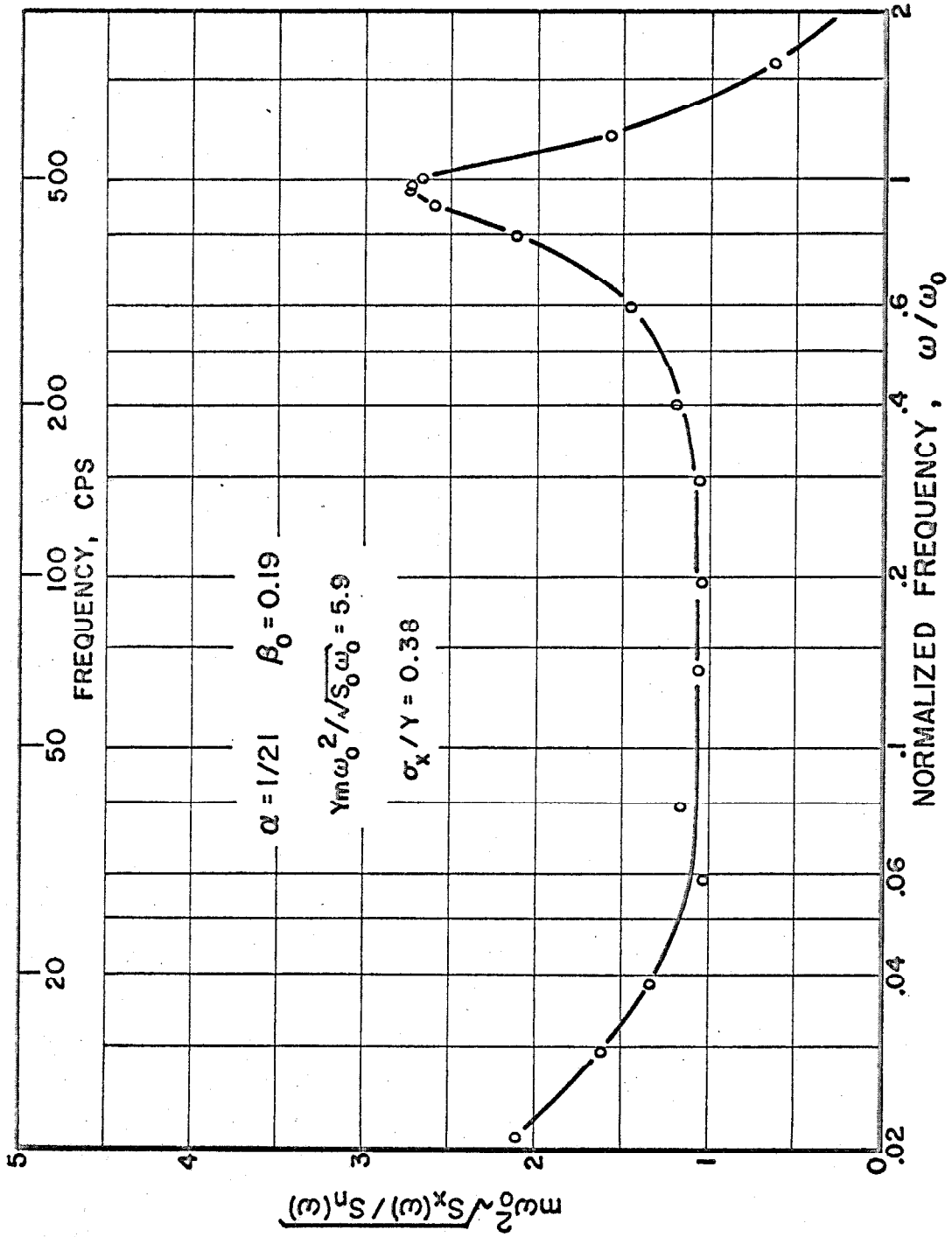
Figure 18. Response Power Spectral Density.
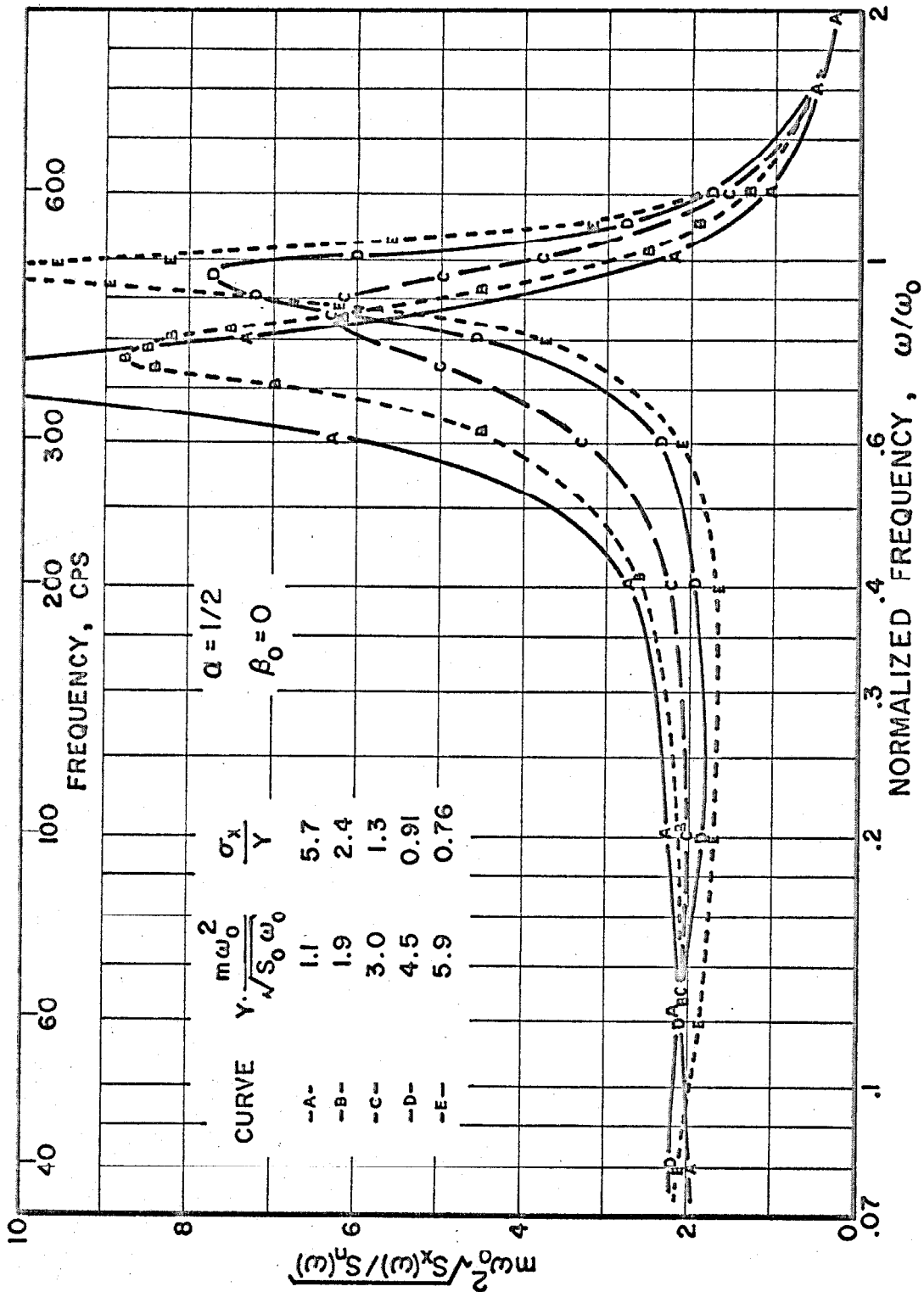
Figure 19. Response Power Spectral Density.

curve A is bounded at $\omega = \sqrt{\alpha}\,\omega_o$, even though the system contained no viscous damping.

Curves G and H reveal that when the ratio of rms response to yield level was less than or equal to unity, the power spectral density of the response near $\omega = \omega_o$ was quite similar to that of a linear damped system with resonant frequency ω_o. The spectral density at low frequency, however, did not tend to the limiting value for a system with resonance at ω_o, but, rather, appears to have approached the limiting value for a resonance at $\sqrt{\alpha}\,\omega_o$. Thus, the predicted limiting condition Number 1 above was not experimentally realized. For this system with no viscous damping it was impossible to decrease the ratio σ_x/Y below approximately 0.55, since a further increase in yield with no change in excitation resulted in a corresponding increase in rms response (see Fig. 9).

One notes from curves C, D and E that the power spectral density of the response of this bilinear system was monotone decreasing over the entire observed frequency range when σ_x/Y was between 4 and 9. A linear oscillator, for comparison, results in a monotone decreasing power spectral density only when it has greater than 70% of critical viscous damping.

Figure 18 presents the spectral density of the system with $\alpha = 1/21$, but with considerable viscous damping introduced, for $\sigma_x/Y = 0.38$. The effect of the nonlinearity on the low frequency power spectral density, within the frequency range of the experiments, is not as great in this instance as when σ_x/Y is larger, but it is still

clearly apparent in Fig. 18.

The power spectral density of the response of the less severely nonlinear system, $\alpha = 1/2$, for several different yield levels, is presented in Fig. 19. Each of the response curves for this system has a definite peak, and the peak is shifted gradually from frequency ω_0 to $\sqrt{\alpha}\,\omega_0$ as σ_x/Y is increased from a small value to a large value. As with the system with $\alpha = 1/21$, though, the low frequency component is like that for a system with resonance at $\sqrt{\alpha}\,\omega_0$, even when the peak response is near ω_0.

From the characteristics of the curves in Figures 15-19, it appears that the proper limiting conditions of the response of the bilinear system, rather than the three postulated above, are:

1.   When $\omega \to 0$ then $m\omega_0^2\sqrt{S_x(\omega)/S_n(\omega)} \to 1/\alpha$ for all σ_x/Y

2.   When $\omega \to \infty$ then $m\omega_0^2\sqrt{S_x(\omega)/S_n(\omega)} \to \omega_0^2/\omega^2$ for all σ_x/Y .

The forms of the spectral density curves in Figs. 15, 16 and 17 show that the response of a severely nonlinear hysteretic oscillator is not, in general, contained in a narrow frequency band. Figure 20 further illustrates this fact by showing plots of displacement response versus time. For comparison, curve (a) shows the response of a linear system with approximately 1% of critical viscous damping. The displacement of this system has a clearly defined principal frequency and a slowly varying amplitude, as is typical of a narrow-band process. Curve (b), for $\alpha = 1/21$ and $\sigma_x/Y = 1.6$, has a fairly well defined

(a) Linear System, $\beta_o = 0.01$

(b) $\alpha = 1/21$, $\beta_o = 0$, $\sigma_x/Y = 1.6$
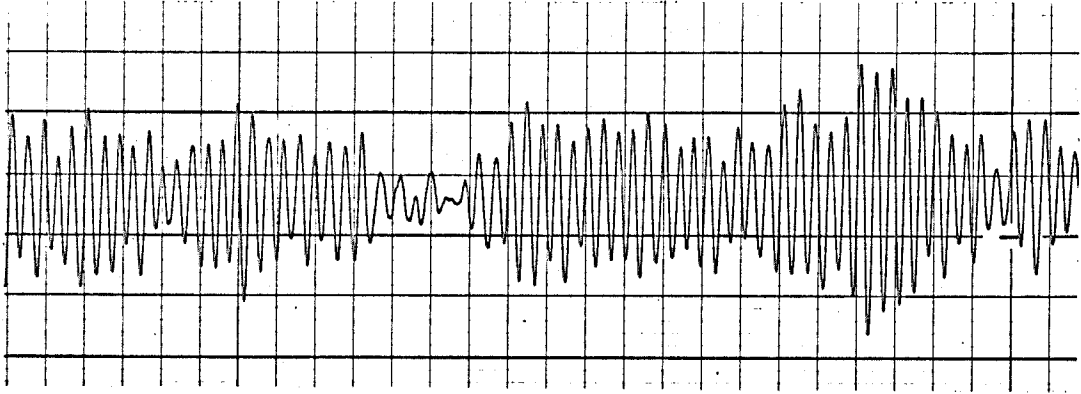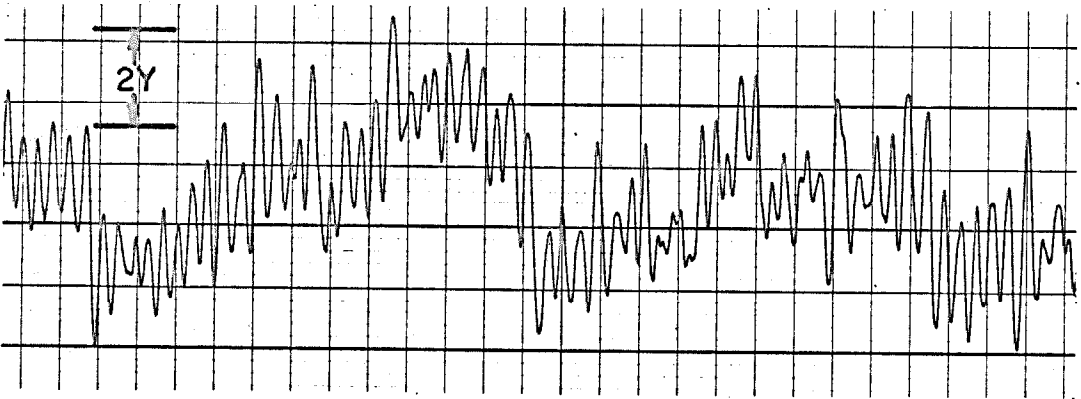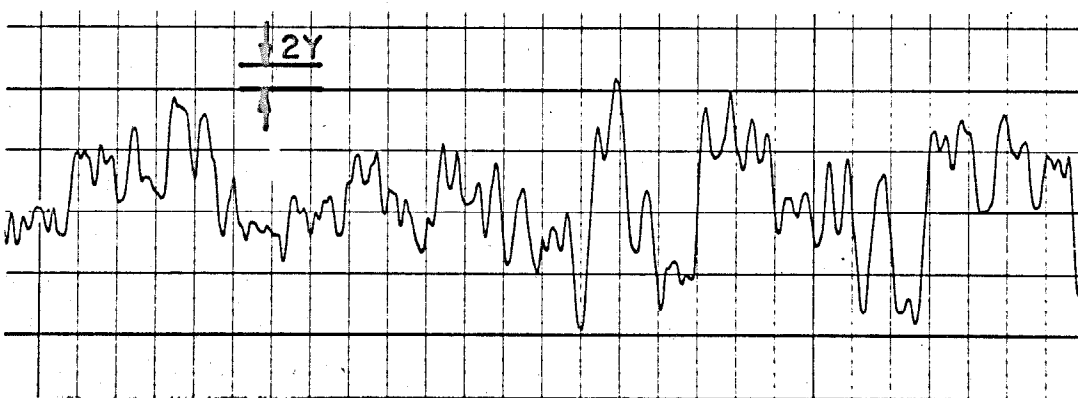
(c) $\alpha = 1/21$, $\beta_o = 0$, $\sigma_x/Y = 5.7$

Figure 20. Time Histories of Random Response.

high frequency component which looks similar to curve (a), but it also contains a large low frequency component which gives a wandering effect to the result. The response of a system with $\alpha = 1/21$ and $\sigma_x/Y = 5.7$, as shown in curve (c), shows almost no similarity to a narrow-band process.

The magnitudes of the yield level are shown for curves (b) and (c) of Fig. 20. At any time and absolute displacement the bilinear system can execute oscillations of amplitude less than the yield level while acting in a purely elastic manner. The high frequency component in curve (b) clearly shows such elastic oscillations taking place at the natural frequency of the linear system. Curve (c), also, shows some indication of elastic oscillations at the linear system natural frequency, but due to the low yield level the amplitude of such oscillations is very small as compared to the lower frequency components present in the displacement. All the curves in Fig. 20 were obtained from a system with a small-amplitude natural frequency near 50 cps, and are plotted with a horizontal scale of 0.05 second per line.

2.4. Probability Distribution Measurements

The probability that a stationary signal exceeds a given level is simply the fraction of the time that the signal exceeds that level. The Quan-Tech Laboratories Amplitude Distribution Analyzer, Model 317, contains a Schmitt trigger device, the output of which is 6.3 volts whenever the input signal is greater than the comparison level and is zero whenever the input signal is less than the comparison level. Thus

the ratio of the mean level of the Schmitt trigger output to 6.3 volts is the fraction of the time that the input signal exceeds the comparison level. The comparison level in the Quan-Tech instrument is continuously adjustable by means of a potentiometer.

Appendix B.2 discusses the probable error introduced by using a finite sampling time in determining the probability distribution of a stationary signal. It is found that the normalized standard error can be expected to be approximately inversely proportional to the square root of the product of the sampling time multiplied by the probability being determined. It is also pointed out why it was necessary to use an external filter and voltmeter to measure the mean output of the Quan-Tech Schmitt trigger in this study. An RC filter having a time constant of 25 seconds was used and this apparently allowed determination of a probability as small as 0.002 within about 10% accuracy. Appendix A.3 gives the details of the slight modification of the distribution analyzer which was necessary in order to use the external filter and voltmeter.

The first stage of the Quan-Tech analyzer is an A.C. amplifier with normalized transmissibility as shown in Figure 21. A low frequency signal passing through the amplifier experiences a phase shift as well as the attenuation shown. Inasmuch as the power spectral density measurements indicated that low frequency components were quite significant in the response of nearly elasto-plastic systems, a test case was checked using an external D.C. amplifier to bypass the A.C. amplifier stage. The test case chosen was the bilinear system
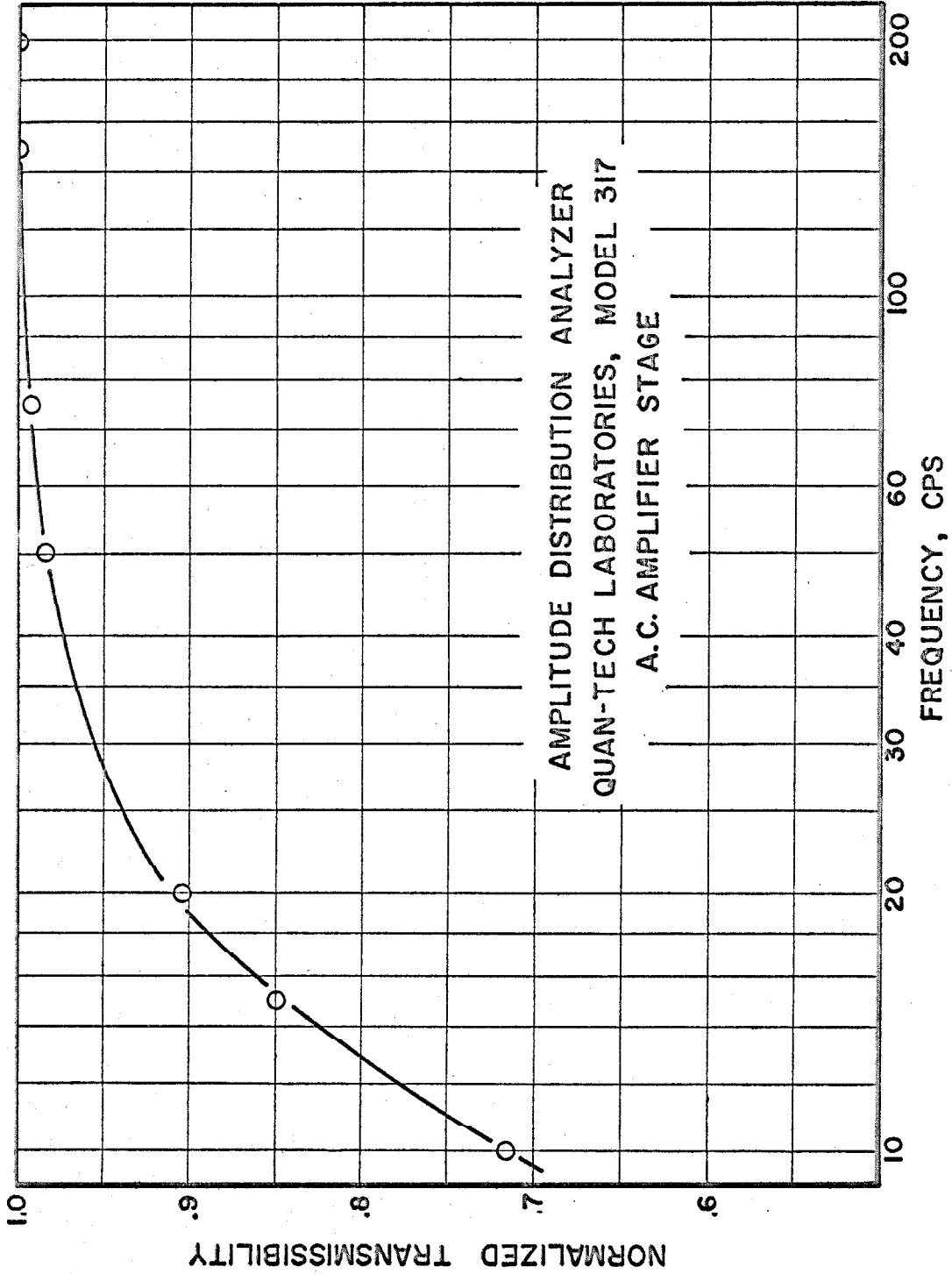
Figure 21. Attenuation of Amplitude Distribution Analyzer.

with $\alpha = 1/21$, $\beta_o = 0$ and $\sigma_x/Y = 6.2$. This was deemed to be a fairly

severe test since the power spectral density of the response of this

system was monotone decreasing with frequency (see Figs. 16 and 17).

The results showed that the A. C. amplifier resulted in no measurable

change in the probability distribution of the response of this particular

system, and, hence, it was concluded that the A. C. amplifier had

negligible effect on all the probability distributions obtained in this

study.

Figure 22 shows probability distributions for the nearly

elasto-plastic oscillator, $\alpha = 1/21$, with no viscous damping. For low

yield levels the response has a significantly greater probability of

being at large displacements, as compared to the rms level, than for

a Gaussian distribution. For example, when $\sigma_x/Y = 6.4$ the bilinear

system response spends approximately 0. 4% of the time beyond $3\sigma_x$,

whereas a signal with a Gaussian distribution spends only about 0. 13%

of the time beyond 3 σ. On the other hand, when the yield level is high

there is a much smaller probability of the system response being at

large amplitudes than for a Gaussian distribution. For example,

when $\sigma_x/Y = 0.55$ the response of the bilinear system spends only

about 0. 3% of the time beyond $2\sigma_x$, whereas a signal with a Gaussian

distribution spends about 2. 3% of the time beyond 2 σ. This latter

effect, which occurs for high yield levels, will be referred to as

amplitude limiting.

Figure 23, for the bilinear system with $\alpha = 1/2$ and $\beta_o = 0.01$,

reveals the same basic tendencies as Figure 22, although not so
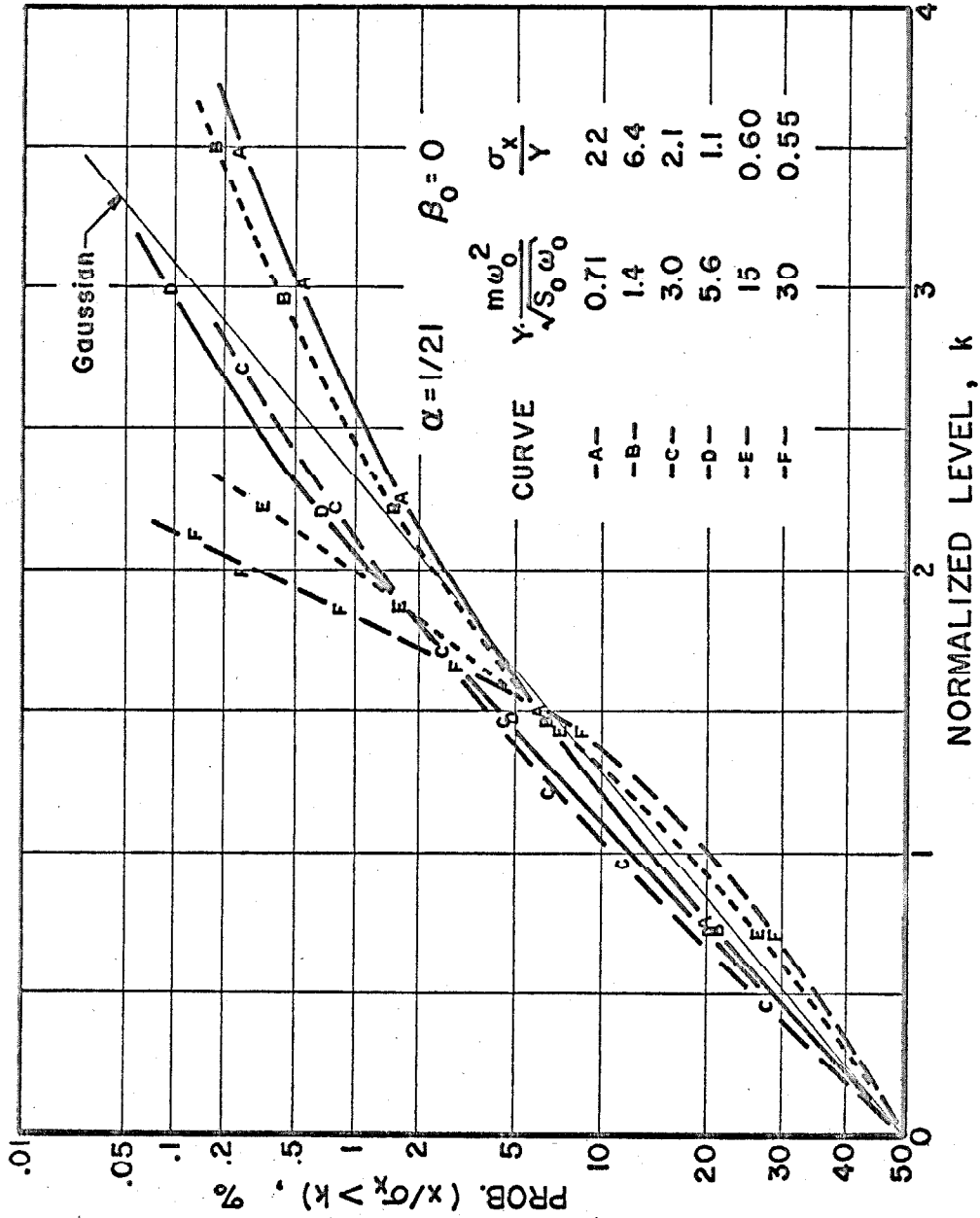
Figure 22. Response Probability Distribution.

-50-
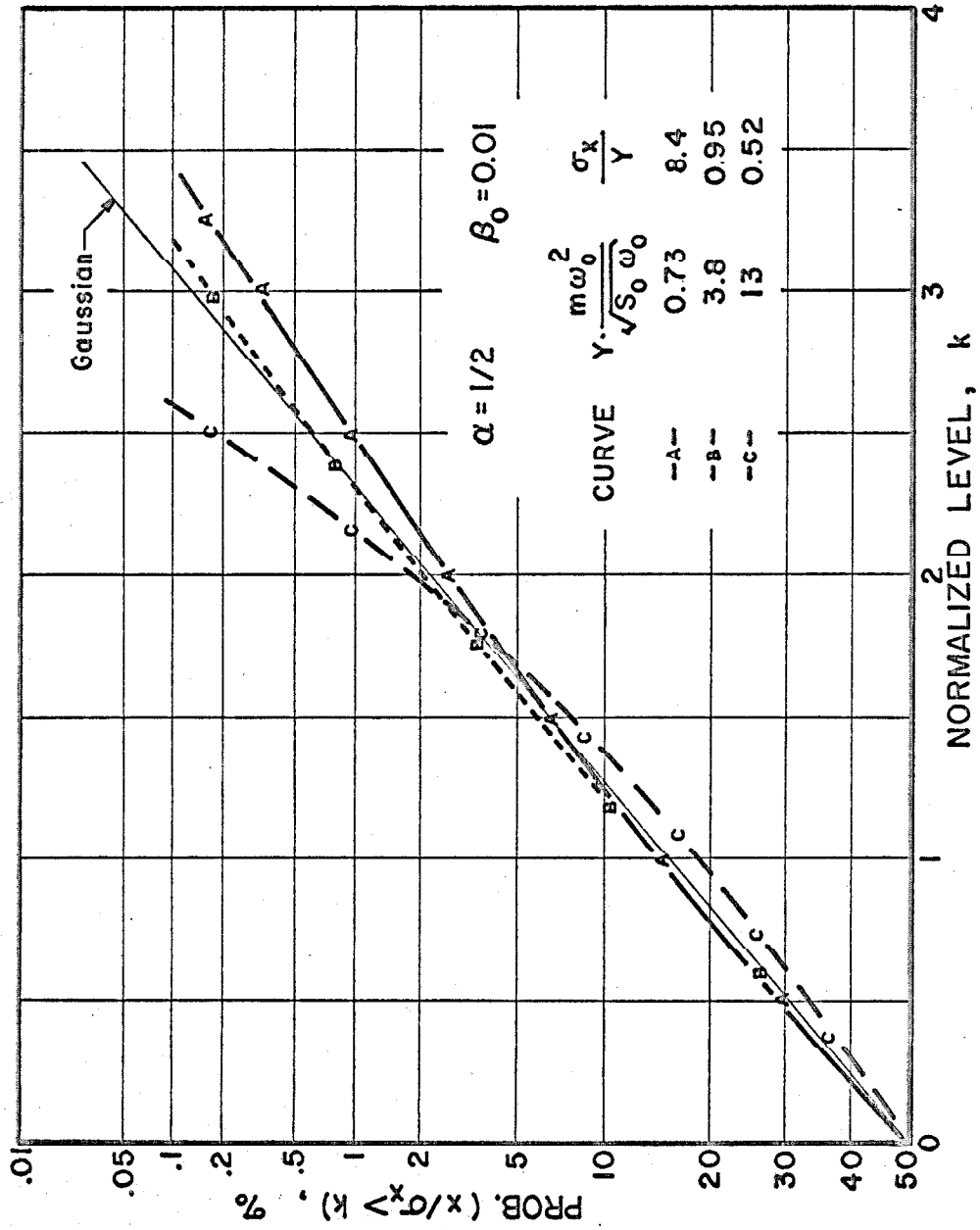
Figure 23. Response Probability Distribution.
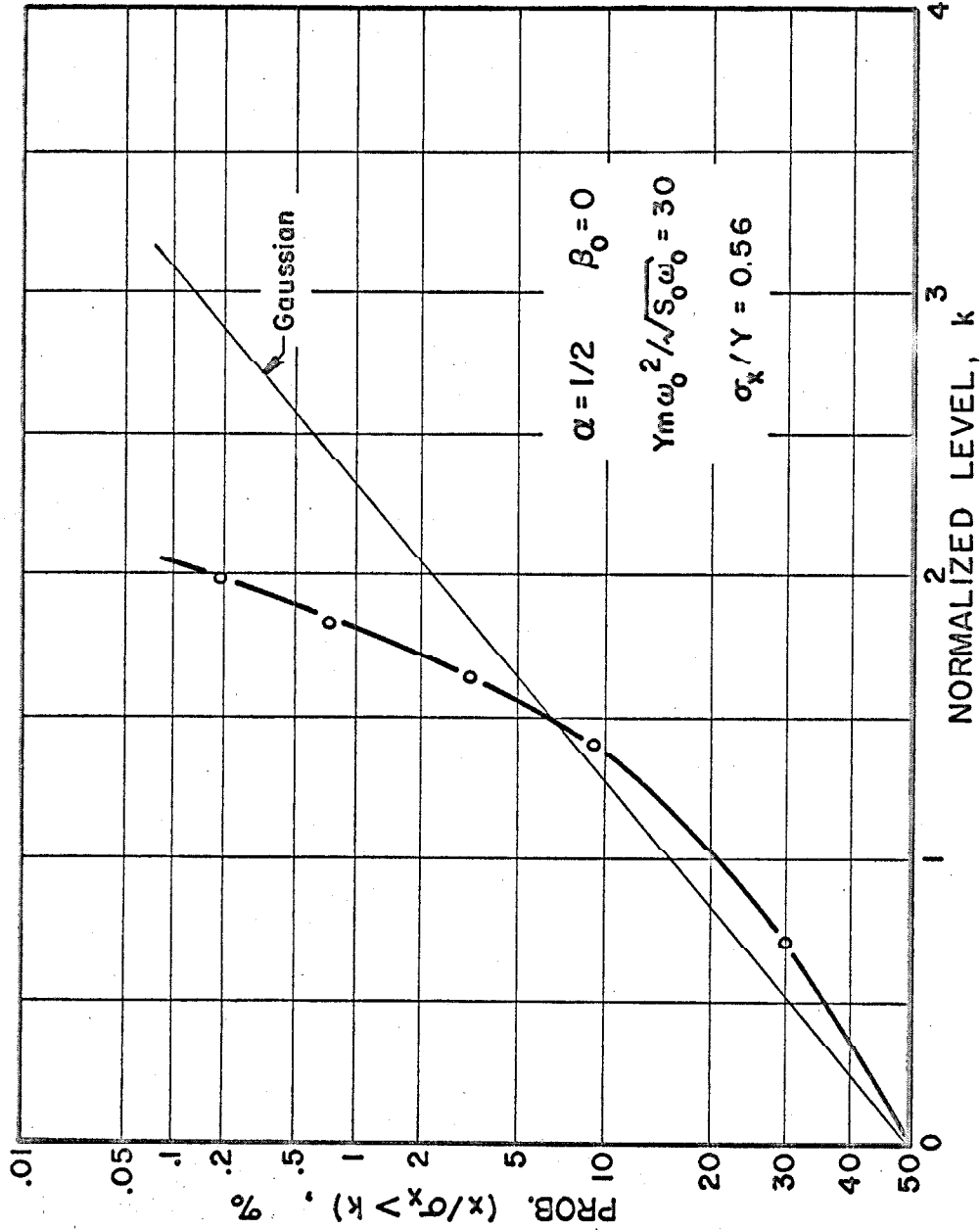
Figure 24. Response Probability Distribution.

pronounced. For example, when $\sigma_x/Y = 8.4$ the response spent approximately 0.3% of the time beyond $3\sigma_x$, and when $\sigma_x/Y = 0.52$ it spent about 1.8% of the time beyond $2\sigma_x$. When the yield level of this damped system was increased until $\sigma_x/Y = 0.2$ the nonlinearity had no detectable effect on the probability distribution of the response, the result being a Gaussian distribution. Figure 24, however, reveals that severe amplitude limiting does occur for high yield levels in the system with $\alpha = 1/2$ when viscous damping is not present.

III. EQUIVALENT LINEAR SYSTEMS

3.1. Krylov-Bogoliubov Method

The statistics of the response of a simple linear oscillator to random excitation are well known. Hence, the statistics of a non-linear oscillator may be readily obtained if one can find an equivalent linear system. A straight-forward method of finding an approximately equivalent linear system is the Krylov-Bogoliubov method of equivalent linearization as adapted by T. K. Caughey for nonlinear dynamic systems with random excitation[8]. Caughey has applied this technique to the particular problem of a bilinear hysteretic oscillator with certain assumptions of small nonlinearity[16]. This analysis will be summarized pointing out the reasons for various assumptions, and the predicted responses will be compared with the measured responses reported in the previous chapter.

Consider the differential equation for the nonlinear system

$$\ddot{x} + 2\beta_o \omega_o \dot{x} + \omega_o^2 \varphi(x) = \frac{N(t)}{m} \tag{3.1}$$

where the excitation $N(t)$ is Gaussian and has a white power spectrum. This equation can be rewritten as

$$\ddot{x} + 2\beta_{eq}\omega_{eq}\dot{x} + \omega_{eq}^2 x + \epsilon(x, \dot{x}, t) = \frac{N(t)}{m} \tag{3.2}$$

where the deficiency term ϵ is given by

$$\epsilon(x, \dot{x}, t) = 2(\beta_o\omega_o - \beta_{eq}\omega_{eq})\dot{x}$$

$$+ \omega_o^2\varphi(x) - \omega_{eq}^2 x \ . \tag{3.3}$$

The basic assumption of equivalent linearization is that it is possible to choose ω_{eq} and β_{eq} in such a way that the effect of the deficiency term is small enough that the statistics of the response of the nonlinear system can be approximated by those of the linear system described by

$$\ddot{x} + 2\beta_{eq}\omega_{eq}\dot{x} + \omega_{eq}^2 x = \frac{N(t)}{m} \quad . \tag{3.4}$$

The statistics of the response of the linear system with ω_{eq} and β_{eq} are readily obtained. From expressions (2.7) and (2.9) of the previous chapter one can write the mean squared displacement and velocity as

$$\sigma_x^2 = \frac{\pi S_o}{4m^2 \beta_{eq} \omega_{eq}^3} \tag{3.5}$$

and

$$\sigma_{\dot{x}}^2 = \frac{\pi S_o}{4m^2 \beta_{eq} \omega_{eq}} \tag{3.6}$$

where S_o is the power spectral density of $N(t)$. Further, using expressions (2.3) and (2.4) gives the power spectral density of the response as

$$S_x(\omega) = \frac{S_o}{m^2 \omega_{eq}^4 \left[\left(1 - \frac{\omega^2}{\omega_{eq}^2} \right)^2 + \left(2\beta_{eq} \frac{\omega}{\omega_{eq}} \right)^2 \right]} \quad . \tag{3.7}$$

Finally, the probability distribution of the response of the linear system must be Gaussian, since N(t) was specified as Gaussian.

When the response of a nonlinear system is known not to have a Gaussian probability distribution the validity of the basic assumption about the existence of an equivalent linear system is obviously limited. It is impossible to choose ω_{eq} and β_{eq} by any technique so as to match a non-Gaussian probability distribution.

For any nonlinear system there exist infinitely many combinations of ω_{eq} and β_{eq} such that either (3.5) gives the proper σ_x or (3.6) gives the proper $\sigma_{\dot{x}}$. However, there exists only one combination of ω_{eq} and β_{eq} such that both (3.5) and (3.6) give the true system response.

If the power spectral density of the response of the nonlinear system is such that it can be approximated by (3.7), then the choice of ω_{eq} and β_{eq} which gives the proper σ_x and $\sigma_{\dot{x}}$ should result in such an approximation. This follows from the fact that both σ_x and $\sigma_{\dot{x}}$ for any system are completely determined by knowledge of the power spectral density of the system response. Specifically

$$\sigma_x^2 = \int_{-\infty}^{\infty} S_x(\omega)d\omega \qquad (3.8)$$

and

$$\sigma_{\dot{x}}^2 = \int_{-\infty}^{\infty} \omega^2 S_x(\omega)d\omega \ . \qquad (3.9)$$

Caughey's equivalent linearization technique is to choose ω_{eq} and β_{eq} so as to minimize the mean squared value of the deficiency term. Minimizing the mean squared value of (3.3) with respect to

$\beta_{eq}\omega_{eq}$ gives

$$\beta_{eq}\omega_{eq} = \beta_o\omega_o + \frac{1}{2}\omega_o^2 \ \overline{\dot{x}\varphi(x)} \Big/ \overline{\dot{x}^2} \qquad (3.10)$$

since $\overline{x\dot{x}}$ must equal zero for a stationary, differentiable signal, where bars denote time averages[*]. Similarly, minimizing with respect to ω_{eq}^2 gives

$$\omega_{eq}^2 = \omega_o^2 \ \overline{x\varphi(x)} \Big/ \overline{x^2}. \qquad (3.11)$$

If one knew certain probability density functions for the non-linear system described by expressions (3.1) and (3.2) it would be possible to use expressions (3.10) and (3.11) to truly minimize the mean squared value of ε. It is not obvious that such a minimization would necessarily ensure that the solution of (3.4) was a good approximation to that of (3.2). Even the minimum level of ε in equation (3.2) for some nonlinear systems might have significant effect on the response. However, it can be shown that true minimization of the mean squared value of the deficiency term requires a choice of ω_{eq} and β_{eq} which yields exact values for σ_x and $\sigma_{\dot{x}}$ for all the nonlinear second order systems for which exact solutions have been obtained to date[13]. These systems which have been solved exactly are all nonhysteretic.

In practice one does not normally know the probability density

---

[*]The time averages used throughout this study are equivalent to ensemble averages if one assumes ergodicity.

functions necessary to evaluate expressions (3.10) and (3.11) so must approximate them. For a nonhysteretic system only the joint probability density of x and $\dot{x}$ is necessary (since $\varphi(x)$ is uniquely determined by x) and this would usually be approximated by a two-dimensional Gaussian distribution. For a hysteretic system $\varphi(x)$ depends on the past history of x so assumptions must be made about the way x varies over time.

If β_o is small and if the effect of the nonlinearity is sufficiently small, the response of the nonlinear system will be contained in a narrow frequency band and can be written as

$$x = A(t) \cos\left(\omega_{eq} t + \theta(t)\right)$$

$$\dot{x} = -A(t)\omega_{eq} \sin\left(\omega_{eq} t + \theta(t)\right)$$

$$\tag{3.12}$$

where $A(t)$ and $\theta(t)$ are slowly varying, i.e., have nearly constant values over any one cycle of frequency ω_{eq}. Expressions (3.12) give relationships between the variables in equations (3.10) and (3.11) over each cycle, so that the only probability density function required to determine $\beta_{eq}\omega_{eq}$ and ω_{eq}^2 is that of the amplitude, p(A).

Using expressions (3.12) gives

$$\overline{x^2} = \frac{1}{2}\overline{A^2} = \frac{1}{2}\int_o^\infty A^2 p(A)dA$$

$$\overline{\dot{x}^2} = \frac{1}{2}\omega_{eq}^2 \overline{A^2} = \frac{1}{2}\omega_{eq}^2 \int_o^\infty A^2 p(A)dA \qquad \left.\right\} \tag{3.13}$$

$$\overline{x\varphi(x)} = \frac{1}{2}\overline{AC(A)} = \frac{1}{2}\int_0^\infty AC(A)p(A)dA \qquad \Bigg\} \qquad (3.13)$$

$$\overline{\dot{x}\varphi(x)} = -\frac{1}{2}\omega_{eq}\overline{AS(A)} = -\frac{1}{2}\omega_{eq}\int_0^\infty AS(A)p(A)dA \qquad \Bigg\}$$

where

$$C(A) = \frac{1}{\pi}\int_0^{2\pi}\cos\psi\,\varphi(A\cos\psi)d\psi \qquad \Bigg\}$$

$$\qquad (3.14)$$

$$S(A) = \frac{1}{\pi}\int_0^{2\pi}\sin\psi\varphi(A\cos\psi)d\psi \quad . \qquad \Bigg\}$$

Evaluating $C(A)$ and $S(A)$ for the bilinear hysteretic system with $\varphi(x)$ as shown in Fig. 1 gives

$$C(A) = \begin{cases} A & \text{for } A \le Y \\ \dfrac{A}{\pi}\left[\alpha\pi + (1-\alpha)\cos^{-1}\left(\dfrac{A-2Y}{A}\right)\right. \\ \qquad\qquad \left. -2(1-\alpha)\dfrac{A-2Y}{A^2}\sqrt{Y(A-Y)}\right] & \text{for } A > Y \end{cases} \qquad (3.15)$$

and

$$S(A) = \begin{cases} 0 & \text{for } A \le Y \\ -\dfrac{4}{\pi}(1-\alpha)\dfrac{Y(A-Y)}{A} & \text{for } A > Y \quad . \end{cases} \qquad (3.16)$$

Both $C(A)$ and $S(A)$ are significant parameters of nonlinear hysteretic systems, apart from their role in equivalent linearization. The equation

$$\omega_r^2(A) = \frac{C(A)}{A}\omega_o^2$$

gives the approximate locus of the peaks of the response curves when the nonlinear system with no viscous damping is excited by various levels of harmonic excitation [14]. The expression $-\pi AS(A)$ is the area enclosed in the hysteresis loop and thus is the energy dissipated per cycle of steady state motion for the nonlinear system with no viscous damping. This latter fact can be easily noted for the bilinear system by rewriting expression (3.16) as

$$-\pi AS(A) = 4Y(A - Y)(1 - \alpha)$$

which is in fact the area of the hysteresis loop.

If one knew the amplitude probability distribution $p(A)$ it would be possible to find the values of $\beta_{eq}\omega_{eq}$ and ω_{eq}^2 which minimize ϵ by substituting from expressions (3.13), (3.15) and (3.16) into (3.10) and (3.11). The only approximation would be that of assuming narrow-band response such that $A(t)$ and $\theta(t)$ are slowly varying parameters in expressions (3.12). In fact, however, $p(A)$ is not known for hysteretic systems so it must be approximated.

The response of a linear system to a Gaussian excitation is Gaussian. Further, if the Gaussian response is narrow-band so that expressions (3.12) can adequately describe it, then the amplitude A has a Rayleigh distribution. Thus, by assuming that the nonlinearity has small effect on the probability density of the response of the hysteretic system, one can approximate the probability density of the amplitude by the Rayleigh distribution:

$$p(A) = \frac{A}{\sigma_x^2} \exp(-A^2/2\sigma_x^2) \tag{3.17}$$

where

$$\sigma_x^2 = \overline{x^2} \ .$$

From expressions (3.11) and (3.13)

$$\left(\frac{\omega_{eq}}{\omega_o}\right)^2 = \frac{1}{2\sigma_x^2} \int_0^\infty AC(A)p(A)dA \ . \tag{3.18}$$

Defining new variables

$$z = \frac{A}{Y} \tag{3.19}$$

and

$$\lambda = 2\frac{\sigma_x^2}{Y^2} \tag{3.20}$$

and substituting (3.15) and (3.17) into (3.10) gives

$$\left(\frac{\omega_{eq}}{\omega_o}\right)^2 = \frac{2}{\lambda^2} \int_0^1 z^3 e^{-z^2/\lambda} dz$$

$$+ \frac{2\alpha}{\lambda^2} \int_1^\infty z^3 e^{-z^2/\lambda} dz$$

$$+ \frac{2(1-\alpha)}{\pi\lambda^2} \int_1^\infty z^3 \cos^{-1}(1-\frac{2}{z})e^{-z^2/\lambda} dz$$

$$- \frac{4(1-\alpha)}{\pi\lambda^2} \int_1^\infty z^2 (1-\frac{2}{z})\sqrt{z-1}\, e^{-z^2/\lambda} dz \ . \tag{3.21}$$

Expression (3.21) is simplified in Appendix C to give expression (C.4):

$$\left(\frac{\omega_{eq}}{\omega_o}\right)^2 = 1 - \frac{8(1-\alpha)}{\pi} \int_1^\infty \left(\frac{1}{z^3} + \frac{1}{\lambda z}\right)\sqrt{z-1}\, e^{-z^2/\lambda} dz \tag{3.22}$$

which can be rewritten as

$$\frac{1-(\omega_{eq}/\omega_0)^2}{1-\alpha} = \frac{8}{\pi}\int_1^\infty \left(\frac{1}{z^3} + \frac{1}{\lambda z}\right)\sqrt{z-1}\, e^{-z^2/\lambda}\, dz \ . \tag{3.23}$$

Caughey has numerically integrated (3.23) and graphed the result as a function of λ [16]. This graph is reproduced in Fig. 25. For large values of λ an asymptotic expansion which allows determination of ω_{eq}/ω_0 without numerical integration is derived in Appendix C. Expression (C.18) gives

$$\left(\frac{\omega_{eq}}{\omega_0}\right)^2 = \alpha + \frac{8(1-\alpha)}{\pi}\left(0.6043\,\lambda^{-3/4} - 0.2451\,\lambda^{-5/4}\right.$$

$$\left. -0.1295\,\lambda^{-7/4}\right) \text{for } \lambda \gg 1. \tag{3.24}$$

For an infinite yield level ($\lambda = 0$) expression (3.22) reduces to

$$\omega_{eq}^2 = \omega_0^2$$

due to the exponential term. For the other limiting case of zero yield level ($\lambda = \infty$) expression (3.24) reduces to

$$\omega_{eq}^2 = \alpha\omega_0^2 \ .$$

The restoring force $\varphi(x)$ is exactly $\omega_0^2 x$ and $\alpha\omega_0^2 x$ when $Y = \infty$ and $Y = 0$, respectively, for the bilinear system. Thus, expressions (3.22) and (3.24) give the limiting values that one would expect for ω_{eq}^2.

Similarly, using expressions (3.10) and (3.13) with the assumption of p(A) being a Rayleigh distribution gives
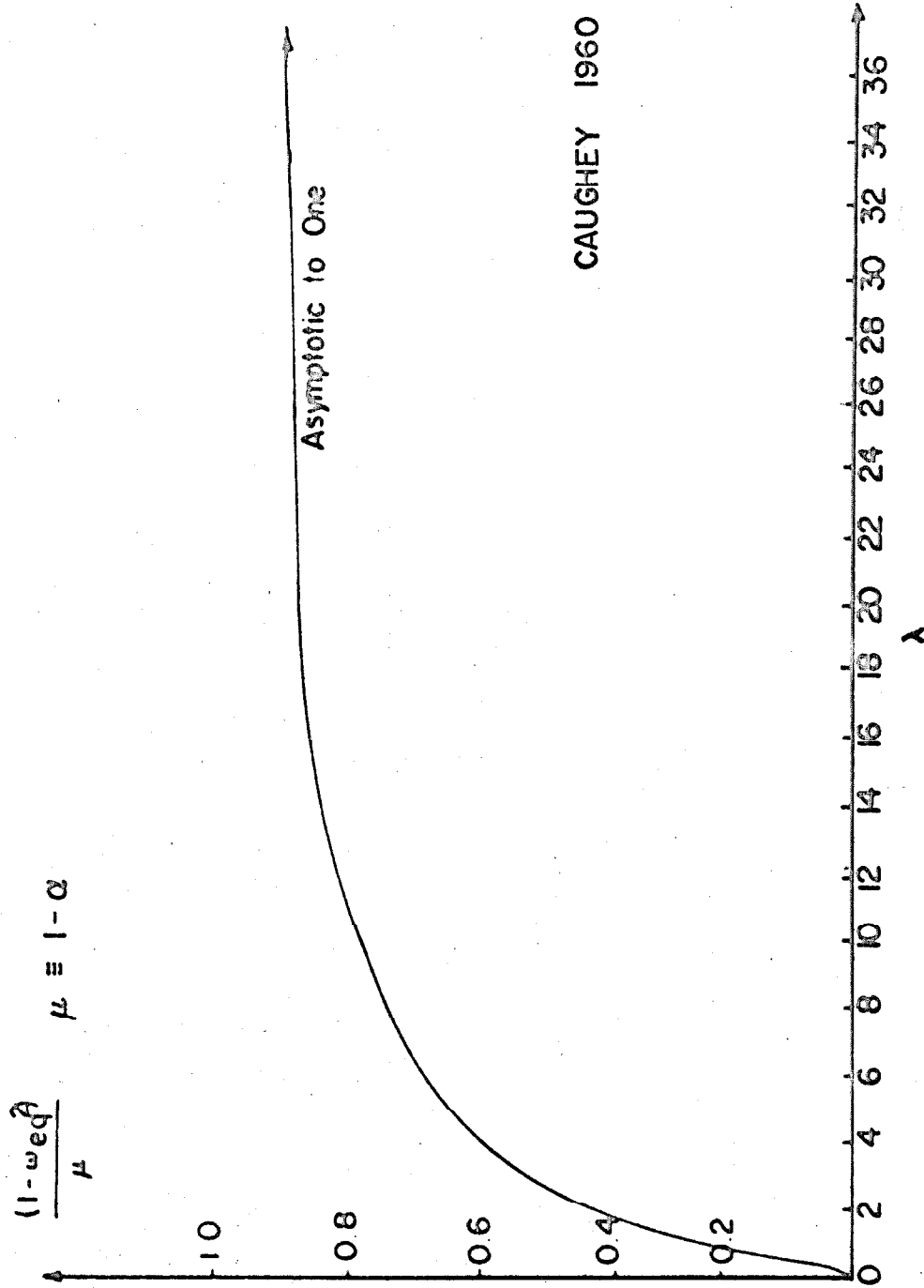
Figure 25. Equivalent Freqeuncy Term.

$$\beta_{eq}\omega_{eq} = \beta_o\omega_o - \frac{\omega_o^2}{4\omega_{eq}\sigma_x^2} \int_0^\infty AS(A)p(A)d(A) \ .$$

Substitution of (3.16) and (3.17) into this expression gives

$$\beta_{eq}\omega_{eq} = \beta_o\omega_o + \frac{\omega_o^2(1-\alpha)Y}{\omega_{eq}\pi\sigma_x^2}\left[\int_Y^\infty \frac{A^2}{\sigma_x^2} \exp\left(-\frac{A^2}{2\sigma_x^2}\right) dA \right.$$

$$\left. - Y\int_Y^\infty \frac{A}{\sigma_x^2} \exp\left(-\frac{A^2}{2\sigma_x^2}\right) dA \right] \ .$$

The second integral in this expression can be integrated directly and the first one integrated by parts to yield

$$\beta_{eq} = \beta_o\left(\frac{\omega_o}{\omega_{eq}}\right) + \left(\frac{\omega_o}{\omega_{eq}}\right)^2 \frac{1-\alpha}{\sqrt{\pi}} \frac{Y}{\sqrt{2}\,\sigma_x} \text{erfc}\left(\frac{Y}{\sqrt{2}\,\sigma_x}\right) \qquad (3.25)$$

where erfc denotes the complimentary error function. In terms of λ this is

$$\beta_{eq} = \beta_o\left(\frac{\omega_o}{\omega_{eq}}\right) + \left(\frac{\omega_o}{\omega_{eq}}\right)^2 \frac{1-\alpha}{\sqrt{\pi}} \lambda^{-1/2}\text{erfc}(\lambda^{-1/2}) \ . \qquad (3.26)$$

The value of ω_{eq}/ω_o from (3.22) or (3.24) above must be used with (3.26) to determine the value of β_{eq} for some particular value of λ.

The assumptions made in this derivation of ω_{eq} and β_{eq} were:

1. The response of the nonlinear system was assumed to be contained within a narrow frequency band;

2. The probability density of the amplitude of this narrow-band response was assumed to be the Rayleigh distribution.

Violation of either of these assumptions will probably result in a choice of ω_{eq} and/or β_{eq} which does not truly minimize the mean squared value of the deficiency term of the "equivalent" linear system. The basic assumption of equivalent linearization, however, is merely that the effect of the deficiency term on the statistics of the response can be neglected. For some problems the effects of the deficiency term may be negligible even if ω_{eq} and β_{eq} are not chosen so as to exactly minimize the mean squared value of the term. However, in other problems even the minimum mean squared level of the deficiency term may result in significant effects on the system response. Thus, satisfaction of assumptions 1 and 2 may in some cases not be necessary, and in other cases not be sufficient for satisfaction of the basic assumption.

3.2. Comparison with Analog Computer Results

The analog computer investigations reported in the previous chapter revealed that the power spectral density of the response of the severly nonlinear hysteretic system often is not contained within a narrow frequency band. This is particularly true for the nearly elasto-plastic system. Further, determinations of probability distribution showed that the response was not, in general, Gaussian. Thus, it is very unlikely that the above technique for determining ω_{eq} and β_{eq} would result in minimizing the effect of the deficiency term for such systems.

Figures 26 - 29 show the values of σ_x and $\sigma_{\dot{x}}$ predicted by direct application of the above technique (which was based on assumptions of

small nonlinearity) to the severely nonlinear systems of $\alpha = 1/21$ and $\alpha = 1/2$. The values determined using the analog computer are also reproduced from Figs. 9-12 for comparison. Recall that the excitation of the analog computer system was a close approximation of a white, Gaussian source.

For the system with $\alpha = 1/2$ and $\beta_o = 0.01$ the predictions of σ_x and $\sigma_{\dot{x}}$ agree within about 10% with the analog computer measurements for all values of yield level (Figs. 26 and 27). The greatest discrepancy is when $Ym\omega_o^2/\sqrt{S_o\omega_o}$ (the normalized yield level) is in the range from 10 to 20. Figure 23 in the previous chapter shows that the probability distribution of x was noticeably non-Gaussian in this range. For example Prob.$(x > 2.5\sigma_x)$ for $Ym\omega_o^2/\sqrt{S_o\omega_o} = 13$ was about 0.18% as compared to 0.60% for a Gaussian signal. The fact that the predicted values of σ_x and $\sigma_{\dot{x}}$ did not err by more than 10% for this case illustrates the point made above that serious violation of assumption 1 or 2 does not necessarily result in a large error in predicted level of response.

Figures 26 and 27 also reveal that for $\alpha = 1/2$ and $\beta_o = 0$ the predicted values of σ_x and $\sigma_{\dot{x}}$ agree with the analog computer results within about 15% when $Ym\omega_o^2/\sqrt{S_o\omega_o}$ is in the range from 0.6 to 10. This range corresponds to σ_x/Y varying from about 20 down to 0.6. The very noticeable error of the prediction for higher yield levels can be attributed to the severe amplitude limiting revealed in Fig. 24 for this system with no viscous damping.

It appears that for systems with $\alpha = 1/2$ the above equivalent
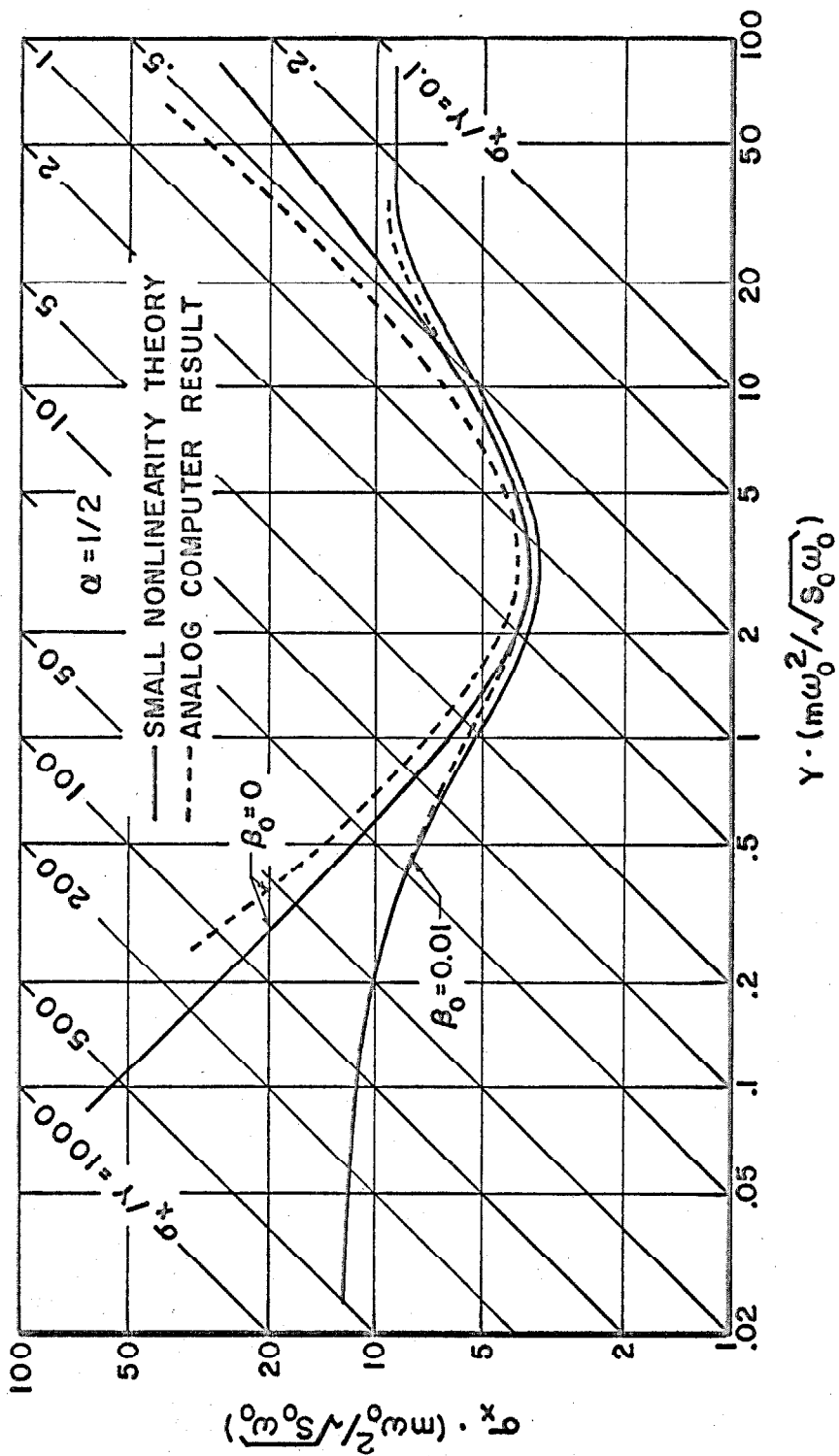
Figure 26. RMS Displacement Response.
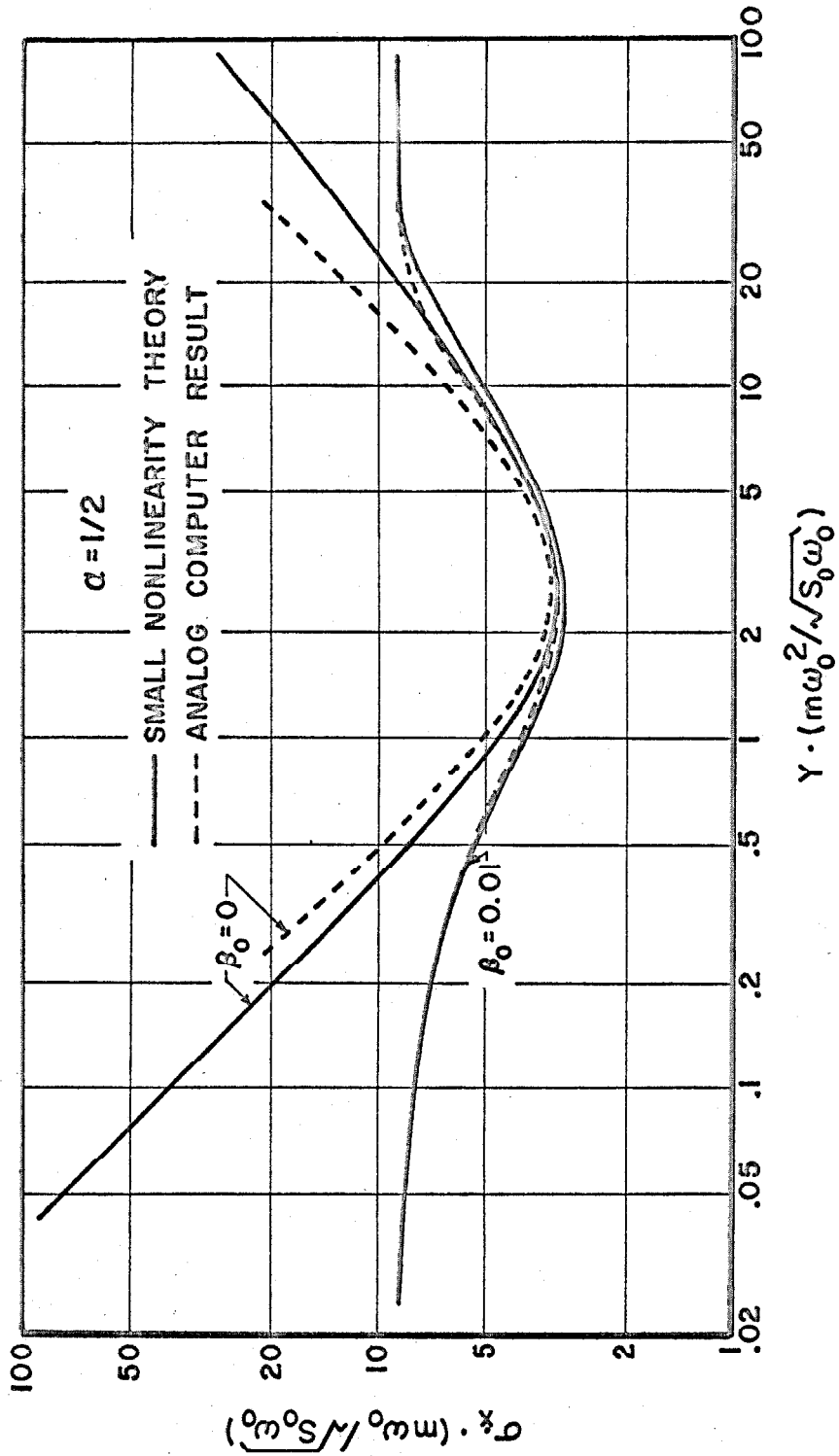
Figure 27. RMS Velocity Response.
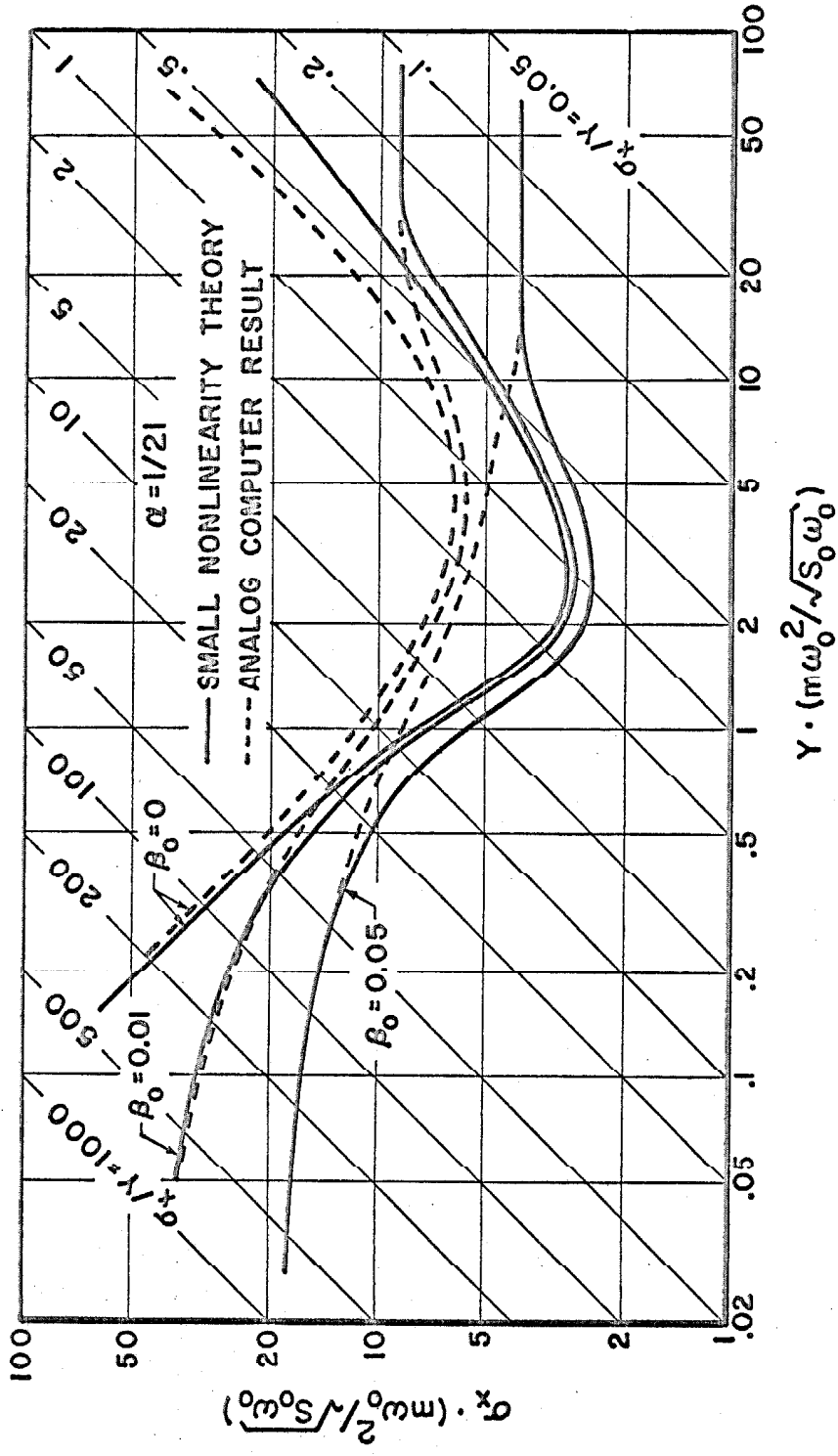
Figure 28. RMS Displacement Response.
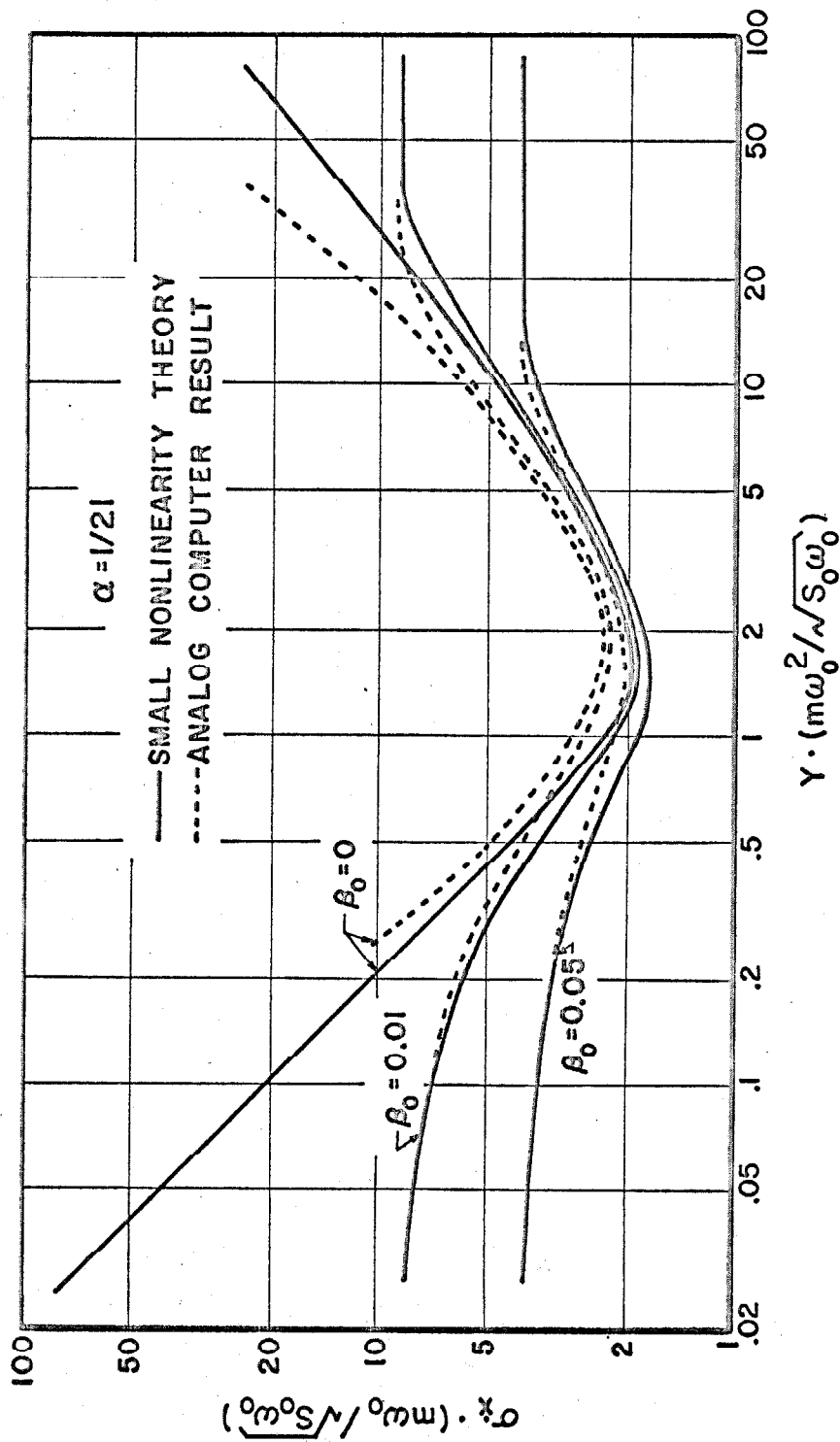
Figure 29. RMS Velocity Response.

linearization technique can be used to predict both displacement and velocity response within about 15% except when β_o is less than 0.01 and the yield level is so low or high that $Ym\omega_o^2 / \sqrt{S_o \omega_o}$ falls outside the range of 0.6 to 10. For physical systems where yielding corresponds to actual ductile yielding of the material or to buckling of some component, values of σ_x/Y as great as 20 could not normally be tolerated without failure. Thus, for such systems the only practical limitation of the region of applicability of the equivalent linearization technique for $\alpha = 1/2$ is that of very small damping and high yield level.

The predicted response based on the assumption of small nonlinearity in the equivalent linearization technique is much less satisfactory for the nearly elasto-plastic system with $\alpha = 1/21$ than for $\alpha = 1/2$. The only instances in which the theory accurately predicts the effect of the nonlinearity on σ_x, as shown in Fig. 28, are when σ_x/Y is greater than about 30. The predicted results also agree with the analog computer results when σ_x/Y is less than 0.3 for the systems having viscous damping, but in this case the nonlinearity has no significant effect on the response.

When the yield level of the system with $\alpha = 1/21$ is such that σ_x/Y is between 1 and 2, the small nonlinearity theory predicts values of σ_x which are only about 50% of the values determined from the analog computer. Note that for $\beta_o = 0.05$ the theory based on small nonlinearity fails to predict even the general character of the effect of yielding on σ_x. In particular, for $\sigma_x/Y = 1$ the small nonlinearity theory predicts a 38% decrease in σ_x as compared to a system with infinite yield level,

whereas the analog computer studies revealed a 22% increase in σ_x due to yielding.

Figure 29 reveals that the small nonlinearity equivalent linearization technique is somewhat more accurate for predicting the velocity response than the displacement response of the nearly elasto-plastic system. For β_o greater than or equal to 0.01 the predicted $\sigma_{\dot{x}}$ is at least 80% of that determined from the analog computer for all yield levels, and for the system with no viscous damping the predicted $\sigma_{\dot{x}}$ is at least 75% of the proper value except for high yield levels $(Ym\omega_o^2 / \sqrt{S_o\omega_o} > 15)$.

For nearly elasto-plastic systems it appears that the equivalent linearization technique based on assumptions of small nonlinearity may be useful for obtaining a rough estimate of the effect of yielding on $\sigma_{\dot{x}}$. However the technique yields useful information about the effect of yielding on σ_x only when σ_x/Y is greater than about 30.

3.3. Linear System Parameters Based on Analog Computer Results

It was mentioned early in this chapter that it is always possible to find a linear system which has the same values of σ_x and $\sigma_{\dot{x}}$ as some particular nonlinear system subjected to the same excitation. This is true even though the response of the linear system may not have a power spectral density or probability distribution which is similar to that of the nonlinear system response. One can find the values of ω_{eq} and β_{eq} for a linear system which has particular values of σ_x and $\sigma_{\dot{x}}$ by using rearranged forms of expressions (3.5) and (3.6); namely

$$\omega_{eq} = \frac{\sigma_{\dot{x}}}{\sigma_x} \qquad (3.27)$$

and

$$\beta_{eq} = \frac{\pi}{4} \frac{S_o(\omega_o)}{(m\omega_o\sigma_{\dot{x}})^2} \frac{\omega_o}{\omega_{eq}} \quad . \qquad (3.28)$$

The fact that the small nonlinearity equivalent linearization technique was considerably more accurate in predicting $\sigma_{\dot{x}}$ than σ_x for the system with $\alpha = 1/21$ suggests that there was considerable error in determining ω_{eq}. In order to show the errors in ω_{eq}/ω_o and β_{eq}, expressions (3.27) and (3.28) have been used with the analog computer results for $\alpha = 1/21$ and $\beta_o = 0$ to find a linear system which is equivalent on the basis of rms response. The results are presented in Figs. 30 and 31 along with the values of ω_{eq}/ω_o and β_{eq} determined from the small nonlinearity equivalent linearization technique. Figure 30 shows the expected discrepancy in ω_{eq}/ω_o. This discrepancy becomes small when σ_x/Y is greater than 30 because then both curves for ω_{eq}/ω_o essentially reach a constant value determined by the second slope of the restoring force curve.

Figure 31 reveals that for σ_x/Y between 5 and 50 the value of β_{eq} determined using assumptions of small nonlinearity agrees well with that determined from the analog computer results. In particular, both the small nonlinearity theory and the analog computer results give a maximum value of β_{eq} of about 0.53 near $\sigma_x/Y = 5.5$. For σ_x/Y less than 5 the two curves for β_{eq} begin to diverge quite rapidly differing by
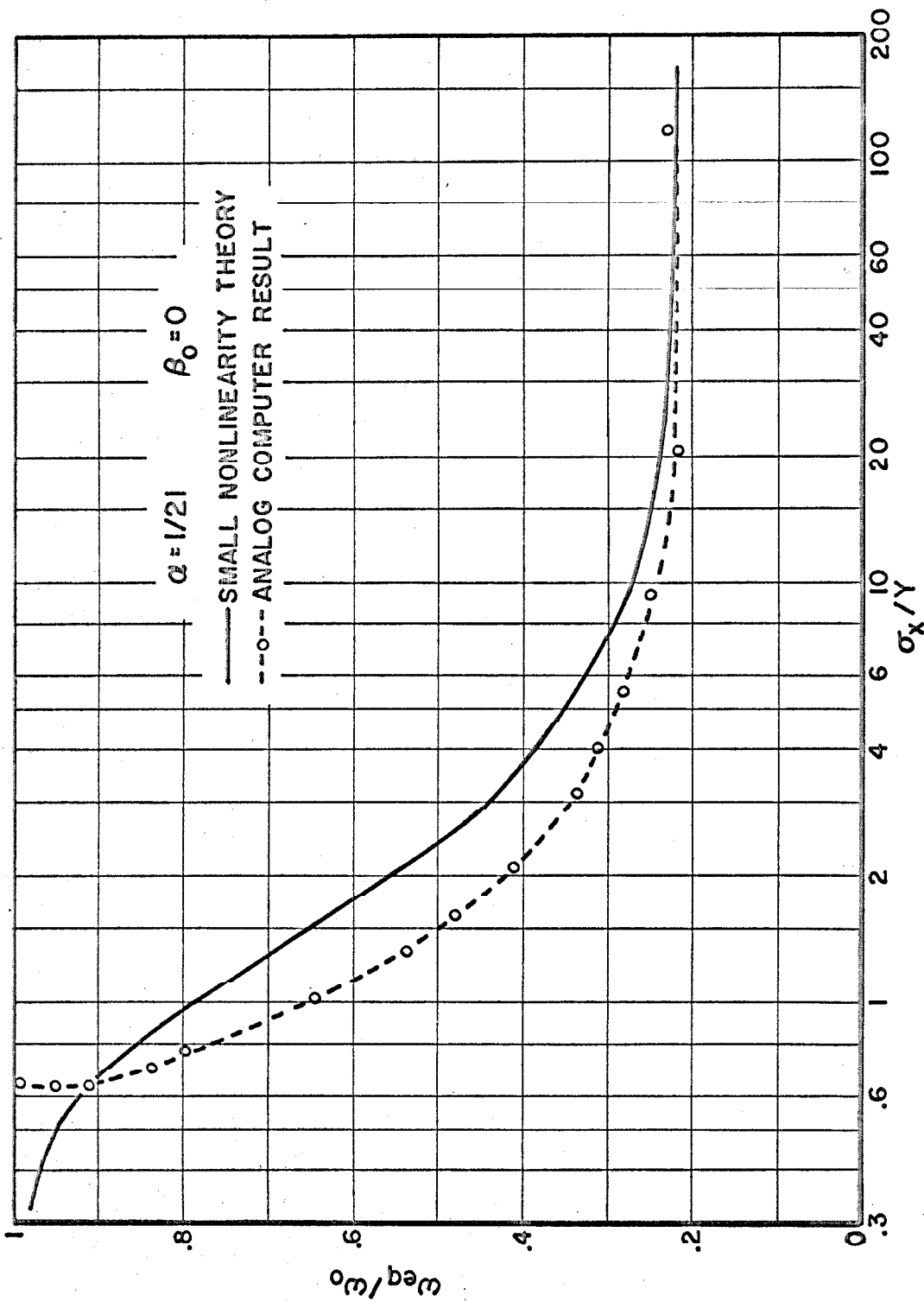
Figure 30. Equivalent Frequeuncy.
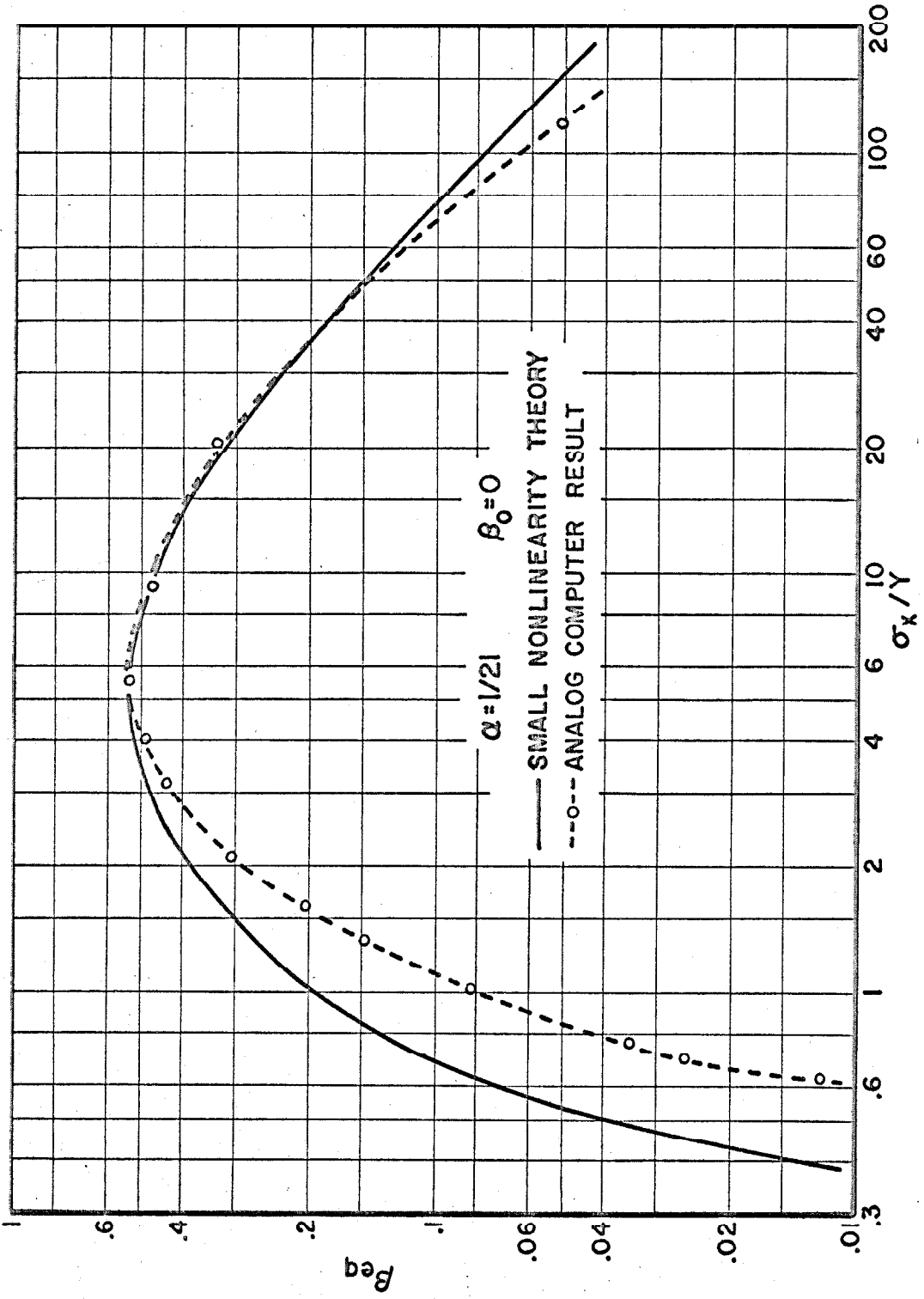
Figure 31. Equivalent Viscous Damping.

about 30% at $\sigma_x / Y - 2$.

It should be emphasized that the linear system derived from expressions (3.27) and (3.28) is known to be equivalent to the non-linear system only on the basis of rms response to an excitation which is nearly white and Gaussian. From the results in the previous chapter it is clear that the power spectral density and probability distribution of the nonlinear system response cannot in general be achieved by any such linear system. Further, the rms response of the "equivalent" linear system may not match that of the nonlinear system for some other excitation.

IV. EQUIVALENT NONLINEAR SYSTEMS

4.1. Use of Fokker-Planck Equation

A Markoff random process is one for which the statistics are completely determined by the transitional or conditional probability function for the process. Further, this probability function is the fundamental solution to the Fokker-Planck equation for the system[12]. The response of a single mass oscillator to a stationary, Gaussian, white excitation is a two-dimensional Markoff process. Specifically, if one knows the location of the mass in the two-dimensional displacement-velocity phase space at any one instant, then the transitional probability function gives the probability of the mass being in the neighborhood of any point in the phase space at any future time. Unfortunately, however, no solution of the Fokker-Planck equation for the transitional probability function of a nonlinear second order system has yet been obtained.

It is sometimes possible to find a solution to the Fokker-Planck equation for a probability function which is independent of time and initial conditions, even though the general solution cannot be found. Such a time-independent solution exists only for a random process which is stationary after a long passage of time, and it is actually the ordinary probability density function for the stationary process. The most general class of nonlinear oscillators for which the stationary probability density function has been obtained is that

described by

$$\ddot{x} + f(H)\dot{x} + g(x) = N(t) \tag{4.1}$$

where:

g(x) is an odd function and $xg(x) > 0$ for $x > 0$,

$$G(x) \equiv \int_0^x g(y)\,dy$$

$$H = \frac{1}{2}\dot{x}^2 + G(x)$$

f(H) is a positive function, and

N(t) is a Gaussian, white process with mean zero.

T. K. Caughey has solved the Fokker-Planck equation for this system to give the stationary probability density function as[13]

$$p(x, \dot{x}) = \frac{\exp\left(-\frac{1}{D}F\big(H(x, \dot{x})\big)\right)}{\displaystyle\int_{-\infty}^{\infty}\int_{-\infty}^{\infty}\exp\left(-\frac{1}{D}F\big(H(x, \dot{x})\big)\right)dx\,d\dot{x}} \tag{4.2}$$

where

$$F(H) = \int_0^H f(h)\,dh$$

and the autocorrelation of N(t) is given by $\overline{N(t)\,N(t+t_1)} = 2D\,\delta(t_1)$. Note that the choice of f(H) is somewhat restricted by the condition that the double integral in the denominator of (4.2) must converge. The class of oscillators described by (4.1) includes all the cases for which exact solutions are known.

Obviously hysteretic systems are not included in the class of oscillators described by expression (4.1). However, one possible technique for finding an approximate solution for a hysteretic system

is to seek a nonlinear system which is described by (4. 1) and which approximates, in some way, the hysteretic system. One might expect the results of applying this technique to severely nonlinear systems to be somewhat better than those obtained by the technique of approximating by a linear system as discussed in the previous chapter. This general approximation scheme has previously been used by J. M. J. Pereira[26] to investigate problems of transient response of elastoplastic oscillators.

The response of a lightly damped linear oscillator to white random excitation can be approximated as a harmonic signal with slowly varying amplitude and phase. The basic frequency of the harmonic signal is the resonant frequency of the linear system. The reason for the response being a slowly varying harmonic signal is that the amount of energy contained in the lightly damped system varies slowly as compared to the rate of change of displacement and velocity. The oscillator accomodates this energy by vibrating in what resembles free vibration.

One may expect that the energy contained in a nonlinear oscillator with random excitation will also vary slowly as compared to the rate of change of displacement and velocity, at least when energy dissipation per cycle is small. Further, one can assume that the nonlinear oscillator will accomodate this energy by executing a motion that resembles free vibration. This leads to the assumption that the response of a nonlinear system to random excitation will be approximately a periodic signal with slowly varying amplitude, phase and

frequency. The frequency of each cycle will be a function of the amplitude of that cycle and will be approximately the resonant frequency of the nonlinear system for that amplitude of vibration. The form of the periodic motion will be similar to that of free vibration of the system.

The resonant frequency of a nonlinear system without energy dissipation is simply the frequency of free vibration of a given amplitude. For a nonlinear system with energy dissipation this definition is inadequate since free vibration is characterized by decreasing amplitude and, hence, changing frequency. Several different logical definitions of resonant frequency could be suggested for nonlinear systems with energy dissipation, but all would give very nearly the same result. One simple definition is to say that for a nonlinear system with energy dissipation the resonant frequency is that frequency of steady state periodic excitation which results in the maximum ratio of response to excitation.

The actual choice of a nonhysteretic system to approximate a hysteretic system could be based on any one of several methods of comparison of the two systems. The method chosen here is primarily a physical comparison.

It is postulated that so long as the assumption of slowly varying periodic response is valid two different nonlinear oscillators should have approximately the same statistics of response to random excitation if:

1.   The two oscillators have the same functional

     relationship between resonant frequency and

     amplitude of vibration, and

2.   The two oscillators have equal energy dissipation

     during a cycle of vibration at any amplitude and

     at the resonant frequency corresponding to that

     amplitude.

This assumes that the exciting force will add approximately the same

amount of energy to each of the oscillators as they vibrate with equal

amplitude and frequency.

The following section will be an attempt to find a nonhysteretic

system which can be described by equation (4.1) and which is similar

to a bilinear hysteretic system in the two ways listed above.

4.2.   Approximation of the Bilinear Hysteretic System by a

Nonhysteretic System

Consider the free vibration of a nonlinear nonhysteretic system

governed by

$$\ddot{x} + \omega_o^2 \varphi(x) = 0 .$$ (4.3)

The periodic vibration can be written as a Fourier series:

$$x = A_1 \cos \omega t + \sum_{j=2}^{\infty} (A_j \cos j\omega t + B_j \sin j\omega t) .$$ (4.4)

No term $\sin \omega t$ is included since it can be eliminated by proper choice

of the time origin.   Assume that the harmonics contribute relatively

little to x so that the restoring force can be approximated as

$$\varphi(x) \approx \varphi(A_1 \cos \omega t) . \tag{4.5}$$

Define

$$C_j(A) = \frac{1}{\pi} \int_0^{2\pi} \cos(j\psi)\varphi(A \cos \psi)d\psi \tag{4.6}$$

and

$$S_j(A) = \frac{1}{\pi} \int_0^{2\pi} \sin(j\psi)\varphi(A \cos \psi)d\psi . \tag{4.7}$$

Using approximation (4.5) while substituting (4.4) into (4.3) then multiplying by $\cos(j\omega t)$ or $\sin(j\omega t)$ and integrating over a complete cycle gives

$$-j^2\omega^2 A_j + \omega_o^2 C_j(A_1) = 0 \qquad \text{where } j = 1, 2, \ldots \tag{4.8}$$

and

$$-j^2\omega^2 B_j + \omega_o^2 S_j(A_1) = 0 \qquad \text{where } j = 2, 3, \ldots \tag{4.9}$$

If $\varphi(x)$ is an odd function then symmetry leads to the following simplifications:

$$S_j(A_1) = 0 \qquad \text{for all } j$$

$$C_j(A_1) = 0 \qquad \text{for all even } j.$$

Thus (4.8) and (4.9) show that

$$B_j = 0 \qquad \text{for all } j$$

$$A_j = 0 \qquad \text{for all even } j. \tag{4.10}$$

Rearranging (4.8) gives

$$\frac{\omega^2}{\omega_o^2} = \frac{C_1(A_1)}{A_1}$$

(4.11)

and

$$A_j = \frac{\omega_o^2}{\omega^2} \frac{1}{j^2} C_j(A_1)$$

or

$$\frac{A_j}{A_1} = \frac{1}{j^2} \frac{C_j(A_1)}{C_1(A_1)} \qquad \text{for } j = 3, 5, \ldots \ . \qquad (4.12)$$

Expression (4.12) confirms the assumption that the lowest frequency component contributes most of the displacement. In addition to the $1/j^2$ factor it is normally found that the $C_j(A_1)$ terms decrease as j increases. Expression (4.11) gives a relationship between resonant frequency and amplitude of vibration based on the assumption of the predominance of the lowest frequency component.

Consider now the energy dissipation if a linear dashpot c is added to the system of equation (4.3) and the system is excited such that it executes vibration which is identical to free vibration. The energy dissipation per cycle is

$$E. D. = \int_0^{2\pi/\omega} c\dot{x}^2 dt.$$

Using expression (4.4) for x, with the restrictions of expressions (4.10) gives

$$\text{E. D.} = \pi c \omega \sum_{j=1,3,5}^{\infty} j^2 A_j^2 \ .$$

Substituting for A_j according to (4.12) yields

$$\text{E. D.} = \pi c \omega A_1^2 \sum_{j=1,3,5}^{\infty} \frac{1}{j^2} \left(\frac{C_j(A_1)}{C_1(A_1)} \right)^2 \ . \tag{4.13}$$

Thus the energy dissipated by a linear dashpot is also predominantly determined by the lowest frequency component of x. Note that the maximum velocity is given by

$$\dot{x}_{max} = \omega \sum_{j=1,3,5}^{\infty} (-1)^{\left(\frac{j-1}{2} \right)} j A_j$$

or

$$\dot{x}_{max} = \omega A_1 \sum_{j=1,3,5}^{\infty} (-1)^{\left(\frac{j-1}{2} \right)} \frac{1}{j} \frac{C_j(A_1)}{C_1(A_1)} \ .$$

The contribution of the higher frequency terms to $\dot{x}_{max}$ decreases as $1/j$ and hence is considerably more significant than the contribution to x or to E. D.

One can also write x as in expression (4.4) for the steady-state response of a hysteretic system to periodic excitation, where ω is now the frequency of excitation. Doing this and using the assumption that the displacement is dominated by the component of frequency ω results in response curves of A_1 versus ω which peak at the frequency given by expression (4.11). W. D. Iwan has compared the response curves obtained in this way with those obtained by an exact

numerical solution for the bilinear hysteretic system with harmonic excitation[27]. The results indicate that the location of the resonant frequency given by expression (4.11) is a very good approximation. For the bilinear hysteretic system $C_1(A)$ is given by

$$\frac{C_1(A)/A - \alpha}{1 - \alpha} = \begin{cases} 1 & \text{for } A \leq Y \\ \frac{1}{\pi}\cos^{-1}\left(1 - \frac{2Y}{A}\right) - \frac{2}{\pi}\left(1 - \frac{2Y}{A}\right)\sqrt{\frac{Y}{A}\left(1 - \frac{Y}{A}\right)} \end{cases}$$

$$\text{for } A > Y. \tag{4.14}$$

One possible choice of a nonhysteretic system to approximate the bilinear hysteretic system is a bilinear nonhysteretic system. In fact this appears to be the obvious choice. Using $\varphi(x)$ as

$$\varphi(x) = \begin{cases} x & \text{for } |x| \leq Y \\ Y(1-\alpha) + \alpha x & \text{for } x > Y \\ -Y(1-\alpha) + \alpha x & \text{for } x < -Y \end{cases} \tag{4.15}$$

yields

$$\frac{C_1(A)/A - \alpha}{1 - \alpha} = 1 - \frac{2}{\pi}\cos^{-1}\left(\frac{Y}{A}\right) + \frac{2}{\pi}\frac{Y}{A}\sqrt{1 - \frac{Y^2}{A^2}} \tag{4.16}$$

$$\text{for } A > Y.$$

Figure 32 shows a comparison of the parameter $(C_1(A)/A-\alpha)/(1-\alpha)$ versus A/Y for the bilinear hysteretic and nonhysteretic systems. It is obvious that the two curves diverge as A/Y increases. Since resonant frequency is related to $C_1(A)/A$ by expression (4.11), Fig. 32 indicates that the bilinear hysteretic and bilinear nonhysteretic systems with the same value of α and Y do not have the same functional relationship between resonant frequency and amplitude of vibration.
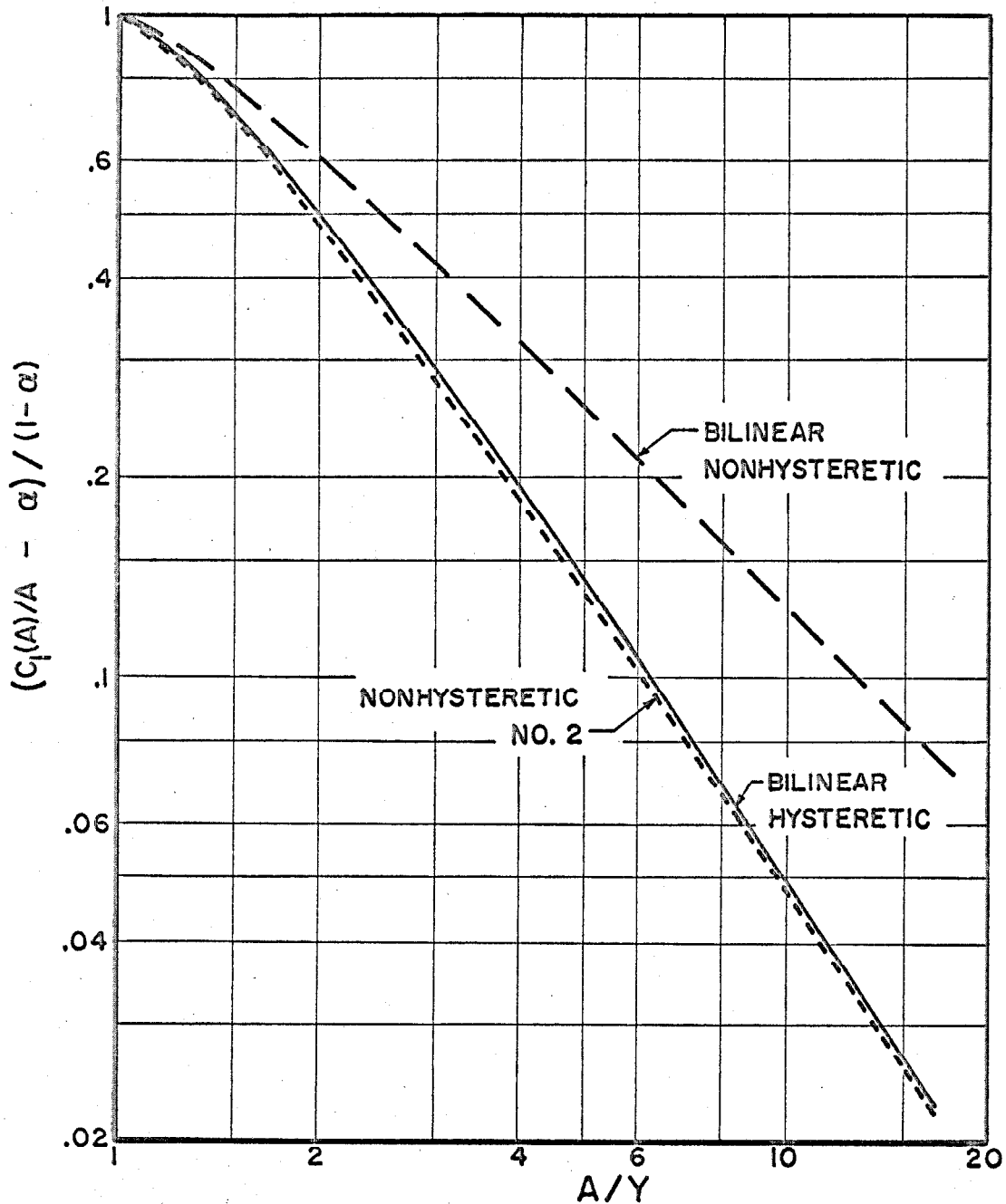
Figure 32.   Resonant Frequency Term.

A different nonhysteretic system has been found to have its resonance frequency much nearer to that of the corresponding bilinear hysteretic system. This system will be referred to as nonhysteretic system No. 2, and it is defined by

$$\varphi(x) = \begin{cases} x & \text{for } |x| \leq Y \\ (1-\alpha) Y^{3/2} x^{-1/2} + \alpha x & \text{for } x > Y \\ -(1-\alpha) Y^{3/2} (-x)^{-1/2} + \alpha x & \text{for } x < -Y. \end{cases} \tag{4.17}$$

For this sytem one finds

$$\frac{C_1(A)/A - \alpha}{1-\alpha} = \begin{cases} 1 & \text{for } A \leq Y \\ 1 - \frac{2}{\pi} \cos^{-1}(Y/A) - \frac{2}{\pi} \frac{Y}{A} \sqrt{1 - Y^2/A^2} \\ \quad + \frac{4}{\pi} \left(\frac{Y}{A}\right)^{3/2} \int_0^{\cos^{-1}(Y/A)} \sqrt{\cos\psi}\, d\psi & \text{for } A > Y. \end{cases} \tag{4.18}$$

Figure 32 shows the numerical values of expression (4.18). It was necessary to numerically integrate the final term of (4.18) to obtain these values. The agreement between $(C_1(A)/A-\alpha)/(1-\alpha)$ for nonhysteretic system No. 2 and a bilinear hysteretic system can be seen to be within about 5% for all levels of A/Y shown in the figure.

It is easily verified that nonhysteretic system No. 2 also matches the bilinear hysteretic system for values of A/Y larger than those shown in Fig. 32. For A/Y >> 1 expression (4.18) can be approximately evaluated without numerical integration since[28]

$$\int_0^{\pi/2} \sqrt{\cos\psi}\, d\psi = \frac{\pi}{2\sqrt{2}} \frac{\Gamma(3/2)}{\Gamma(5/4)\Gamma(5/4)} .$$

Evaluation of the gamma functions[29] gives

$$\int_0^{\pi/2} \sqrt{\cos \psi'} \, d\psi = 1.198 \ .$$

Using this information one finds that expression (4.18) gives

$$\frac{C_1(A)/A - \alpha}{1 - \alpha} \approx \frac{4.792}{\pi} (Y/A)^{3/2} \qquad \text{for } A/Y \gg 1 \qquad (4.19)$$

for nonhysteretic system No. 2. Similarly taking the limiting conditions of expression (4.14) gives

$$\frac{C_1(A)/A - \alpha}{1 - \alpha} \approx \frac{5}{\pi} (Y/A)^{3/2} \qquad \text{for } A/Y \gg 1 \qquad (4.20)$$

for a bilinear hysteretic system.

The close comparison between expressions (4.19) and (4.20) along with the results shown in Fig. 32 confirm that nonhysteretic system No. 2 and a bilinear hysteretic system with the same values of α and Y have nearly the same functional relationship between resonant frequency and amplitude of vibration for all amplitudes. It thus appears that $\omega_0^2 \varphi(x)$ as given in expression (4.17) will be a reasonable choice for $g(x)$ in approximating the bilinear hysteretic system by expression (4.1).

Using

$$g(x) = \omega_0^2 \varphi(x)$$

for nonhysteretic system No. 2 gives

$$G(x) = \begin{cases} \omega_o^2 x^2/2 & \text{for } |x| \le Y \\ \\ -\dfrac{3\omega_o^2}{2}(1-\alpha)Y^2 + 2\omega_o^2(1-\alpha)Y^{3/2}x^{1/2} \\ \\ \qquad + \alpha\omega_o^2 x^2/2 & \text{for } x > Y. \end{cases} \qquad (4.21)$$

The next problem in using expression (4.1) to approximate a bilinear hysteretic system is that of choosing an appropriate damping function f(H). As stated above one seeks a damping function for the nonhysteretic system which results in energy dissipation equal to that of the bilinear hysteretic system for a cycle of vibration at any amplitude and at the resonant frequency corresponding to that amplitude.

As previously explained the idea of the response of a nonlinear system with random excitation being a slowly varying periodic function is based on the expectation that the energy contained within the system will vary slowly. Thus the energy for a cycle of amplitude A can be written as

$$H = G(A) . \qquad (4.22)$$

The damping function f(H) is, hence, only a function of the amplitude of vibration.

The energy dissipated per cycle of amplitude A(A > Y) by the bilinear system without viscous damping is

$$\text{E. D.} = 4\omega_o^2(1-\alpha)Y(A-Y) .$$

Neglecting the higher harmonic contribution to x and E. D. expression (4.13) results in

$$\text{E. D.} - 4\omega_o{}^2(1-\alpha)Y(A-Y)+\pi c_o\omega A^2 \qquad (4.23)$$

if a dashpot c_o is added to the bilinear hysteretic system.

For the nonhysteretic system with dashpot $f(H)$ the energy dissipation is approximately

$$\text{E. D.} = \pi f(H)\omega A^2 \qquad (4.24)$$

where the higher frequency contributions to x and E. D. have again been neglected. Equating (4.23) and (4.24) and solving for $f(H)$ gives

$$f(H) = c_o + \frac{4}{\pi}\frac{\omega_o{}^2}{\omega}(1-\alpha)\frac{Y}{A(H)}\left(1-\frac{Y}{A(H)}\right) \qquad (4.25)$$

where $A(H)$ is the inverse of expression (4.22); that is $H = G(A(H))$. The frequency ω in (4.25) is given by

$$\omega^2 = \omega_o{}^2\frac{C_1(A(H))}{A(H)}$$

where either (4.14) or (4.17) can be used for $C_1(A)/A$. Expression (4.25) can be rearranged to a nondimensional form without explicit dependence on α in the right hand side as

$$\frac{f(H)-c_o}{\omega_o(1-\alpha)} = \frac{4}{\pi}\sqrt{\frac{A(H)}{C_1(A(H))}}\ \frac{Y}{A(H)}\left(1-\frac{Y}{A(H)}\right). \qquad (4.26)$$

The right hand side of this expression still involves α since the relationships between $C_1(A)/A$ and A and between A and H both depend on α. Unfortunately the complicated nature of the expressions involved does not allow a general analytical solution for $f(H)$ as a function of H.

Expressions (4.14), (4.21), (4.22) and (4.26) have been used to obtain numerical values for the damping function as a function of H

for a few values of α. These results are presented in Fig. 33 where

the damping function in the form of (4.26) is plotted versus H nor-

malized by the lowest value of H at which yielding occurs (i.e. $\omega_o^2 Y^2/2$).

Curves are plotted for $\alpha = 1/2$ and $\alpha = 1/21$, the systems which have

been given particular emphasis in this study, and also for the two

limiting cases of $\alpha - 0$ and $\alpha - 1$. As mentioned in a prior chapter the

system with $\alpha = 0$ is not acceptable for the investigation of stationary

response since when this system is subjected to random excitation the

response wanders endlessly rather than achieving a stationary state.

The system with $\alpha = 1$ is also trivial for this study since it is a linear

system with $f(H) \equiv c_o$.

The curve in Fig. 33 for $\alpha = 1$, in addition to being a limiting

case of the systems under consideration, is interesting inasmuch as

it is possible to write $f(H)$ as a fairly simple analytical function of H

in this instance. For $\alpha = 1$ expression (4.14) gives

$$\frac{C_1(A)}{A} = 1$$

and expressions (4.21) and (4.22) give

$$A(H) = \sqrt{2H/\omega_o^2}.$$

Use of these expressions in (4.26) gives

$$\frac{f(H)-c_o}{\omega_o(1-\alpha)} = \frac{4}{\pi}\left(\frac{2H}{\omega_o^2 Y^2}\right)^{-1/2}\left[1-\left(\frac{2H}{\omega_o^2 Y^2}\right)^{-1/2}\right] \quad \text{for } \alpha = 1. \qquad (4.27)$$

For all values of α except $\alpha = 0$ the curves of $(f(H)-c_o)/\omega_o(1-\alpha)$
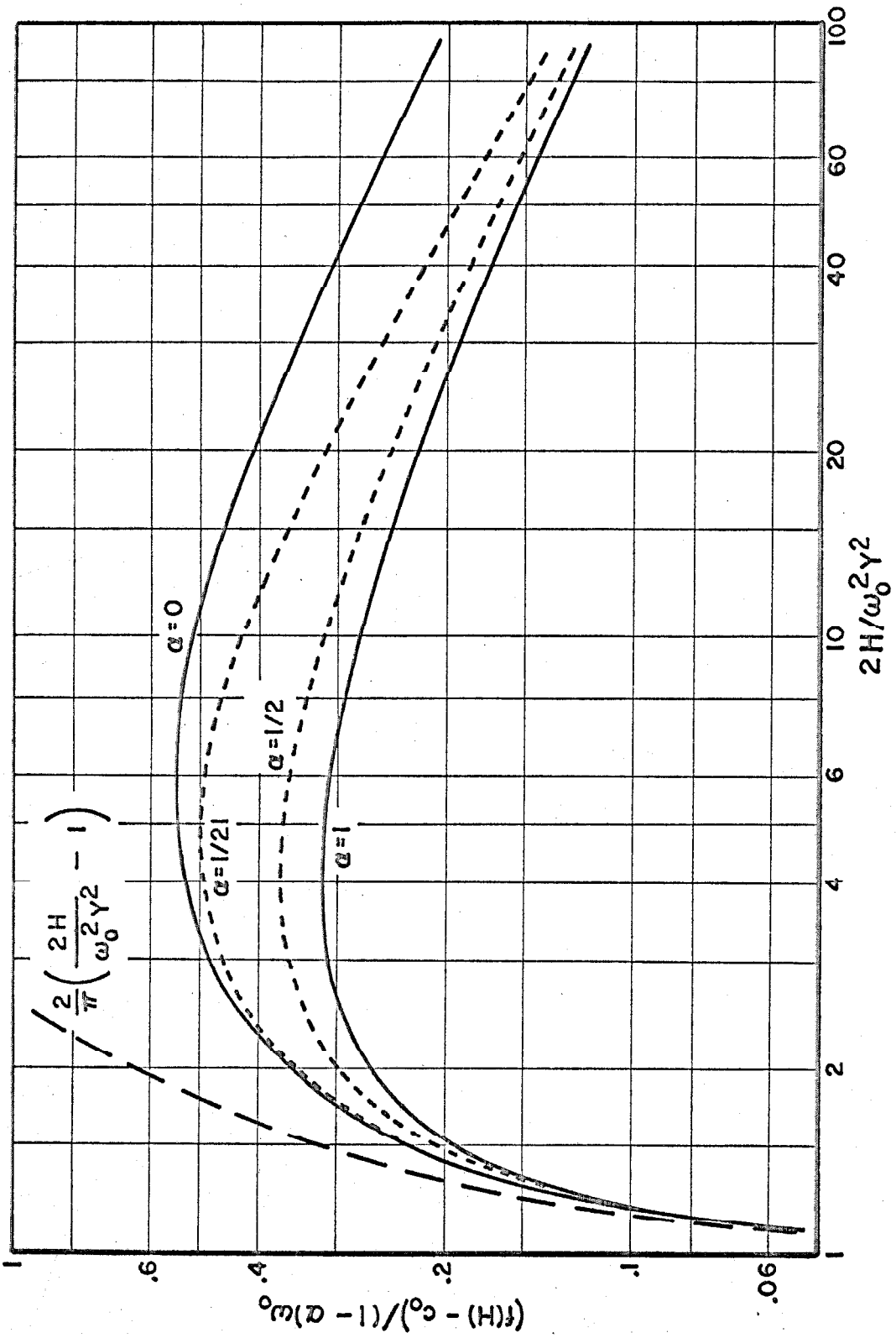
Figure 33. Damping Coefficient Term.

tend to a single asymptote for large H. This follows from the fact
that for $A/Y \gg 1$

$$C_1(A)/A \approx 2H/\omega_o^2 Y^2 \approx \alpha.$$

Expression (4.26) then gives this asymptote as

$$\frac{f(II) - c_o}{\omega_o(1-\alpha)} = \frac{4}{\pi}\left(\frac{2H}{\omega_o^2 Y^2}\right)^{-1/2} \quad \text{for } H \gg \omega_o^2 Y^2/2 \text{ and } \alpha \neq 0.$$

When $\alpha = 0$ the expression $C_1(A)/A$ and $2H/\omega_o^2 A^2$ do not become equal
for large A/Y; hence the asymptote is different for this case.

In order to determine the probability density function $p(x, \dot{x})$ as
given in expression (4.2) for a particular problem one needs to know
the function

$$F(H) = \int_0^H f(h)dh.$$

An approximate expression for this function can be obtained by approx-
imating $f(h)$ as given in Fig. 33 by an analytic or piecewise analytic
function.

Certain predictions about the general tendencies of the proba-
bility density function can be based on the form of expression (4.2) and
the shape of the curves in Fig. 33. For $H < \omega_o^2 Y^2/2$ the joint proba-
bility density $p(x, \dot{x})$ will be like that for a linear system, but the sharp
increase in damping for slightly greater values of H will result in
$p(x, \dot{x})$ decreasing more rapidly with increasing H than is true for a
linear system. Thus the damping function introduces an amplitude

limiting effect for x slightly greater than Y. On the other hand for $H > 3\omega_0^2 Y^2$ the damping function decreases with increasing H so in this range $p(x, \dot{x})$ will decrease less rapidly than for a linear system. In particular for systems oscillating with $\sigma_x >> Y$ the principal effect of the damping function will be to increase the probability of large excursions as compared to a linear system. If the system contains considerable linear viscous damping in addition to the damping corresponding to Fig. 33 the effect of the nonlinear damping function on the probability density will obviously be diminished.

The effect of a nonlinear spring is to change the relationship between $p(x, \dot{x})$ and $p(x)$. A given level of the energy H corresponds to larger values of displacement for a system with a softening spring than for a linear system. Thus in the limiting case when the damping function is a constant so that $p(x, \dot{x})$ is the same function of H as for a linear system a softening spring will result in a greater than normal probability of large displacements.

For nonhysteretic system No. 2 with damping as shown in Fig. 33 both the nonlinear damping and nonlinear spring effects will influence the probability density $p(x)$. For large values of σ_x / Y both effects will tend to increase the probability of large displacements. For somewhat smaller values of σ_x / Y the two effects will be opposite so that general predictions about $p(x)$ cannot be made within this domain of moderate values of σ_x / Y. When there is very little viscous damping in the system the increase of damping at initiation of yield is

particularly abrupt, whereas the softening spring effect is somewhat more gradual. Thus for small σ_x/Y and little or no viscous damping one may expect the nonlinear damping effect to predominate over the softening spring effect so that p(x) will have an amplitude limited characteristic.

The analog computer results for the bilinear hysteretic system as presented in Figs. 22-24 of Chapter II have the characteristics predicted above for nonhysteretic system No. 2 with damping as shown in Fig. 33. For small excitation p(x) clearly reveals amplitude limiting, while for large excitation the oppostie characteristic is dominant.

4. 3. System with Small Excitation

For a system with sufficiently small excitation the response will spend very little time at large values and the amount of damping in the system for large values of the energy H will have little effect on the response. For such cases one needs to closely approximate the damping function f(H) only for relatively small values of H. The simplest approximation for f(H) to fit nonhysteretic system No. 2 for H only slightly greater than $\omega_o^2 Y^2/2$ is

$$f(H) = \begin{cases} c_o & \text{for } H \leq \omega_o^2 Y^2/2 \\ \\ c_o + \omega_o(1-\alpha)\dfrac{2}{\pi}\left(\dfrac{2H}{\omega_o^2 Y^2} - 1\right) & \text{for } H > \omega_o^2 Y^2/2 \ . \end{cases} \qquad (4.28)$$

This function is shown in Fig. 33. For all values of α the function f(H) for nonhysteretic system No. 2 tends to (4.28) as H tends to $\omega_o^2 Y^2/2$.

Using (4.28) gives the function $F(H)$ as

$$F(H) = \begin{cases} c_o H & \text{for } H \leq \omega_o^2 Y^2/2 \\ \frac{2}{\pi} \frac{1-\alpha}{\omega_o^2 Y^2} H^2 + \left[c_o - \frac{2}{\pi} \omega_o (1-\alpha) \right] H + \frac{1-\alpha}{2\pi} \omega_o^3 Y^2 \\ \qquad\qquad\qquad\qquad\qquad\qquad \text{for } H > \omega_o^2 Y^2/2. \end{cases}$$
(4.29)

Substitution into expression (4.2) gives the probability density as

$$p(x, \dot{x}) = \begin{cases} \frac{1}{K_4} \exp\left(-\frac{c_o}{D} H(x, \dot{x}) \right) & \text{for } H \leq \omega_o^2 Y^2/2 \\ \frac{1}{K_4} \exp\left[-\frac{K_3}{D} \left(H^2(x, \dot{x}) + K_2 H(x, \dot{x}) + K_1 \right) \right] \\ \qquad\qquad\qquad\qquad\qquad\qquad \text{for } H > \omega_o^2 Y^2/2 \end{cases}$$
(4.30)

where

$$\left. \begin{aligned} K_1 &= \frac{\omega_o^4 Y^4}{4} \\[2ex] K_2 &= \frac{\pi}{2} \frac{\omega_o^2 Y^2}{1-\alpha} c_o - \omega_o^2 Y^2 \\[2ex] K_3 &= \frac{2}{\pi} \frac{1-\alpha}{\omega_o^2 Y^2} \\[2ex] K_4 &= \int_{-\infty}^{\infty} \int_{-\infty}^{\infty} \exp\left(-F(H)/D \right) dx d\dot{x} \, . \end{aligned} \right\}$$
(4.31)

Substituting $H = \dot{x}^2/2 + G(x)$ gives

$$p(x, \dot{x}) = \begin{cases} \dfrac{1}{K_4} \exp\left[-\dfrac{c_o}{D}\left(\dfrac{\dot{x}^2}{2}+G(x)\right)\right] & \text{for } \dot{x}^2/2 + G(x) \le \omega_o^2 Y^2/2 \\[4mm] \dfrac{1}{K_4} \exp\left\{-\dfrac{K_3}{D}\left[\dfrac{\dot{x}^4}{4}+\left(G(x)+\dfrac{K_2}{2}\right)\dot{x}^2+G^2(x)+K_2 G(x)+K_1\right]\right\} \\[4mm] & \text{for } \dot{x}^2/2 + G(x) > \omega_o^2 Y^2/2 \,. \end{cases}$$

(4. 32)

The one-dimensional probability density function p(x) is simply an integral of (4. 32):

$$p(x) = \int_{-\infty}^{\infty} p(x, \dot{x}) d\dot{x} \,.$$

An analytic expression for this integral of (4. 32) is not readily obtainable. However, one could obtain values of p(x) by numerical integration of (4. 32).

It is possible to approximate the mean squared levels of response for this system with small excitation without resorting to numerical integration. To do so consider a new variable u defined by

$$u = \sqrt{2H/\omega_o^2} \,.$$

(4. 33)

Since $H = \omega^2 A^2/2$ for vibration of frequency ω and amplitude A it is obvious that u is like the amplitude of vibration.

The probability that u is less than some particular value u_1 is given by

$$\text{Prob. } (u < u_1) = \text{Prob.}\left(\frac{\dot{x}^2}{\omega_o^2}+\frac{2G(x)}{\omega_o^2} < u_1^2\right) \,.$$

Since symmetry requires that $p(x, \dot{x})$ be an even function of both x and $\dot{x}$ one can write

$$\text{Prob.}(u < u_1) = 4 \int_0^{W(u_1)} dx \int_0^{\sqrt{\omega_o^2 u_1^2 - 2G(x)}} p(x, \dot{x}) \, d\dot{x}$$

where $W(u_1)$ is defined by

$$G\Big(W(u_1)\Big) = H(u_1) = \frac{\omega_o^2 u_1^2}{2} \, . \tag{4.34}$$

Then the probability density of u is given by

$$p(u_1) = \frac{\partial}{\partial u_1} \text{Prob}(u < u_1)$$

or

$$p(u) = 4\frac{dW}{dx} \int_0^{W(u)} \frac{\omega_o^2 u \, p\Big(x, \sqrt{\omega_o^2 u^2 - 2G(x)}\Big)}{\sqrt{\omega_o^2 u^2 - 2G(x)}} \, dx \ \ .$$

The term $p\Big(x, \sqrt{\omega_o^2 u^2 - 2G(x)}\Big)$ actually depends only on u, not on x. This term is in fact given by expression (4.30) with

$$H = \frac{\omega_o^2 u^2}{2} \, .$$

Thus

$$p(u) = 4\omega_o^2 u \, p\Big(x, \sqrt{\omega_o^2 u^2 - 2G(x)}\Big) \frac{dW}{du} \int_0^{W(u)} \frac{dx}{\sqrt{\omega_o^2 u^2 - 2G(x)}} \, . \tag{4.35}$$

Recall that the approximation for the damping was based on the assumption that H does not much exceed $\omega_o^2 Y^2 / 2$. For this case it is possible to further approximate that

$$G(x) = \frac{\omega_o^2 x^2}{2} \quad . \tag{4.36}$$

This assumption with (4.34) gives

$$W(u) = u \; .$$

Note that u is now exactly the amplitude of vibration. Expression (4.35) then gives

$$p(u) = 2\pi\omega_o \, u \, p\left(x, \sqrt{\omega_o^2 u^2 - 2G(x)}\right)$$

or

$$p(u) = \begin{cases} \dfrac{2\pi\omega_o}{K_4} \, u \exp\left[-\dfrac{c_o}{D} \dfrac{\omega_o^2 u^2}{2}\right] & \text{for } u \leq Y \\[4mm] \dfrac{2\pi\omega_o}{K_4} \exp\left[-\dfrac{K_3}{D}\left(K_1 - \dfrac{K_2^2}{4}\right)\right] u \exp\left[-\dfrac{K_3}{D}\left(\dfrac{\omega_o^2 u^2}{2} + \dfrac{K_2}{2}\right)^2\right] & \\ & \text{for } u > Y \; . \end{cases} \tag{4.37}$$

The normalizing constant K_4 can be evaluated from the expression

$$\int_o^\infty p(u)du = 1 \; .$$

Doing this yields

$$\frac{K_4}{2\pi\omega_o} = \frac{D}{c_o\omega_o^2}\left(1 - e^{-r_1}\right) + \exp\left[-\frac{K_3}{D}\left(K_1 - \frac{K_2^2}{4}\right)\right]\frac{1}{\omega_o^2}\sqrt{\frac{D}{K_3}} \, \frac{\sqrt{\pi}}{2} \, \text{erfc}(r_2) \tag{4.38}$$

where

$$r_1 = \frac{c_o}{D} \frac{\omega_o^2 Y^2}{2}$$

$$r_2 = \sqrt{\frac{K_3}{D} \left(\frac{\omega_o^2 Y^2}{2} + \frac{K_2}{2} \right)} \quad . \tag{4.39}$$

In a similar manner the mean squared value of u can be obtained. It is given by

$$\sigma_u^2 = \int_o^\infty u^2 p(u) du \quad . \tag{4.40}$$

Substitution and integration gives

$$\sigma_u^2 = \frac{2\pi\omega_o}{K_4} \left(\frac{2D}{c_o \omega_o^2} \right)^2 \frac{1}{2} \left[1 + (1 + r_1) e^{-r_1} \right]$$

$$+ \frac{2\pi\omega_o}{K_4} \exp \left[-\frac{K_3}{D} \left(K_1 - \frac{K_2^2}{4} \right) \right] \frac{2}{\omega_o^4} \sqrt{\frac{D}{K_3}} \left[\sqrt{\frac{D}{K_3}} \frac{e^{-r_2^2}}{2} - \frac{K_2}{2} \frac{\sqrt{\pi}}{2} \mathrm{erfc}(r_2) \right] \tag{4.41}$$

where r_1 and r_2 are as given in (4.39).

Assumption (4.36) gives

$$H = \frac{\omega_o^2 u^2}{2} = \frac{\dot{x}^2}{2} + \frac{\omega_o^2 x^2}{2} \quad .$$

Since the mean value of $x\dot{x}$ is zero for a stationary differentiable signal this expression yields

$$\sigma_u^2 = \frac{\sigma_{\dot{x}}^2}{\omega_o^2} + \sigma_x^2 \quad .$$

Further, since $p(x, \dot{x})$ depends only on H, and H depends on x and $\dot{x}/\omega_o$ in an identical manner one can conclude that

$$\sigma_x^2 = \sigma_{\dot{x}}^2 / \omega_o^2 .$$

These two expressions require that

$$\sigma_x^2 = \sigma_{\dot{x}}^2 / \omega_o^2 = \sigma_u^2 / 2 . \qquad (4.42)$$

Some of the above expressions are somewhat simpler in the special case with $c_o = 0$. In this instance one obtains the following:

$$p(x, \dot{x}) = \begin{cases} \dfrac{1}{K_4} & \text{for } H \leq \omega_o^2 Y^2 / 2 \\[4mm] \dfrac{1}{K_4} \exp\left[-\dfrac{K_3}{D}\left(H(x, \dot{x}) - \dfrac{\omega_o^2 Y^2}{2} \right)^2 \right] & \text{for } H > \omega_o^2 Y^2 / 2 \end{cases} \qquad (4.43)$$

$$p(u) = \begin{cases} \dfrac{2\pi\omega_o}{K_4} u & \text{for } u \leq Y \\[4mm] \dfrac{2\pi\omega_o}{K_4} u \exp\left[-\dfrac{K_3}{D}\left(\dfrac{\omega_o^2 u^2}{2} - \dfrac{\omega_o^2 Y^2}{2} \right)^2 \right] & \text{for } u > Y \end{cases} \qquad (4.44)$$

$$\frac{K_4}{2\pi\omega_o} = \frac{Y^2}{2} + \frac{1}{\omega_o^2} \sqrt{\frac{D}{K_3}} \cdot \frac{\sqrt{\pi}}{2} \qquad (4.45)$$

and

$$\sigma_u^2 = \frac{2\pi\omega_o}{K_4}\left(\frac{Y^4}{4} + \frac{1}{\omega_o^2} \sqrt{\frac{D}{K_3}} \frac{\sqrt{\pi}}{2} Y^2 + \frac{1}{\omega_o^4} \frac{D}{K_3} \right) . \qquad (4.46)$$

Consider now how this relates to the analog computer results of Chapter II. The definition of D was

$$\overline{N(t)N(t+t_1)} = 2D \, \delta(t_1) .$$

This corresponds to the power spectral density of N(t) being

$$S_n(\omega) = \frac{D}{\pi} \qquad \text{for } -\infty < \omega < \infty$$

or the equivalent situation where

$$S_N(\omega) = \begin{cases} 0 & \text{for } \omega < 0 \\[2ex] \dfrac{2D}{\pi} & \text{for } \omega \geq 0 \ . \end{cases}$$

The white excitation for equation (2.1) was $n(t)/m$ where (see (2.6))

$$S_n(\omega) = \begin{cases} 0 & \text{for } \omega < 0 \\[2ex] S_o & \text{for } \omega \geq 0 \ . \end{cases}$$

Using this excitation for the N(t) of expression (4.1) gives

$$D = \frac{\pi}{2} \frac{S_o}{m^2} \ . \tag{4.47}$$

The constant by which Y and σ_x were normalized in Figs. 9 and 11 is

$$\frac{\sqrt{S_o \omega_o}}{m \omega_o^2} = \sqrt{\frac{2}{\pi} \frac{D}{\omega_o^3}} \ .$$

Further recall that the dashpot coefficient in Chapter II was given by $2\beta_o \omega_o$. Thus

$$c_o = 2\beta_o \omega_o \ . \tag{4.48}$$

Substituting for D and K_3 when $c_o = 0$ yields

$$\sigma_u^2 = \frac{Y^2}{2}\left[\frac{1 + \dfrac{\pi^{3/2}}{\sqrt{1-\alpha}}\;\dfrac{\sqrt{S_o\omega_o}}{m\omega_o^2 Y} + \dfrac{\pi^2}{1-\alpha}\;\dfrac{S_o\omega_o}{m^2\omega_o^4 Y^2}}{1 + \dfrac{1}{2}\dfrac{\pi^{3/2}}{\sqrt{1-\alpha}}\;\dfrac{\sqrt{S_o\omega_o}}{m\omega_o^2 Y}}\right] . \qquad (4.49)$$

Figure 34 shows a comparison of σ_x for $\alpha = 1/21$ as determined by expressions (4.42) and (4.49) with the analog computer result previously presented in Fig. 9. When $Ym\omega_o^2/\sqrt{S_o\omega_o}$ is in the neighborhood of 20 to 30 the agreement is within about 7%. However for larger yield levels the ratio σ_x/Y for the analog computer results begins to increase, whereas the ratio determined by expression (4.49) tends uniformly to the value $1/2$.

It was pointed out in Section 2.2 that the increase of σ_x/Y when $Ym\omega_o^2/\sqrt{S_o\omega_o}$ is increased beyond about 30, as is noticeable in both Figs. 9 and 11, must be due to the small amount of negative damping which was present in the analog computer circuit with nominally zero viscous damping. In Appendix A.1 it is noted that the rate of build up of oscillation of the system with no excitation was no greater than that for a system with 0.05% of negative viscous damping. It is possible to use expressions (4.38), (4.41) and (4.42) to predict the response of a system having negative viscous damping. This has been done for $\alpha = 1/21$ and $c_o/\omega_o = -0.001$, which corresponds to $\beta_o = -0.0005$, and the result is presented in Fig. 34. One notes that this prediction agrees with the analog computer result with an accuracy of about 6% for $Ym\omega_o^2/\sqrt{S_o\omega_o} > 20$.
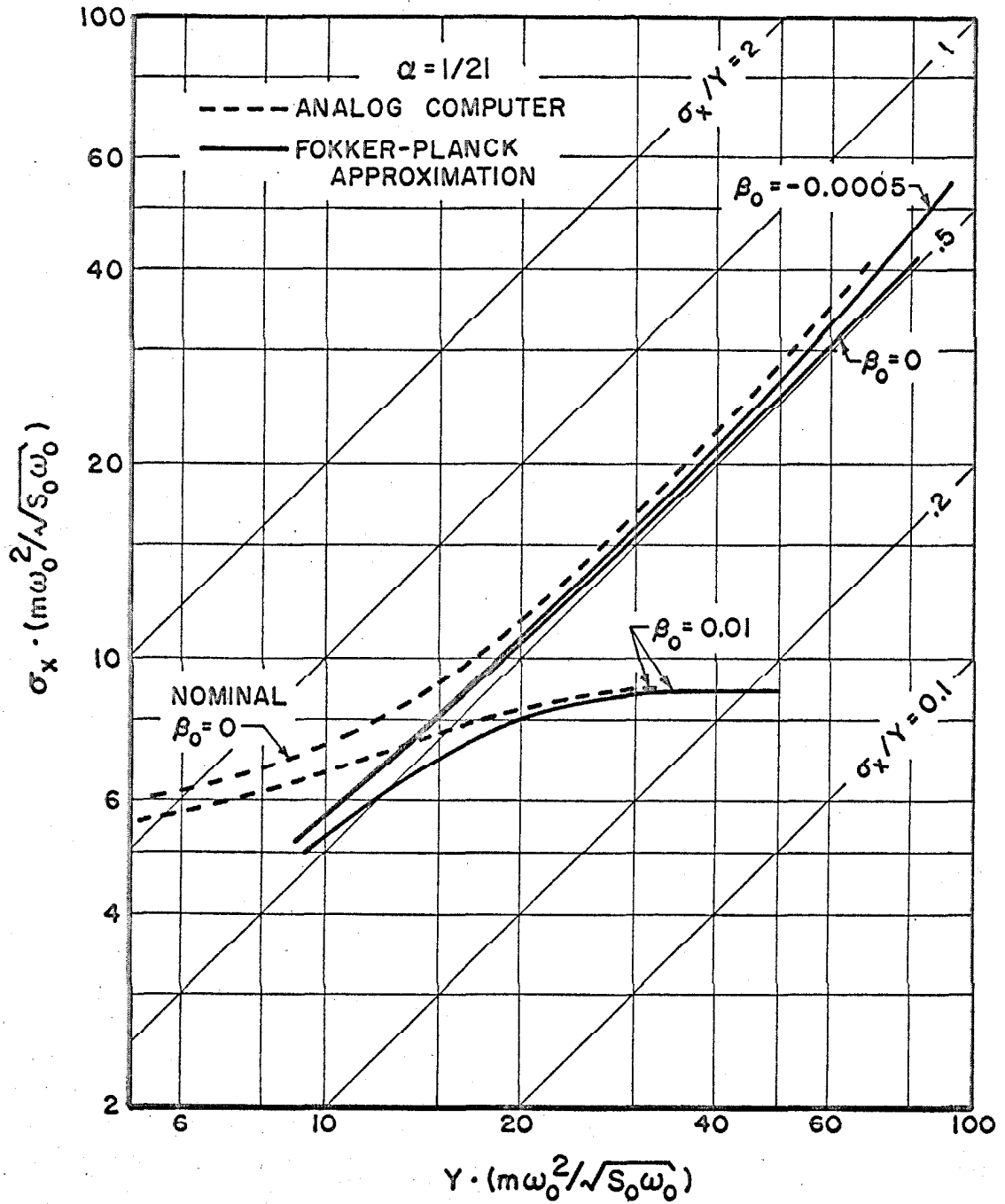
Figure 34. RMS Displacement Response.

Figure 34 also shows a comparison of σ_x as determined by the analog computer for $\beta_o = 0.01$ with the result of expressions (4.38) and (4.41) for that value of damping. Again the results agree within about 5% for $Ym\omega_o^2/\sqrt{S_o\omega_o} > 20$. This result is not particularly valuable, though, since for this damped system with $Ym\omega_o^2/\sqrt{S_o\omega_o} > 20$ the response can be predicted within about 8% by completely neglecting the effect of the nonlinearity and applying expression (2.10).

Figure 35 shows the response predicted by expressions (4.38) and (4.41) for the system with $\alpha = 1/2$ along with the analog computer results previously presented in Fig. 11. When $Ym\omega_o^2/\sqrt{S_o\omega_o} > 10$ the results agree within about 7% for $\beta_o = -0.0005$ and about 5% for $\beta_o = 0.01$. This improved accuracy for somewhat lower yield levels makes this approximate technique more valuable for this system than for the one with $\alpha = 1/21$. Note that for $\alpha = 1/2$ and $\beta_o = 0.01$ this approximate technique predicts σ_x within about 5% even when the effect of yielding is sufficient to reduce σ_x to about 60% of the value for a linear system.

Recall that the two approximations especially made for this case of small excitation (or high yield level) were that the damping function was given by expression (4.28) and that the potential energy was the same as for a linear system with resonance at ω_o (see expression (4.36)). The first of these approximations overestimates the damping and the second one completely neglects the softening spring effect; thus both approximations tend to cause an underestimation of the response. The damping approximation is somewhat more accurate
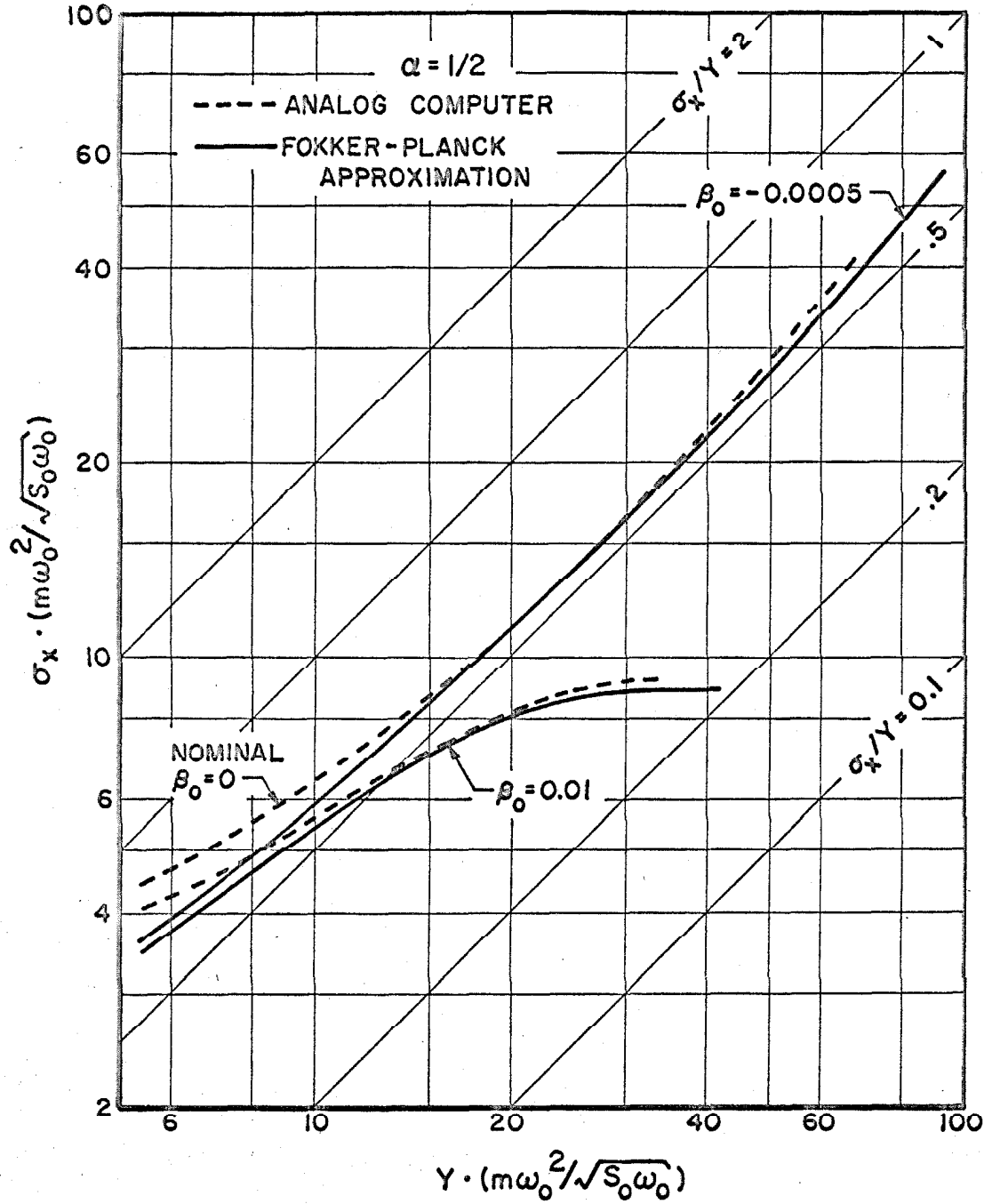
Figure 35.   RMS Displacement Response.

for the system with $\alpha = 1/21$ than for $\alpha = 1/2$, whereas the neglected softening spring effect is greater when $\alpha = 1/21$. Since the predicted responses are noticeably more accurate for the system with $\alpha = 1/2$ than for $\alpha = 1/21$ it can be concluded that the error due to the potential energy approximation is significantly greater than that due to the damping approximation. By replacing expression (4.36) by a more accurate description of the potential energy in nonhysteretic system No. 2 one might extend the range of accurate prediction to a lower value of $Ym\omega_o^2/\sqrt{S_o\omega_o}$, particularly for $\alpha = 1/21$.

4.4 Energy Dissipation Due to Yielding

One measure of the response of a yielding system which has not to this point been considered in the present study is the amount of energy dissipated in yielding. In some instances this quantity may be important since for some materials there is experimental evidence of a correlation between fatigue life and the energy dissipated internally due to yielding[30]. It is possible to use the expressions in the preceding section to obtain an approximate prediction of this quantity for a bilinear hysteretic oscillator with a low level of excitation. D. Karnopp and T. D. Scharton[31] have used a somewhat different approach to this problem and have arrived at an approximate analytical prediction of the energy dissipated due to yielding of an elasto-plastic oscillator. Hence it is of interest to compare the results of the two different approaches.

Since the bilinear hysteretic system with a low level of exci-
tation was approximated in the preceding section by a system with a
linear spring and a nonlinear dashpot it is possible to use expression
(4.24) to determine the total energy dissipated during a cycle of
amplitude u as

$$E. D. = \pi f\left(\omega_o^2 u^2/2\right) \omega_o u^2 .$$

The energy dissipated due to yielding can be considered to be

$$E. D. Y. = \pi\left[f\left(\omega_o^2 u^2/2\right) - c_o\right] \omega_o u^2$$

since c_o represents the viscous damping present in the hysteretic sys-
tem which is being approximated. The mean energy dissipated per
cycle due to yielding can be found from

$$\overline{(E. D. Y.)} = \int_0^\infty (E. D. Y.) \, p(u) du.$$

Using expression (4.28) for the damping function and expression (4.37)
for the probability density of the amplitude, integration yields

$$\overline{(E. D. Y.)} = \frac{8\pi(1-\alpha)}{\omega_o^3 Y^2 K_4} \sqrt{\frac{D}{K_3}} \; \exp\left[-\frac{K_3}{D}\left(K_1 - \frac{K_2^2}{4}\right)\right]$$

$$\cdot \left[\left(r_2 \sqrt{\frac{D}{K_3}} - K_2 - \frac{\omega_o^2 Y^2}{2}\right)\sqrt{\frac{D}{K_3}} \; e^{-r_2^2}\right.$$

$$\left. + \left(\frac{D}{K_3} + \frac{K_2^2}{2} + \frac{\omega_o^2 Y^2}{2} K_2\right)\frac{\sqrt{\pi}}{2} \; \text{erfc}(r_2)\right] \qquad (4.50)$$

where r_2 is as given in expression (4.39) and K_4 can be evaluated from (4.38).

For Y much greater than σ_x expression (4.50) can be considerably simplified. In this situation r_2 is large so that $\text{erfc}(r_2)$ can be approximated by an asymptotic expansion. The first two terms of the expansion are [32]

$$\text{erfc}(r_2) = \frac{e^{-r_2^2}}{\sqrt{\pi}\ r_2} \left(1 - 1/2r_2^2\right).$$

Using this two term approximation for $\text{erfc}(r_2)$ and substituting for the various constants in expression (4.50) yields

$$\overline{(\text{E.D.Y.})} \approx 4(1-\alpha)\omega_o^2 \sigma_x^2 \exp\left(-Y^2/2\sigma_x^2\right) \qquad \text{for } Y >> \sigma_x. \qquad (4.51)$$

This expression was put in terms of σ_x by noting that

$$\sigma_x^2 \approx \frac{\pi S_o}{4\beta_o \omega_o^3 m^2} \qquad \text{for } Y >> \sigma_x.$$

Karnopp and Scharton's analysis is based on the assumption that the statistics of the response of an elasto-plastic oscillator can be approximated by those for a linear oscillator with "infinitely rigid, perfectly inelastic barriers" at $x = \pm Y$. The amount of energy dissipated due to yielding of the elasto-plastic system is assumed to be the same as that dissipated by the inelastic barriers in the linear system. The amount of energy dissipated during a single impact with one of the barriers in the linear system is the kinetic energy of the system at the time of impact.

Assume that the joint probability density $p(x, \dot{x})$ is known for a linear system with inelastic barriers. Then $p(Y, \dot{x})dxd\dot{x}$ is the probability of being in an incremental square located at $x = Y$. Dividing this probability by the time required to cross the incremental distance dx at the velocity $\dot{x}$ gives the probable rate of crossings of dx with velocity $\dot{x}$ as $\dot{x}p(Y, \dot{x})d\dot{x}$. Note that this probable number of crossings per unit time is independent of dx and thus is exactly the probable rate of impacts with the barrier at $x = Y$ with velocity $\dot{x}$. Integrating over all positive $\dot{x}$ gives the probable frequency of impacting the barrier at x. This result is identical to the probable frequency of crossing the line $x = Y$ with positive $\dot{x}$ as determined by S. O. Rice[33].

Karnopp and Scharton determine the average kinetic energy of the system when it impacts the barrier at $x = Y$ as

$$\int_0^\infty \frac{\dot{x}^2}{2}p(Y, \dot{x})d\dot{x} \bigg/ \int_0^\infty p(Y, \dot{x})d\dot{x} \; .$$

This average kinetic energy at impact is then the average amount of energy dissipated per impact. Karnopp and Scharton multiply this average energy dissipated per impact times the probable frequency of impacting the barrier to estimate the average energy dissipated per unit time due to yielding at $x = Y$. Since $p(-Y, -\dot{x}) = p(Y, \dot{x})$, due to symmetry, an equal amount of energy is dissipated per unit time by the barrier at $x = -Y$.

Rather than multiplying the average energy dissipated per impact times the probable frequency of impacting it is possible to exactly evaluate the probable total amount of energy dissipated by

impacts during a unit time. It was found above that $\dot{x}p(Y,\dot{x})d\dot{x}$ was

the probable number of impacts per unit time with velocity $\dot{x}$. Since

the energy dissipated at each impact is simply the kinetic energy of

the system immediately prior to impact, each of these impacts with

velocity $\dot{x}$ results in an energy dissipation of $\dot{x}^2/2$. Integrating over

all positive $\dot{x}$ gives the probable energy dissipated per unit time due

to impacts on the barrier at $x = Y$. An equal rate of energy dissipation

will be expected at $x = -Y$. Adding these then dividing by the natural

frequency of the system gives the probable energy dissipated per

cycle due to yielding as

$$\overline{(E.\ D.\ Y.)} = \frac{2\pi}{\omega_0} \int_0^\infty \dot{x}^3 p(Y,\dot{x})d\dot{x}. \qquad (4.52)$$

This will be referred to as an improved Karnopp and Scharton approx-

imation since it is based on the same assumptions as their analysis

except that it avoids the assumption that the product of two averages

is equal to the average of the product.

For cases of "infrequent plastic deformations" Karnopp and

Scharton suggest that $p(Y,\dot{x})$ can be approximated from a Gaussian

distribution:

$$p(Y,\dot{x}) = \frac{1}{2\pi\sigma_x\sigma_{\dot{x}}} \exp\left[-\frac{Y^2}{2\sigma_x^2} - \frac{\dot{x}^2}{2\sigma_{\dot{x}}^2} \right]$$

$$\text{for } \dot{x} > 0. \qquad (4.53)$$

No method is given for determining σ_x and $\sigma_{\dot{x}}$ other than to assume

that they are the same as for the linear system with no barriers.

These assumptions appear to be valid when Y is much greater than σ_x.

Substituting expression (4.53) into (4.52) and assuming that $\sigma_{\dot{x}}$ is equal to $\omega_o \sigma_x$ yields

$$\overline{(\text{E. D. Y.})} = 2\omega_o^2 \sigma_x^2 \exp\left(-Y^2/2\sigma_x^2\right). \qquad (4.54)$$

This result is twice as large as that obtained by Karnopp and Scharton.

Figure 36 shows levels of $\overline{(\text{E. D. Y.})}$ normalized by $\omega_o^2 Y^2$ as determined both from expression (4.54) and from expression (4.50) with $\alpha = 0$. Expressions (4.41) and (4.42) have been used to determine the values of σ_x corresponding to expression (4.50) so that Fig. 36 could be plotted as a function of σ_x/Y. The figure reveals that the two approximate analyses give results which are of the same order of magnitude over the range of σ_x/Y values shown. The results of the analysis using the solution of the Fokker-Planck equation reveal considerable dependence on the amount of viscous damping in the system, whereas the Karnopp and Scharton analysis assumes that σ_x/Y is the only parameter affecting $\overline{(\text{E. D. Y.})}$ for systems with "infrequent plastic deformations".

Both expression (4.53) for the probability distribution in the Karnopp and Scharton analysis and expression (4.36) for the potential energy in the analysis using the solution of the Fokker-Planck equation are based on the assumption that the system does not often go far beyond the yield level. It thus seems logical to expect both of the
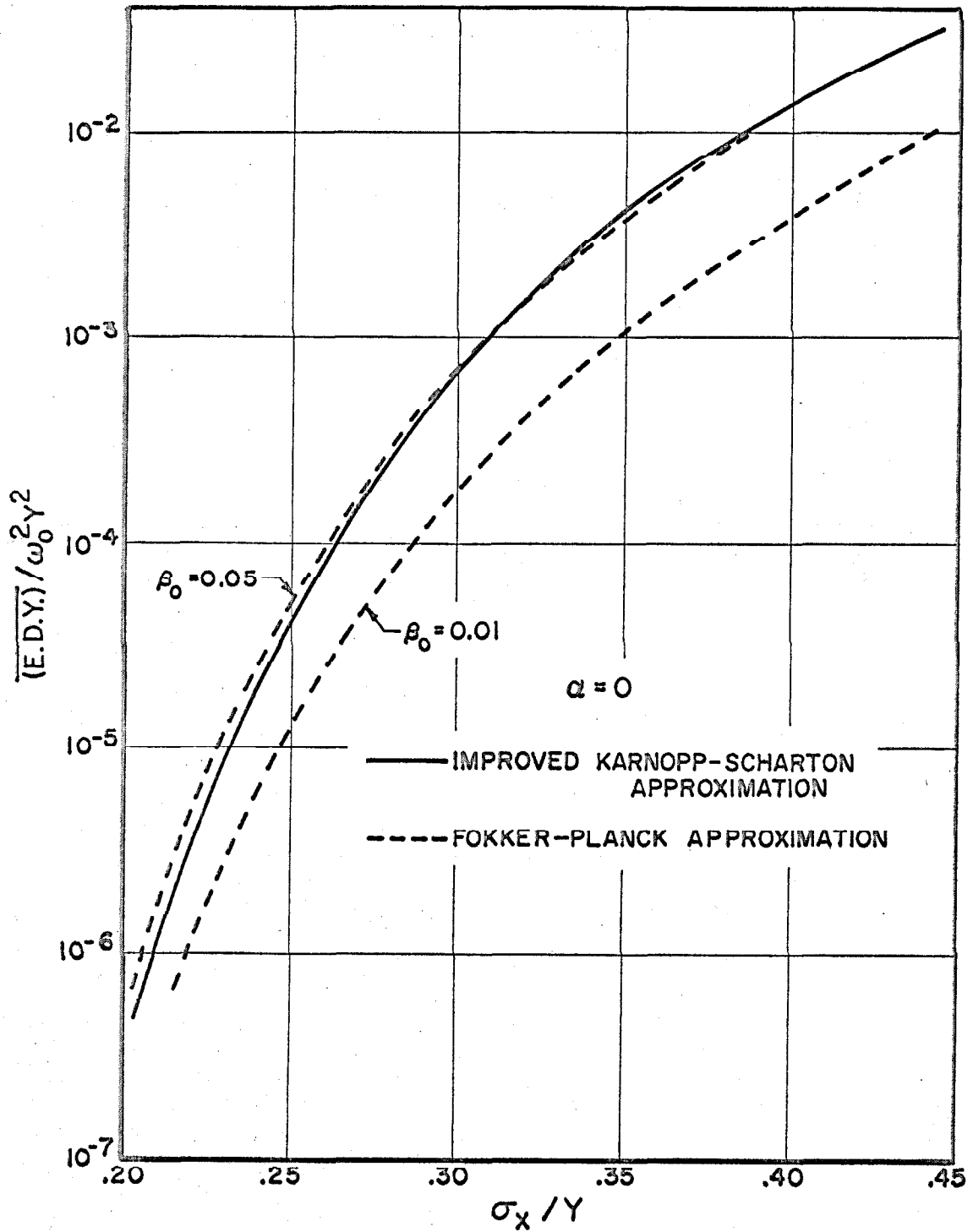
Figure 36. Energy Dissipated Due to Yielding.

approximate analyses to be most accurate when Y is much greater

than σ_x. One notes however that for $Y >> \sigma_x$ expressions (4.51) with

$\alpha = 0$ gives a mean value of E. D. Y. which is twice that given by expres-

sion (4.54) for the improved Karnopp and Scharton approximation.

It appears that the origin of this difference between the two

results can be found by a comparison between the choice of the damp-

ing factor f(H) in Section 4.2 and the determination of the energy

dissipated in the Karnopp and Scharton analysis. The nonhysteretic

system used in Section 4.2 to approximate a bilinear hysteretic sys-

tem always executes vibrations about a fixed center position. The

damping function was chosen to equate the energy dissipated in a cycle

of vibration amplitude u to that which would be dissipated by the

hysteretic system during a complete cycle of amplitude u about a

fixed center position; that is, an amount corresponding to yielding

equally in the positive and negative directions.

Karnopp and Scharton properly note that whenever the elasto-

plastic system ($\alpha = 0$) yields, the center position of the vibration shifts

by the amount of the yielding. Hence yielding an amount (u-Y) in the

positive direction during one half-cycle of vibration shifts the center

position a distance (u-Y) in the positive direction so that the following

half-cycle of vibration starts with an initial amplitude of Y rather

than u. For Y much greater than σ_x this sudden decrease in ampli-

tude of vibration upon yielding results in a very small probability of

yielding in both directions during a single cycle of vibration. In fact

yielding in one direction results in absolutely no increased probability

of yielding in the opposite direction at any future time.

From the above it appears that the Karnopp and Scharton analysis may be more accurate than the analysis of Section 4.2 for the special case of $\alpha = 0$ and Y much greater than σ_x. However, it should be emphasized that this special case cannot be expected to be typical of the general class of bilinear systems. In particular, all systems with α greater than zero must execute stationary vibration about a fixed mean position, rather than wandering endlessly. Hence the analysis of Section 4.2 should give more accurate results for the general case of α not equal zero. The Karnopp and Scharton analysis is restricted to the special case of α equal zero.

V. DISCUSSION

The course of this study has been largely determined by the fact that no exact analytical solutions for the response of hysteretic systems to random excitation have yet been found. The study thus consists of experimental investigations using an analog computer, and various approximate analytical investigations which are compared with the analog computer results. The principal approximate analytical investigations are reported in Chapters III and IV. This chapter will discuss advantages and limitations of various approximation techniques.

Since the characteristics of the response of a linear system are well known it is natural to discuss the response of a nonlinear system in terms of how it differs from that of a linear system. When the level of excitation of a linear system is raised or lowered the levels of all measures of response are raised or lowered in direct proportion. Thus, ratios of mean squared level of response to level of excitation, or power spectral density of response to power spectral density of excitation are independent of the level of excitation for a linear system. Similarly for a linear system response the probability distribution normalized by the rms level of the response is independent of the level of excitation.

The analog computer results presented in Chapter II clearly indicate differences between the characteristics of the response of bilinear hysteretic systems and linear systems. A change in the level

of excitation of a particular bilinear hysteretic system sometimes
resulted in significant decreases and sometimes significant increases
in the ratios of mean squared levels of response to level of excitation.
Further, the shape of the curves showing the ratio of power spectral
density of response to power spectral density of excitation was found to
vary considerably as the level of excitation was changed. The frequency
location of the peak of these curves shifted significantly and for the
nearly elasto-plastic system the peak completely disappeared giving
a monotone decreasing power spectral density for some levels of exci-
tation. The normalized probability distribution of the bilinear system
response was also found to be considerably influenced by the level of
excitation. Since the excitation was Gaussian a linear system would
have had a Gaussian response but any particular bilinear system was
found to sometimes have a greater than Gaussian and sometimes a
smaller than Gaussian probability of large displacements, depending on
the level of excitation.

The mathematical simplicity of linear system analysis makes
very attractive the idea of attempting to apply linear analysis to non-
linear problems. To do this one must devise a method of finding a
linear system which will respond in the same manner as the nonlinear
system. Such a linear system could be referred to as an equivalent
linear system. The considerable differences noted above between the
response of linear and bilinear hysteretic systems make it clear that
no linear system will be equivalent to a bilinear system except in a
quite limited sense. However by specifying a particular basis for

comparison of the response to a particular excitation one may be able

to find a linear system which is equivalent to a nonlinear system in

such a limited sense.

L. S. Jacobson in 1930 first drew attention to the idea of seek-

ing an equivalence between nonlinear and linear systems by finding

equivalent damping factors for some nonlinear oscillators with har-

monic excitation[34]. The basis of comparison of the response of the

linear and nonlinear systems was the steady state displacement ampli-

tude. The oscillators considered in this original study had nonlinear

damping mechanisms but linear springs.

More recently, possible techniques for using an equivalent

viscous damping factor to characterize systems with nonlinear hyster-

etic restoring forces have been discussed by various authors, particu-

larly Jacobsen[9,35] and D. E. Hudson[10]. Jacobsen compares the

linear and nonlinear systems on the basis of energy dissipated per

cycle and potential energy stored in the system. This type of compar-

ison was shown to lead to equivalence in terms of level of response for

the systems with nonlinear damping treated in the 1930 study. It has

not been demonstrated, however, how this basis of comparison relates

to the response of systems with softening hysteretic restoring forces.

Hudson compares the response of the linear and nonlinear systems to

harmonic excitation on the basis of maximum amplitude of displace-

ment due to a given amplitude of excitation force. The stiffness of the

equivalent linear system is always taken to be the same as the initial

tangent stiffness of the nonlinear system. On this basis of comparison

one finds that the maximum value of equivalent viscous damping for any bilinear hysteretic system is about 16% and that this maximum value can only be achieved when the system is elasto plastic ($\alpha = 0$).

Hudson also compares the response of linear and nonlinear systems to earthquake-like excitation. The basis of comparison in this situation is the maximum value of the transient displacement due to the excitation. The nonlinear system considered in this case is a yielding structure with a curved hysteresis loop. The equivalent linear system again has a stiffness equal to the initial tangent stiffness of the nonlinear system. Using this analysis Hudson finds that for thirty seconds of strong earthquake-like excitation the equivalent viscous damping is about 4%. By comparison, for harmonic excitation of this particular yielding system the maximum equivalent viscous damping (using Hudson's definition) for any level of excitation is about 12%.

By analogy to the work of Hudson one could compare the stationary response of linear and nonlinear systems to white, Gaussian excitation on the basis of rms displacement. The analog computer results presented in Figs. 9 and 11 can then be used to evaluate viscous damping factors for equivalent linear systems with stiffness equal to the initial tangent stiffness of the bilinear systems. The equivalent damping factor for a bilinear system with a specific restoring force curve is, of course, a function of the level of excitation. For the nearly elasto-plastic system ($\alpha = 1/21$) the above definition of equivalence gives a maximum equivalent damping factor of about 2% and for the system with $\alpha = 1/2$ it gives a maximum equivalent damping factor of about 5%.

These upper bounds compare reasonably with Hudson's results.

To talk of characterizing the effect of yielding by an equivalent amount of viscous damping implies that yielding always acts to decrease the level of response. Figs. 9 and 11 show that this is not true when the response under consideration is the stationary level of displacement due to random excitation. The fact that the rms level of response is always finite indicates that yielding does always act to limit the response of the bilinear system containing no viscous damping, since without yielding this system would have unbounded response. However, when the bilinear system also contains some viscous damping yielding sometimes acts to increase the level of response. Of the cases treated with the analog computer this increased response effect is most notable when $\alpha = 1/21$ and $\beta_o = 0.05$. In this instance yielding results in no appreciable decrease in displacement response, and for σ_x/Y greater than about 0.3 yielding tends to increase the level of displacement up to as much as 4.5 times the level for no yielding. If one is to characterize yielding solely by an equivalent damping factor this suggests that the equivalent damping factor must sometimes be negative, since yielding sometimes acts to increase the level of response. The total damping effect due to the combined action of viscous damping and yielding is still positive but it is smaller than the effect of the viscous damping by itself.

The explanation of the fact that yielding in some situations acts to decrease the level of response and in other situations acts to increase

the level of response is fairly simple. The nonlinearity of typical

softening hysteretic systems actually has two, sometimes opposite,

effects on the system response. The softening spring in addition to

shifting resonance to a lower frequency normally tends to increase

displacement response for a given level of exciting force, while the

hysteretic energy dissipation tends to decrease the system response.

In some instances the energy dissipation effect is greater than the

softening spring effect so that the net result is a decrease in level of

response; in other instances the softening spring effect predominates

resulting in a net increase in level of response. In all instances the

two effects counteract such that great reductions in displacement re-

sponse are not realized even when there is a large amount of hysteretic

energy dissipation.

A somewhat different method of comparing linear and nonlinear

systems forms the basis of the Krylov-Bogoliubov method of equivalent

linearization as presented in Chapter III. Here the mean squared level

of the difference between the differential equations for the linear and

nonlinear systems is considered. The particular linear system which

results in the minimum mean squared difference between the equations

is called the equivalent linear system. The finding of both an equiva-

lent stiffness and an equivalent damping factor in this method makes

possible a better approximation of the response of a nonlinear system.

Unfortunately in order to adapt the Krylov-Bogoliubov method

to problems of random excitation it was necessary to make certain

assumptions which are normally only valid for systems with small
nonlinearities. Nonetheless the method served to predict the levels
of displacement and velocity response within about 15% for the bi-
linear system with $\alpha = 1/2$, except when the viscous damping was
very small while the yield level was either quite high or very low.
For a nearly elasto-plastic system ($\alpha = 1/21$) the equivalent linear-
ization method gave a rough estimate (20 to 25% error) of the effect
of yielding on the velocity response, but failed almost completely
to predict the effect of yielding on the displacement response.

The spring constant and damping factor of the Krylov-
Bogoliubov equivalent linear system are dependent on the level of
excitation for any particular nonlinear system. For the bilinear
hysteretic system with $\alpha = 1/21$ the maximum value of the equiva-
lent damping factor was about 53%, and for the system with $\alpha = 1/2$
the maximum equivalent damping was about 10%. The great dif-
ference between these factors and the 2% and 5% damping factors
determined above using a basis of comparison similar to that used
by Hudson is explained by the difference in stiffness of the equiva-
lent linear systems determined by the two methods.

Hudson's method of defining an equivalent linear system keeps
the stiffness of the linear system equal to the initial tangent stiffness
of the nonlinear system, whereas the Krylov-Bogoliubov method allows
a decreased linear system stiffness in order to account for the soften-

ing spring effect of a bilinear hysteretic system. The mean squared

level of displacement response of a linear system with white excitation

is inversely proportional to the product of the damping factor times the

cube of the resonance frequency. Therefore if two linear systems are

to have the same level of response the system with the greater stiffness

must have a smaller damping factor than the system with the lesser

stiffness.

Since, as mentioned above, the Krylov-Bogoliubov method

almost completely failed to predict the effect of yielding on the dis-

placement response of the system with $\alpha = 1/21$ it might appear to be

meaningless to compare the 53% maximum damping factor determined

by the Krylov-Bogoliubov method with the 2% maximum damping factor

determined using Hudson's method of comparison for this system.

However this comparison is not as meaningless as it might appear.

Consider the results obtained in Chapter III using a definition of an

equivalent linear system based on matching the levels of response of

the nonlinear system. For any particular level of excitation the reso-

nance frequency and damping factor were computed for a linear sys-

tem which would have the same rms levels of both displacement and

velocity response as the levels experimentally determined for the bi-

linear hysteretic system with $\alpha = 1/21$. The stiffness of this linear

system, as with the Krylov-Bogoliubov equivalent linear system, was

less than the initial tangent stiffness of the nonlinear system. The

maximum damping factor for any level of excitation of this newly de-

fined equivalent linear system was found to be the same as that for the

Krylov-Bogoliubov system, that is about 53%.

In some instances one may wish to predict the power spectral density of the response of a nonlinear system. To do this by an approximate method requires a somewhat better approximation than is necessary to predict rms levels of response. The softening spring of commonly encountered hysteretic systems results in the peak power spectral density of the response to white random excitation being at a lower frequency for a low yield level than for a high yield level. Thus the usefulness of the method of equivalent viscous damping with initial tangent stiffness to predict power spectral density is limited to cases with very little yielding. Krylov-Bogoliubov linearization using both an equivalent stiffness and an equivalent damping should give a somewhat better prediction of power spectral densities for systems with somewhat more yielding.

The results of Chapter II, however, indicate that one can never have more than limited success in using a single-mass linear oscillator to predict the power spectral density of a bilinear hysteretic system. It was found, for example, that the low frequency power spectral density of a bilinear hysteretic system is always like that for a linear system with a stiffness equal to the smaller of the two slopes of the bilinear restoring force curve. Thus choosing an equivalent linear stiffness on the basis of fitting the center frequency portion of the bilinear system power spectral density will always result in error in the low frequency power spectral density.

The difference between the curve for the power spectral density of a nearly elasto-plastic system and those appropriate to single-mass linear systems is particularly marked. It appears, in fact, that the curves for the nearly elasto-plastic system are more like those for a linear system with two uncoupled modes of vibration. For such an uncoupled system the power spectral density and mean squared level of response due to each mode can be computed separately and summed to obtain these measures of the total system response.

Figure 37 shows an attempt to approximate some of the power spectral density curves previously presented in Figs. 16 and 17 by those for a two mode linear system. The linear system chosen has one mode with resonance at ω_o and damping factor β_1, and another mode with resonance at $\sqrt{\alpha}\,\omega_o$ and damping factor β_2. For each of the three cases shown in Fig. 37 the damping factors β_1 and β_2 have been chosen somewhat arbitrarily in an attempt to match the curves obtained from the analog computer results. The figure shows that the approximations are far from exact. Nonetheless the general characteristics of the analog computer results are found in the approximations.

The values chosen for β_1 and β_2 of the two mode linear approximation for each case shown in Fig. 37 are given in the lower part of the accompanying table. The table also gives the mean squared displacement and velocity response due to each mode of the approximation and the resulting rms levels of total response. In the table the terms $\left(\sigma_x^2\right)_1$ and $\left(\sigma_x^2\right)_2$ are the mean squared displacement contributions
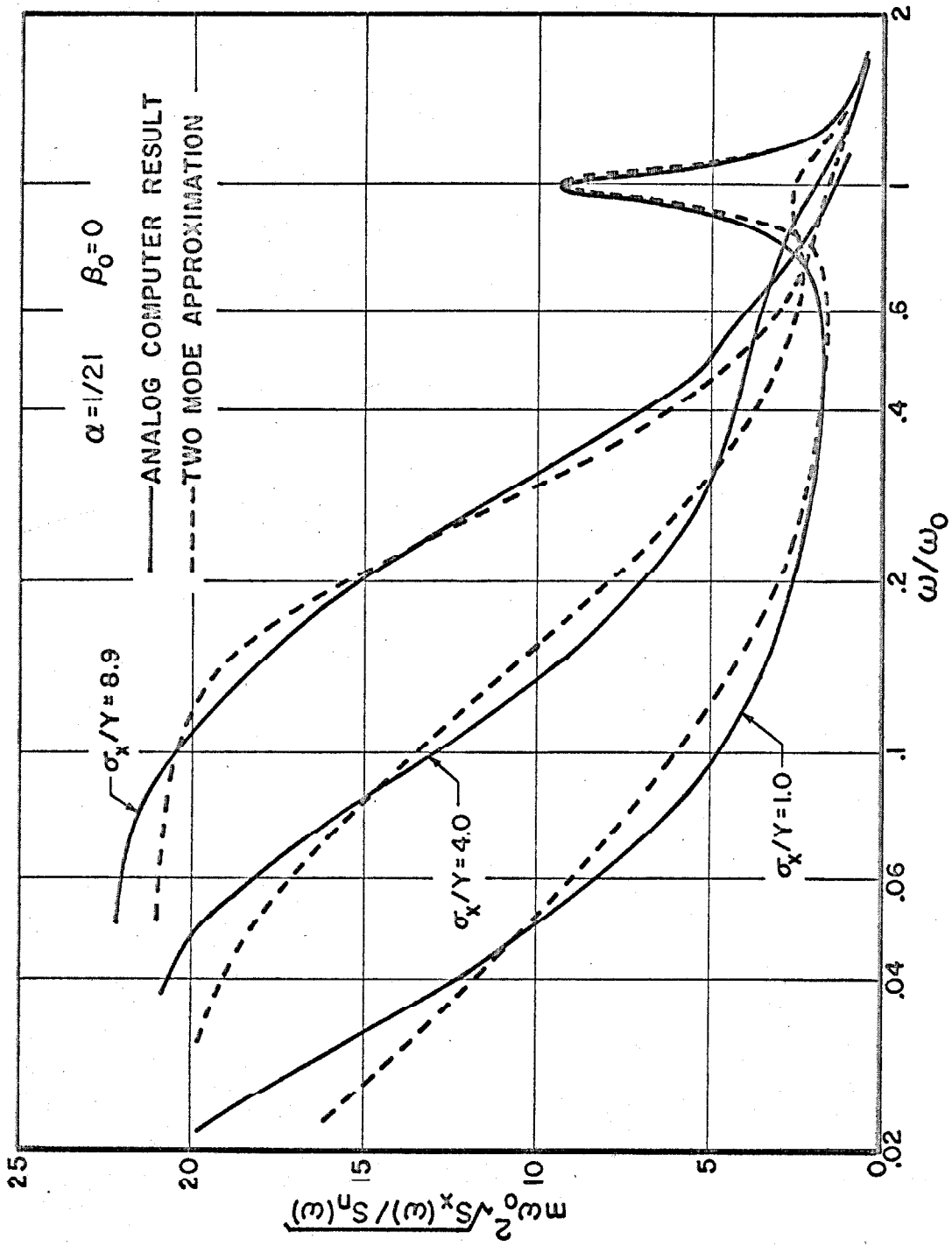
Figure 37. Response Power Spectral Density.

CASES CONSIDERED

	1.0	4.0	8.9
$\dfrac{\sigma_x}{Y}$	1.0	4.0	8.9

ANALOG COMPUTER RESULTS

$\sigma_x \dfrac{m\omega_o^2}{\sqrt{S_o \omega_o}}$	6.0	7.4	10.0
$\sigma_{\dot{x}} \dfrac{m\omega_o}{\sqrt{S_o \omega_o}}$	4.0	2.3	2.6

APPROXIMATION

β_1	0.053	0.20	0.40
β_2	4.00	1.45	0.72
$\left(\sigma_x^2\right)_1 \left(\dfrac{m\omega_o^2}{\sqrt{S_o \omega_o}}\right)^2$	14.8	3.93	1.97
$\left(\sigma_x^2\right)_2 \left(\dfrac{m\omega_o^2}{\sqrt{S_o \omega_o}}\right)^2$	18.9	52.1	105
$\sigma_x \dfrac{m\omega_o^2}{\sqrt{S_o \omega_o}}$	5.8	7.5	10.3
$\left(\sigma_{\dot{x}}^2\right)_1 \left(\dfrac{m\omega_o}{\sqrt{S_o \omega_o}}\right)^2$	14.8	3.93	1.97
$\left(\sigma_{\dot{x}}^2\right)_2 \left(\dfrac{m\omega_o}{\sqrt{S_o \omega_o}}\right)^2$	0.90	2.48	5.01
$\sigma_{\dot{x}} \dfrac{m\omega_o}{\sqrt{S_o \omega_o}}$	3.96	2.53	2.64

due to the modes with resonance at ω_0 and $\sqrt{\alpha}\,\omega_0$ respectively; similar

subscripting is used for the velocity contributions. The levels of total

response for the two mode linear system with the chosen damping func-

tions are seen to be approximately the same as the analog computer

results presented in the upper part of the table for each case considered.

When the yield level is such that $\sigma_x/Y = 1.0$ one might expect the

system response to be principally governed by the small-displacement

part of the restoring force curve. The table shows, however, that for

the two mode approximation of this example the lower frequency mode

(which is based on the large-displacement slope of the restoring force

curve) contributes about 56% of the total mean squared displacement

response. This is even though the damping in the lower frequency

mode is chosen as 400%.

A two mode linear system approximation might be potentially

useful for predicting the power spectral density and the mean squared

levels of response of nearly elasto-plastic systems if one were to find

some analytical technique for choosing the damping factors. As pre-

sented above the approximation obviously gives no prediction of response

since the damping factors were chosen solely on the basis of matching

the known response.

For the bilinear system with $\alpha = 1/2$ the overall shape of the

power spectral density curves is more like that for a single mode

linear system than is true for the nearly elasto-plastic system. Each

of the curves for $\alpha = 1/2$ has a definite peak and the peak shifts gradu-

ally from frequency ω_0 to $\sqrt{\alpha}\,\omega_0$ as σ_x/Y increases. For this system

with a moderate amount of yielding neither Krylov-Bogoliubov linearization or the above suggested two mode linear system approximation yields a very adequate approximation of the power spectral density. Figure 38 shows a comparison of the power spectral density obtained from the two approximate methods with the analog computer result from Fig. 19 for $\sigma_x/Y = 1.3$. The damping constants in the two mode approximation are chosen so as to give the correct mean squared levels of total displacement and velocity response. The Krylov-Bogoliubov approximation for this system predicts rms levels of displacement and velocity response which are within about 6% of the analog computer results. The single mode linear system which gives the same levels of displacement and velocity response as the analog computer results has a peak power spectral density which is higher yet than that for the Krylov-Bogoliubov approximation and hence is a poorer approximation for spectral density. Thus neither a single mode linear system or a two mode linear system with resonances at ω_o and $\sqrt{\alpha'}\omega_o$ seems capable of closely approximating the power spectral density for the bilinear system with $\alpha = 1/2$ and $\sigma_x/Y = 1.3$.

If one wishes to approximate the probability distribution of the response of a nonlinear system none of the above approximation methods is of any help. The suggested methods all consist of approximating the nonlinear system by some linear system and for any linear system with a Gaussian excitation the response also has a Gaussian distribution. The analog computer results reported in Chapter II, however, indicated that the response of a bilinear hysteretic system to
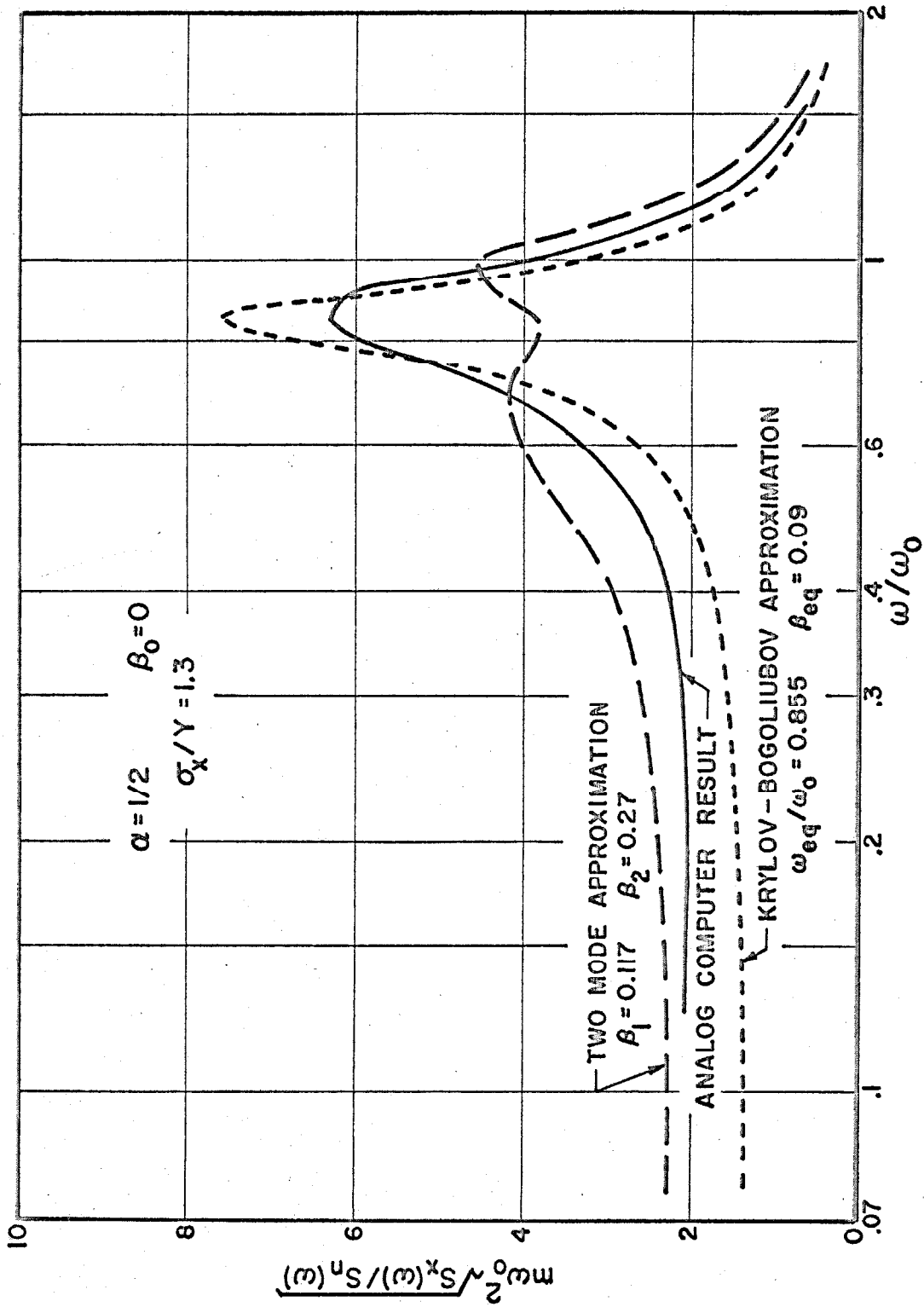
Figure 38. Response Power Spectral Density.

Gaussian excitation may be significantly non-Gaussian.

The stationary joint probability density function $p(x, \dot{x})$ found by T. K. Caughey as the fundamental solution of the appropriate Fokker-Planck equation for a general class of nonlinear nonhysteretic systems is presented in Chapter IV. A possible approximation of a bilinear hysteretic system by such a nonhysteretic system is also discussed. The general characteristics of the probability distribution predicted by the approximation are deduced, although no numerical values are calculated. For an oscillator with a low yield level the nonhysteretic approximation predicts a greater than normal probability of large displacements as normalized by the rms level. For a system with a high yield level and little or no viscous damping, however, the approximation predicts a smaller than normal probability of large normalized displacements. These general trends are seen to be in agreement with the analog computer results.

From the joint probability density function one can, of course, obtain mean squared values of displacement and velocity response in addition to the one dimensional probability density functions. To evaluate these measures of response for the nonhysteretic approximation presented in Chapter IV, however, requires numerical integration in most instances. Such numerical integration was not carried out in this study but may be potentially useful. For a limiting case of a bilinear hysteretic system with a very high yield level it was found possible to use a nonhysteretic approximation which gives predicted mean squared values of response without numerical integration.

The values so predicted compare well with the analog computer results.

The solution of the Fokker-Planck equation presented in Chapter IV does not give any information about the power spectral density of the system response. The general transitional probability solution of the time-dependent Fokker-Planck equation would give power spectral density, but this solution has not yet been found for second order nonlinear systems such as spring-mass oscillators.

VI. SUMMARY AND CONCLUSIONS

6. 1. Analog Computer Investigations

The analog computer was used to experimentally investigate the stationary response of bilinear hysteretic single-mass oscillators to an excitation which was approximately Gaussian and white.   The slope ratio α of the bilinear restoring force curve was given values of 1/21 and 1/2 in order to study one nearly elasto-plastic system and one system intermediate between linear and elasto-plastic.   The characteristics of the response which were determined in the investigation were mean squared level of displacement and velocity response, power spectral density, and probability distribution of displacement response. The following paragraphs summarize the findings of the analog computer investigation.

1.   For a given level of excitation of the bilinear hysteretic systems with no viscous damping the mean squared level of the displacement response was minimized when the yield level was chosen such that the ratio of rms displacement to yield level (σ_x/Y) was between unity and two.   For the system with the slope ratio α equal 1/2 this minimum level of displacement response was about the same as that for the system with infinite yield level and 5% of critical viscous damping.   For the nearly elasto-plastic system ($\alpha = 1/21$) the minimum level of response was about the same as that for 2% viscous damping with infinite yield level.

2. For the bilinear hysteretic systems containing some viscous damping the rms displacement response for a particular level of excitation was greater by a factor of $\sqrt{1/\alpha}$ when the yield level approached zero than when the yield level approached infinity. When the amount of viscous damping was such as to provide 1% damping for small amplitude oscillations ($\beta_o = 0.01$) the rms displacement response was less than that for $Y = \infty$ provided σ_x/Y was less than 30 for $\alpha = 1/2$ or $\sigma_x/Y < 7.5$ for $\alpha = 1/21$. For the nearly elasto-plastic system with $\beta_o = 0.05$ the effect of yielding was to increase the rms displacement response level above that for $Y = \infty$ for virtually all values of yield level.

3. For all yield levels the rms velocity response of the bilinear hysteretic systems was reduced by yielding. The minimum level of velocity response for a given level of excitation occurred when σ_x/Y was near 1.25. For this condition of minimum velocity response the reduction of the velocity due to yielding for the system with $\alpha = 1/2$ was about the same as that which would result from adding 7% viscous damping to the system with infinite yield level. For $\alpha = 1/21$ the maximum reduction in velocity response was like that due to the addition of 15% viscous damping to the system with infinite yield level. For bilinear systems containing some viscous damping the level of velocity response was the same for very high or very low yield levels.

4. Two limiting conditions were found for the power spectral density of the response of the bilinear hysteretic systems. At very high frequencies the response power spectral density of a bilinear

system was like that for a linear system having the same mass and excitation. At frequencies near zero the response power spectral density was like that for a linear system having the same mass and excitation and having a spring constant equal to the smaller of the two slopes of the bilinear restoring force curve. Between these limits it was found that for the system with $\alpha = 1/2$ the power spectral density curve always had a definite peak and the location of the peak shifted gradually from frequency ω_0 to $\sqrt{\alpha}\,\omega_0$ as σ_x/Y was increased from a small value to a large value. For $\alpha = 1/21$ it was found that for σ_x/Y between 4 and 9 the power spectral density was monotone decreasing over the entire frequency range, while higher yield levels resulted in a peak near frequency ω_0 and lower yield levels resulted in a peak near $\sqrt{\alpha}\,\omega_0$.

5. Probability distribution measurements showed that for low yield levels the response of a bilinear hysteretic system had a significantly greater probability of being at large displacements than does a Gaussian signal with the same rms level. On the other hand, when the yield level was high and the bilinear system contained little or no viscous damping there was a much smaller probability of the system response being at large values than for a Gaussian distribution.

6.2. Approximate Analytical Techniques

The possibility of finding a single-mass linear oscillator which has the same displacement and/or velocity response as a particular nonlinear oscillator with the same excitation was discussed. The only

technique suggested for finding such an equivalent linear system for some particular nonlinear system without first knowing the response of the nonlinear system was an extension of the method of Krylov and Bogoliubov. In adapting the Krylov-Bogoliubov method to problems of bilinear hysteretic systems with random excitation certain assumptions were made which one would normally expect to be valid only for systems with small nonlinearities. Nonetheless the response of equivalent linear systems found by this method was compared with the analog computer results for the bilinear systems with $\alpha = 1/2$ and $\alpha = 1/21$.

The possibility of approximating the power spectral density curve for the response of a nearly elasto-plastic system by one for a two mode linear system was also discussed. However, no technique was suggested for determining the parameters of such an equivalent linear system without first knowing the response of the nonlinear system.

Finally there was a discussion of the idea of approximating a hysteretic system by a nonlinear nonhysteretic system for which the solution of the Fokker-Planck equation is known. A particular nonlinear nonhysteretic system to approximate a bilinear hysteretic system was suggested. The general characteristics of the probability distribution of the response of this nonhysteretic system were discussed, and for a limiting case of high yield level numerical values were obtained for its rms response level. These characteristics of the response of the nonhysteretic system were compared with the experimentally determined characteristics of the bilinear hysteretic

system.

The findings of the investigation of approximate analytical techniques are summarized in the following paragraphs.

1. For the bilinear hysteretic oscillator with $\alpha = 1/2$ the Krylov-Bogoliubov method of equivalent linearization serves to predict the rms levels of both displacement and velocity response within about 15% except when the viscous damping factor β_o is less than 0.01 while the yield level is either very low or very high.

2. For a nearly elasto-plastic system ($\alpha = 1/21$) the Krylov-Bogoliubov method of equivalent linearization gives a rough estimate of the rms velocity response (about 25% maximum error). For this system, however, the method yields useful information about the effect of yielding on the displacement response only when the yield level is so low that σ_x/Y is greater than about 30.

3. One cannot, in general, accurately approximate the power spectral density of the response of a bilinear hysteretic oscillator to white excitation by the response power spectral density for a single-mass linear oscillator. This is true even for the bilinear hysteretic system with $\alpha = 1/2$, although the response power spectral density for this particular system does always have a well defined peak.

4. It is possible to roughly approximate the power spectral density of the response of a nearly elasto-plastic oscillator to white excitation by the response power spectral density for a linear system with two uncoupled modes of vibration, where one of the modes has its resonance at frequency ω_o while the other has its resonance at $\sqrt{\alpha}\, \omega_o$.

The approximation is not exact but the general characteristics of the power spectral density for the nearly elasto-plastic system are similar to those for the two mode linear system if the linear system damping factors are properly chosen. It is not possible to approximate the response power spectral density for the bilinear hysteretic system with $\alpha = 1/2$ by that for such a two mode linear system.

5. The technique of approximating a hysteretic system by a nonlinear nonhysteretic system for which the solution of the Fokker-Planck equation is known may be potentially useful for predicting the response of hysteretic systems. The probability distribution of the response of a particular type of nonlinear nonhysteretic system suggested in Chapter IV has the same general characteristics as the probability distribution for bilinear hysteretic systems. In most instances numerical integration will be necessary to determine numerical values for the probability distribution or mean squared values of the response for this particular type of nonlinear nonhysteretic system. For a limiting case of a bilinear hysteretic system with a very high yield level a simpler nonhysteretic approximation is appropriate. This simpler approximation gives mean squared levels of response without numerical integration, and these values agree very well with those for bilinear hysteretic systems within the limitation of high yield level.

REFERENCES

1. Crandall, S. H. and Mark, W. D., Random Vibration in Mechanical Systems, Academic Press, New York, 1963.

2. Davenport, W. B., Jr. and Root, W. L., An Introduction to the Theory of Random Signals and Noise, Lincoln Laboratory Publication, McGraw-Hill, New York, 1958.

3. Bendat, J. S., Principles and Applications of Random Noise Theory, John Wiley and Sons, New York, 1958.

4. Alford, J. L., Housner, G. W., and Martel, R. R., Spectrum Analyses of Strong-Motion Earthquakes, Earthquake Engineering Research Laboratory, California Institute of Technology, revised 1964.

5. Rosenblueth, E. and Bustamante, J. I., "Distribution of Structural Response to Earthquakes", Journal of the Engineering Mechanics Division ASCE, Vol. 88, No. EM3, (June 1962), pp 75-106.

6. Shinozuka, M., "Probability of Structural Failure Under Random Loading", Journal of the Engineering Mechanics Division ASCE, Vol. 90, No. EM5, (Oct. 1964) pp 147-170.

7. Brady, A. G., Studies of Response to Earthquake Ground Motion, Earthquake Engineering Research Laboratory, California Institute of Technology, 1966, (Ph. D. Thesis).

8. Caughey, T. K., "Equivalent Linearization Techniques", Journal of the Acoustical Society of America, Vol. 35, No. 11, (Nov. 1963), pp 1706-1711.

9. Jacobsen, L. S., "Damping in Composite Structures", Proc. of the Second World Conference on Earthquake Engineering, Vol. II, Japan, 1960, pp 1029-1044.

10. Hudson, D. E., "Equivalent Viscous Friction for Hysteretic Systems with Earthquake-Like Excitations", Proc. of the Third World Conference on Earthquake Engineering, Vol. II, New Zealand, 1965, pp II-185-206.

11. Crandall, S. H., "Perturbation Techniques for Random Vibration of Nonlinear Systems", Journal of the Acoustical Society of America, Vol. 35, No. 11, (Nov. 1963), pp 1700-1705.

12. Caughey, T. K. , "Derivation and Application of the Fokker-Planck Equation to Discrete Nonlinear Dynamic Systems Subjected to White Random Excitation", Journal of the Acoustical Society of America, Vol. 35, No. 11, (Nov. 1963), pp 1683-1692.

13. Caughey, T. K. , "On the Response of a Class of Nonlinear Oscillators to Stochastic Excitation", Les Vibrations Forcées Dans Les Systèmes Non-Linéaires, Editions Du Centre National De La Recherche Scientifique, Paris, 1965 (Colloques Internationaux No 148, Marseille, 1964) pp 393-405.

14. Caughey, T. K. , "Sinusoidal Excitation of a System with Bilinear Hysteresis", Journal of Applied Mechanics, Vol. 27, No. 4, (Dec. 1960), pp 640-643.

15. Iwan, W. D. , The Dynamic Response of Bilinear Hysteretic Systems, Earthquake Engineering Research Laboratory, California Institute of Technology, 1961, (Ph. D. Thesis).

16. Caughey, T. K. , "Random Excitation of a System with Bilinear Hysteresis", Journal of Applied Mechanics, Vol. 27, No. 4, (Dec. 1960) pp 649-652.

17. Bycroft, G. N. , Murphy, M. J. , and Brown, K. J. , "Electrical Analog for Earthquake Yield Spectra", Journal of the Engineering Mechanics Division ASCE, Vol. 35, No. EM4 (Oct. 1959), pp 43-64.

18. Newmark, N. M. and Veletsos, A. S. , "Effects of Inelastic Behavior on the Response of Simple Systems to Earthquake Motions", Proc. of the Second World Conference on Earthquake Engineering, Vol. II, Japan, 1960, pp 895-912.

19. Chelapati, C. V. , Response of Simple Inelastic Systems to Ground Motions , Ph. D. Thesis, University of Illinois, 1962.

20. Veletsos, A. S. , Newmark, N. M. , and Chelapati, C. V. , "Deformation Spectra for Elastic and Elasto-Plastic Systems Subjected to Ground Shock and Earthquake Motions", Proc. of the Third World Conference on Earthquake Engineering, Vol. II, New Zealand, 1965, pp II-663-682.

21. Thomaides, S. S. , "Earthquake Response of Systems with Bilinear Hysteresis", Journal of the Structural Division ASCE, Vol. 90, No. ST4, (Aug. 1964), pp 123-143.

22. Berg, G. V., *The Analysis of Structural Response to Earthquake Forces*, Industry Program of the College of Engineering, University of Michigan, 1958.

23. Penzien, J., "Elasto-Plastic Response of Idealized Multi-Story Structures", *Proc. of the Second World Conference on Earthquake Engineering*, Vol. II, Japan, 1960, pp 739-760.

24. Clough, R. W., Benuska, K. L., and Wilson, E. L., "Inelastic Earthquake Response of Tall Buildings", *Proc. of the Third World Conference on Earthquake Engineering*, Vol. II, New Zealand, 1965, pp II-68-89.

25. Hu, P. Y., *Analytical and Experimental Studies of Random Vibration*, Dynamics Laboratory, California Institute of Technology, 1966, (Ph. D. Thesis), pp 153, 156.

26. Pereira, J. M. J., "Behaviour of an Elasto-Plastic Oscillator Acted By Random Vibration", *Proc. of the Third World Conference on Earthquake Engineering*, Vol. II, New Zealand, 1965, pp II-491-501.

27. Reference 15, pp 64-66.

28. Gröbner, W. and Hofreiter, N., *Integraltafel*, Zweiter Teil, Zweite verbesserte Auflage, Springer-Verlag, Wien and Innsbruck, 1958, p 108, No. 332.9.

29. Abramowitz, M. and Stegun, I. A. (editors), *Handbook of Mathematical Functions*, Dover, New York, 1965, p 225.

30. Coffin, L. F., Jr., "Design Aspects of High-Temperature Fatigue with Particular Reference to Thermal Stress", *Journal of Applied Mechanics*, Vol. 23, No. 2, (April 1956) pp 527-532.

31. Karnapp, D. and Scharton, T. D., "Plastic Deformation in Random Vibration", *Journal of the Acoustical Society of America*, Vol. 39, No. 6, (June 1966), pp 1154-1161.

32. Reference 29, p 298.

33. Rice, S. O., "Mathematical Analysis of Random Noise", *Bell System Technical Journal*, Vols. 23, 24 (1944, 1945). Reprinted in *Selected Papers on Noise and Stochastic Processes*, edited by N. Wax, Dover Publications, New York, 1954, pp 133-294.

34. Jacobsen, L. S., "Steady Forced Vibration as Influenced by Damping", Transactions of the ASME Applied Mechanics Division, Vol. 52, No. 22, (Sept. - Dec. 1930), pp 169-181.

35. Jacobsen, L. S., Frictional Effects in Composite Structures Subjected to Earthquake Vibrations, Dept. of Mech. Engrg., Stanford University, Stanford, 1959.

36. Reference 3, p 259.

37. Reference 3, p 270.

38. Bendat, J. S. and Piersol, A. G., Measurement and Analysis of Random Data, John Wiley and Sons, New York, 1966, pp 186-187.

39. Reference 38, pp 188-191, 205.

40. Reference 3, pp 55-57.

41. Reference 28, p 64, No. 314.2.

42. Jolley, L. B. W., Summation of Series, Second Revised Edition, Dover, New York, 1961, p 42, No. 228.

APPENDICES

A. EQUIPMENT DESIGNED OR MODIFIED FOR USE IN
ANALOG COMPUTER INVESTIGATIONS

A. 1. Analog Computer Circuit

The analog computer used was a K7-A10 manifold of Philbrick Model USA-3 Universal Stabilized Amplifiers. The basic circuit for the bilinear oscillator problem is shown in Fig. A. 1, where $\varphi_p(v)$ is an elasto-plastic function of v. The nominal values of the resistors and capacitors in the circuit of Fig. A.1 were chosen as follows:

$$R_1 = 80\,K$$

$$R_3 = 100\,K \qquad C_1 = 0.001\,\mu f$$

$$R_4 = 100\,K \qquad C_2 = 0.01\,\mu f$$

$$R_7 = \frac{R_5 R_6}{R_5 + R_6}$$

The value of the slope parameter α (see Fig. 1) was simply $\alpha = R_6/(R_5 + R_6)$. Resistor R_2 was varied to achieve various values of viscous damping. Measurements of the response of the system indicated that the individual errors of the components combined in such a way that the actual integrator constants were:

$$R_3 C_1 = 1.02 \times 10^{-4}$$

$$R_1 C_1 = 0.79 \times 10^{-4}$$

$$R_4 C_2 = 1.01 \times 10^{-3}$$

The small-amplitude (i. e. linear system) undamped natural frequency was 496 cps.
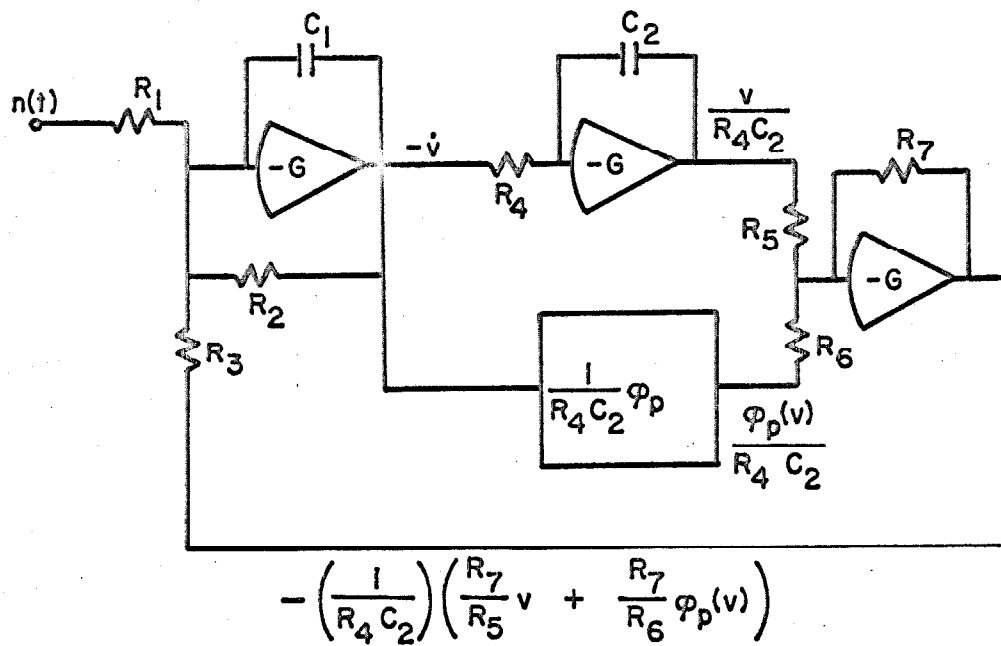
$$\ddot{v} = -\left(\frac{1}{R_3 C_1}\right)\left(\frac{1}{R_4 C_2}\right)\left(\frac{R_7}{R_5} v + \frac{R_7}{R_6} \varphi_p(v)\right) - \frac{\dot{v}}{R_2 C_1} + \frac{n(t)}{R_1 C_1}$$

Figure A. 1.   Analog Circuit for Bilinear Hysteretic Oscillator.

The actual amount of viscous damping for some particular re-sistor R_2 was experimentally determined from the amplification factor when the system was harmonically excited at its undamped natural fre-quency with the amplitude of v/R_4C_2 less than v_0. It was found that when R_2 was infinite (open circuit) the system response slowly built up until it reached yield level, when there was no excitation of the system. This build-up indicates the presence of negative damping in the system under this condition, but measurement of the rate of build-up showed the effect of this negative damping to be less than that of -0.05% vis-cous damping. Because of its small size this negative damping was ignored and the system with R_2 infinite was considered as having no viscous damping. However, in a few instances where excitation was small compared to yield level and when R_2 was infinite the effect of this negative damping could be detected, as is mentioned in Section 2.2.

Probably the most common electrical device for developing an elasto-plastic function is an integrator with either biased simple diodes or a double anode Zener diode to limit the output voltage, as shown in Fig. A.2a. Such a diode feedback device has a current-voltage characteristic with finite slopes and somewhat rounded corners as shown in Fig. A.2b. This type of elasto-plastic function generator works quite well for studying periodic response, since by choosing components correctly the maximum current during each cycle can be made large enough to push the diode well past the corner of the current-voltage characteristic. The finite slopes of the character-istic prevent the hysteresis loop of $\varphi_p(v)$ versus v from being truly
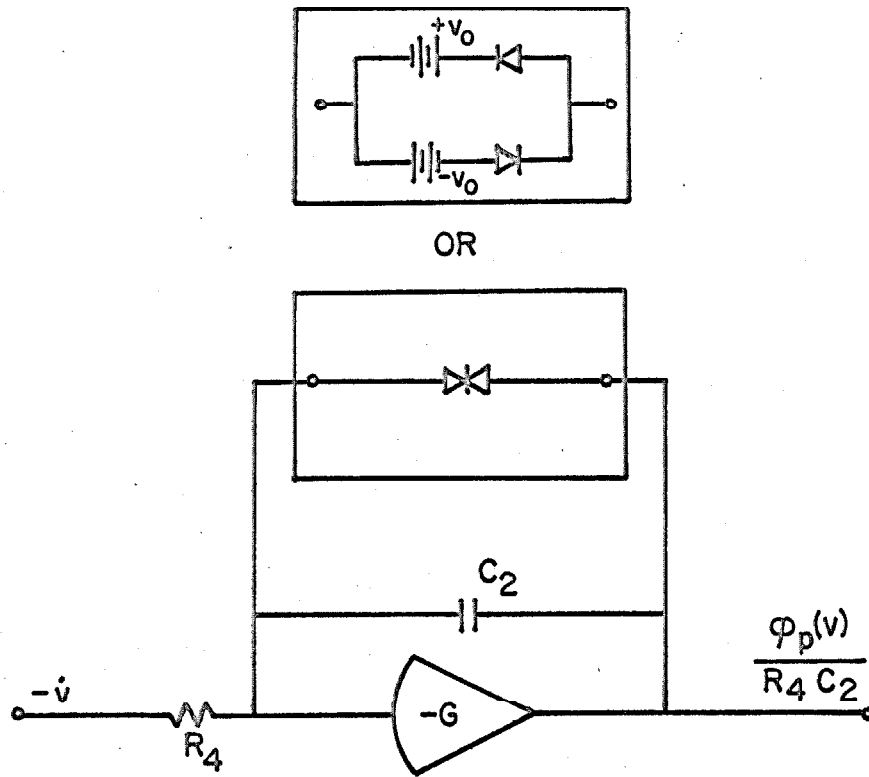
a. Elasto-Plastic Function Generator Using Diode Feedback Devices.
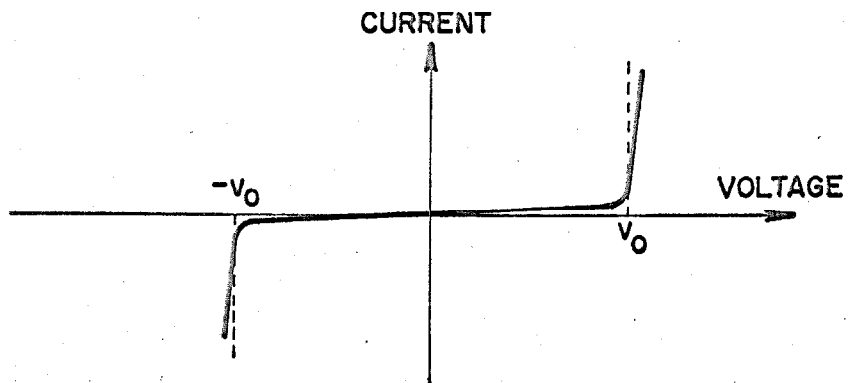
b. Characteristic of Diode Feedback Devices.

Figure A. 2.

elasto-plastic, but the approximation is quite good.

The imperfect current-voltage characteristic of a diode feed-back device is much more of a hindrance to an investigation of response to random excitation, since successive cycles of response can be expected to give greatly differing values of maximum feedback current. Thus one cycle may give yielding at a voltage corresponding to the rounded corner of the current-voltage curve while another cycle will give yielding at a larger voltage corresponding to some point well past the corner. Hence the yield level will vary and the resulting energy dissipation will be distributed incorrectly among the various cycles. Experiments using a 1N475 double anode Zener diode with feedback currents in the range from 10^{-7} to 10^{-3} amp showed that an increase by a factor of ten in the maximum feedback current resulted in a 10% to 25% increase in the effective yield level.

In this study a transistor switching circuit was substituted for the diode feedback devices of Fig. A.2. Figure A.3 illustrates the circuit. The voltage v_o is the nominal yield level and amplifier #1 is merely a sign changer. Amplifier #4 is the integrator and amplifiers #2 and #3 along with the two Zener diodes and four transistors provide the limiting effect on the output voltage.

To understand the operation of the limiting system consider the details of how amplifier #2 and transistors Q_1 and Q_2 limit the output at the upper yield level. The minimum negative gain of each amplifier used is 10^7, and the maximum output voltage of each is 100 volts; thus
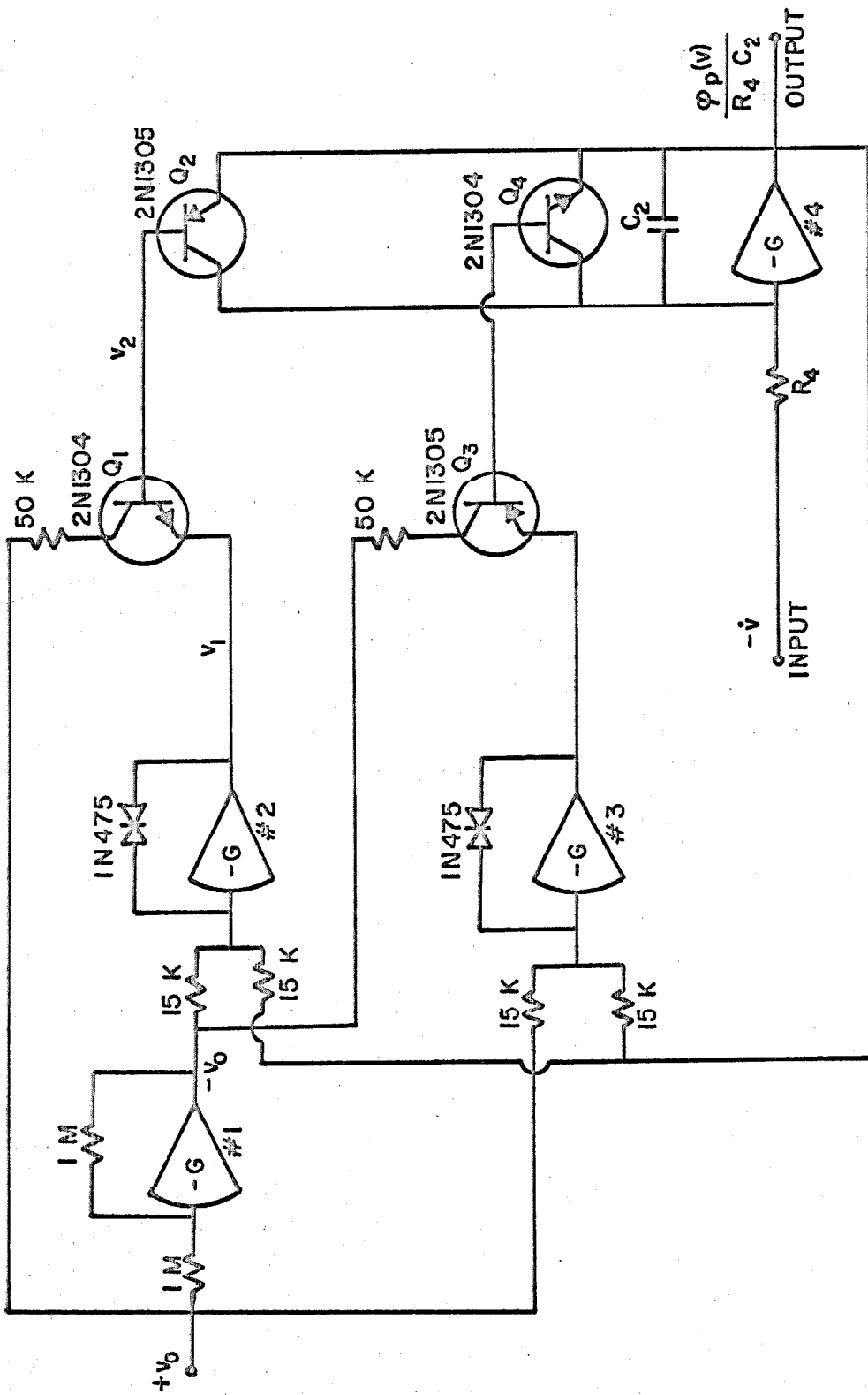
Figure A. 3. Transistor Elasto-Plastic Function Generator.

the absolute value of the voltage at the summing point of any amplifier must be less than or equal to 10^{-5} volts. When $\varphi_p(v)/R_4C_2 - v_o$ is less than zero there must be a current flowing to the left from the summing point of amplifier #2 (since the summing point is so nearly at zero voltage). The input impedance of the amplifier itself is so high that the current from its input must be of the order of 10^{-11} amps. Thus the principal current to the summing point must come through the Zener diode, and the output voltage of #2 must be $v_1 = v_z$, the Zener breakdown voltage of the diode. The nominal yield voltage, v_o, must always be chosen less than v_z, giving a reverse bias from emitter to collector of transistor Q_1 when $v_1 = v_z$. Under this condition the transistor transmits only very small leakage currents and its base voltage is maintained at $v_2 = v_o$. The base of Q_2 is, thus, also held at voltage v_o; and since $\varphi_p(v)/R_4C_2$ is less than v_o (as originally assumed) there is a very high impedance to any current flow through Q_2.

Amplifier #3 and transistors Q_3 and Q_4 operate in a manner directly analogous to that of amplifier #2 and Q_1 and Q_2. Thus, whenever $\varphi_p(v)/R_4C_2 + v_o$ is greater than zero the base of Q_4 is maintained at voltage $-v_o$. Hence when $\varphi_p(v)/R_4C_2$ is between $-v_o$ and v_o both Q_2 and Q_4 are in nonconducting modes of operation due to reverse bias voltage from emitter to base. There is, of course, some leakage current through the transistors even though they have reverse bias. The magnitude and effect of this leakage current is discussed below. Neglecting the leakage current, the current through resistor R_4 due to the

input voltage, $-\dot{v}$, is summed (or integrated) on capacitor C_2 whenever $\varphi_p(v)/R_4C_2$ is between $-v_o$ and v_o.

If $\dot{v}$ is positive then the integration on C_2 leads to an increasing output voltage, $\varphi_p(v)/R_4C_2$. When $\varphi_p(v)/R_4C_2$ approaches the level v_o the current at the summing point of #2 decreases. If $\varphi_p(v)/R_4C_2$ were allowed to exceed v_o the current through the diode on #2 would reverse direction, requiring that $v_1 = -v_z$. However, if v_1 falls below v_2 (which is at level v_o) the transistor Q_1 is "turned on", allowing a current to flow from the collector to the emitter and a much smaller current (not more than 2.5% of that from collector to emitter) to flow from the base to the emitter. Similarly, if $\varphi_p(v)/R_4C_2$ is greater than v_2 transistor Q_2 conducts a current from emitter to collector discontinuing integration on capacitor C_2.

Thus when $\varphi_p(v)/R_4C_2$ reaches the level v_o and $\dot{v}$ is greater than zero the only current at the summing point of #2 is the 10^{-11} amps through the amplifier and a small leakage current through the diode. The resulting situation is that v_1 is maintained slightly below v_o so that a small current is transmitted from collector to emitter of Q_1 and a still smaller current passes from base to emitter of Q_1. This latter current is also the emitter to base current of Q_2, which is passing a current of $\dot{v}/R_4$ from emitter to collector, so that the charge on capacitor C_2 is not changing and $\varphi_p(v)/R_4C_2$ is being maintained at a constant level. This constant level of output, which is the effective yield level, is slightly less than v_o since there is some voltage drop across

any conducting transistor. Experimental measurement, however, showed that the effective yield level was never more than 0.05 volt below the nominal yield level in the tests conducted. The effective yield level was measured in each test and is normally referred to simply as yield level.

When the system is yielding as described above and $\dot{v}$ decreases until it becomes negative, the current through the resistor R_4 to the summing point of the integrator, #4, must reverse direction. But Q_2 will not pass a current in this direction (except for the previously mentioned leakage current) so the charge on C_2 must begin to decrease. Thus integration of $\dot{v}$ begins again when $\dot{v}$ reverses sign, and it starts from an initial value of yield level. When $\varphi_p(v)$ begins to decrease the current at the summing point of amplifier #2 must increase and v_1 returns to the level v_z, where it must remain until $\varphi_p(v)/R_4C_2$ again reaches the level v_0.

The operation of amplifier #3 and transistors Q_3 and Q_4 when $\varphi_p(v)/R_4C_2$ reaches the level $-v_0$ is directly analogous to the above.

It should be mentioned that properly oriented single anode Zener diodes on amplifiers #2 and #3 would work equally as well as the double anode diodes used. The 1N475 diodes were chosen because of their clean switching operation without adverse transient effects. The Zener voltage of the diodes used was about 6 volts, hence yield level was restricted to less than 6 volts.

As mentioned above there is some leakage current through the

feedback transistors in the elasto-plastic function generator. To determine the effect of such leakage, consider the linear integrator with a feedback resistor as shown in Fig. A. 4. For the particular instance where $\dot{v}$ is a harmonic signal of circular frequency ω, the output of this linear device can be written as

$$v^* = \frac{1}{1 + 1/R_8^2 C_2^2 \omega^2} \frac{1}{R_4 C_2} \left(v + \frac{\dot{v}}{R_8 C_2 \omega^2} \right) \qquad (A.1)$$

Substituting this output for $\varphi_p(v)/R_4 C_2$ in the equation of motion for the system in Fig. A. 1 gives

$$\ddot{v} = -\frac{1}{R_3 C_1} \frac{1}{R_4 C_2} \left[\left(\frac{R_7}{R_5} + \frac{R_7}{R_6} \gamma \right) v + \frac{R_7}{R_6} \frac{\gamma \dot{v}}{R_8 C_2 \omega^2} \right] - \frac{\dot{v}}{R_2 C_1} + \frac{n(t)}{R_1 C_1}$$

$$(A.2)$$

where

$$\gamma = \frac{1}{1 + 1/R_8^2 C_2^2 \omega^2} \leq 1 .$$

This differential equation describes harmonic motion with amplitude smaller than the yield level of the system in Fig. A. 1, including the leakage effect of the feedback transistors. The term γ is obviously very nearly unity when $R_8 C_2 \omega$ is large compared to unity.

Since $R_7 = R_5 R_6/(R_5 + R_6)$ the natural circular frequency for linear oscillations of the system of Fig. A. 1 is

$$\omega_o = \sqrt{\frac{1}{R_3 C_1} \frac{1}{R_4 C_2}}$$

Assuming γ to be nearly unity the natural circular frequency of equation (A. 2) is also approximately ω_o. Comparing terms of (A. 2) with
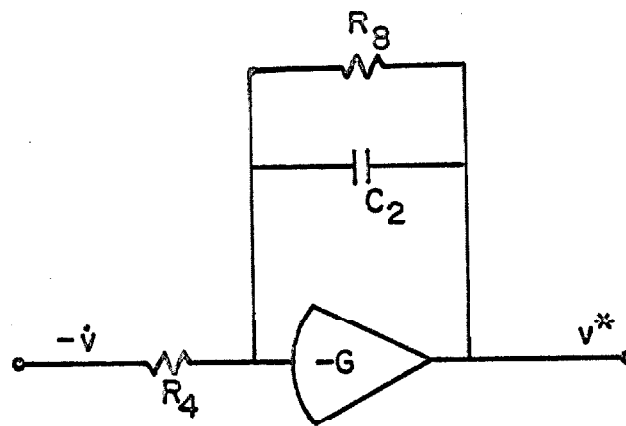
Figure A. 4. Integrator with Leakage Current.

a conventional form of the damped linear oscillator equation:

$$\ddot{v} + 2\beta_o \omega_o \dot{v} + \omega_o^2 v = n(t)/m$$

gives a viscous damping coefficient of

$$\beta_o = \frac{1}{2\omega_o}\left(\frac{1}{R_2 C_1} + \gamma\frac{R_7}{R_6}\frac{1}{R_8 C_2}\frac{\omega_o^2}{\omega^2}\right).$$

Since γ and R_7/R_6 are both less than or equal to unity, the additional damping coefficient due to the leakage current through resistor R_8 can be bounded as follows:

$$\beta_L \leq \frac{\omega_o}{2}\frac{1}{R_8 C_2}\frac{1}{\omega^2}. \qquad (A.3)$$

Since β_L is a function of frequency the effect of the leakage current on the linear system response at frequencies other than resonance can best be seen by looking at the transfer function for the system with nominally zero damping, i.e., $R_2 = \infty$:

$$|H(\omega)| = \frac{1}{m\omega_o^2\sqrt{\left(1 - \frac{\omega^2}{\omega_o^2}\right)^2 + \left(2\beta_L\frac{\omega}{\omega_o}\right)^2}}$$

$$\geq \frac{1}{m\omega_o^2\sqrt{\left(1 - \frac{\omega^2}{\omega_o^2}\right)^2 + \left(\frac{1}{R_8 C_2}\frac{1}{\omega}\right)^2}}. \qquad (A.4)$$

The actual effective value of the leakage resistance of the feed-back transistors used was determined by plotting v^* versus v at low frequencies (0.5 to 5 cps) and measuring the relative magnitude of the

two components of v^* in expression (A. 1). The value determined for the net resistance of the two transistors in parallel was approximately $R_8 - 145$ megohms. At the natural frequency, $\omega_o = 3,120$ rad/sec, the damping contribution from the leakage current was, thus,

$$\beta_L \leq 1,560 \frac{1}{1.45} (1.03 \times 10^{-7}) = 1.1 \times 10^{-4} \, .$$

Substituting into expression (A. 4) shows that the leakage current affected the transfer function for a signal at 5 cps by less than 0.025% and at 0.5 cps by less than 2.5%.

Figure 5 (in Chapter 2) shows that at 1000 cps there was a detectable overshoot of $\varphi_p(v)$ at yield, before it returned to a constant yield level. This overshoot was apparently due to the finite time it took for the output voltage of amplifiers #2 and #3 to change level, and thus initiate yielding. The maximum rate of change of output voltage of the USA-3 amplifiers is in the range of 2 to 8 volts per microsecond, making it possible for there to be a 2 or 3 microsecond lag between the time when $\varphi_p(v)/R_4C_2$ reached nominal yield level and the time when actual yielding began. To establish some measure of the size of error introduced by this overshoot, the hysteresis loop was studied carefully for a case with an effective yield level of 0.1 volt and the steady state amplitude of v/R_4C_2 equal to 20 volts at 1000 cps. For this test case the overshoot effect increased the area of the hysteresis loop by less than two per cent.

Since the overshoot is due to the integration of $\dot{v}$ over some time increment, one can expect that the height of the overshoot will be

approximately proportional to the amplitude of $\dot{v}$. Hence, the height

of the overshoot is approximately proportional to the product of the

amplitude of v times the frequency, for steady state operation. Thus,

the area added to the hysteresis loop by the overshoot varies approx-

imately quadratically with the product of the amplitude of v times the

frequency, whereas the area of the ideal hysteresis loop varies ap-

proximately linearly with the product of the amplitude of v times the

yield level for low yield levels. This predicts that the percentage

error in area of the hysteresis loop will vary approximately like the

frequency squared times the ratio of the amplitude of v to the yield

level.

In the test case above the rms level of v/R_4C_2 was approxi-

mately 144 times greater than the yield level. In Fig. 9 of Chapter 2

results are given for cases of random excitation where this ratio is as

great as 1000, but in that instance the predominant frequency of the

response was near 108 cps, such that the expected error due to over-

shoot is approximately

$$\frac{1000}{144}\left(\frac{108}{1000}\right)^2 (2\%) = 0.16\% \ .$$

In Fig. 11 of Chapter 2 results are presented for a case with the rms

of v/R_4C_2 about 200 times the yield level, and with a predominant

frequency of about 350 cps. This results in a predicted error of about

0.34%. These two cases should have resulted in the most serious

error due to overshoot of any reported in this study.

A.2. A Low-Frequency Elasto-Plastic Function Generator

A device to produce an elasto-plastic restoring force by switching the input to an integrator, rather than using a feedback device to control the output of the integrator, was also developed. This device is more satisfactory than the device used in this study at low frequencies where leakage currents through the feedback device have been seen to introduce some error, however it is not so satisfactory at the higher frequencies used in this study.

Figure A.5 shows the circuit for this low-frequency elasto-plastic function generator. Amplifiers #2 through #5, with their diodes, form simple flip-flop devices, so that

$$\text{when } \frac{\varphi_p(v)}{R_4 C_2} \begin{cases} < v_o \\ > v_o \end{cases} \quad \text{then } v_1 \begin{cases} = v_z \\ = 0 \end{cases} \quad \text{and } v_2 \begin{cases} = -10v_z \\ = 0 \end{cases}$$

and

$$\text{when } \frac{\varphi_p(v)}{R_4 C_2} \begin{cases} > -v_o \\ < -v_o \end{cases} \quad \text{then } v_3 \begin{cases} = -v_z \\ = 0 \end{cases} \quad \text{and } v_4 \begin{cases} = 10v_z \\ = 0 \end{cases} \quad .$$

Thus when $-v_o < \varphi_p(v)/R_4 C_2 < v_o$ and provided that $-10v_z < v_5 < 10v_z$ the diodes D_1 and D_2 conduct no current such that $v_5 = -\dot{v}/2$ and the output of #5 is the desired integral. When the output reaches $+v_o$, though, voltage v_2 becomes zero, and diode D_1 dictates that v_5 must be greater than or equal to zero. Thus if $\dot{v}$ is positive then $v_5 = 0$ and the integrator sees no input signal so the output remains constant, but if $\dot{v}$ becomes negative then $v_5 = -\dot{v}/2$ and integration proceeds. Diode D_2 similarly grounds the input to the integrator when the system reaches
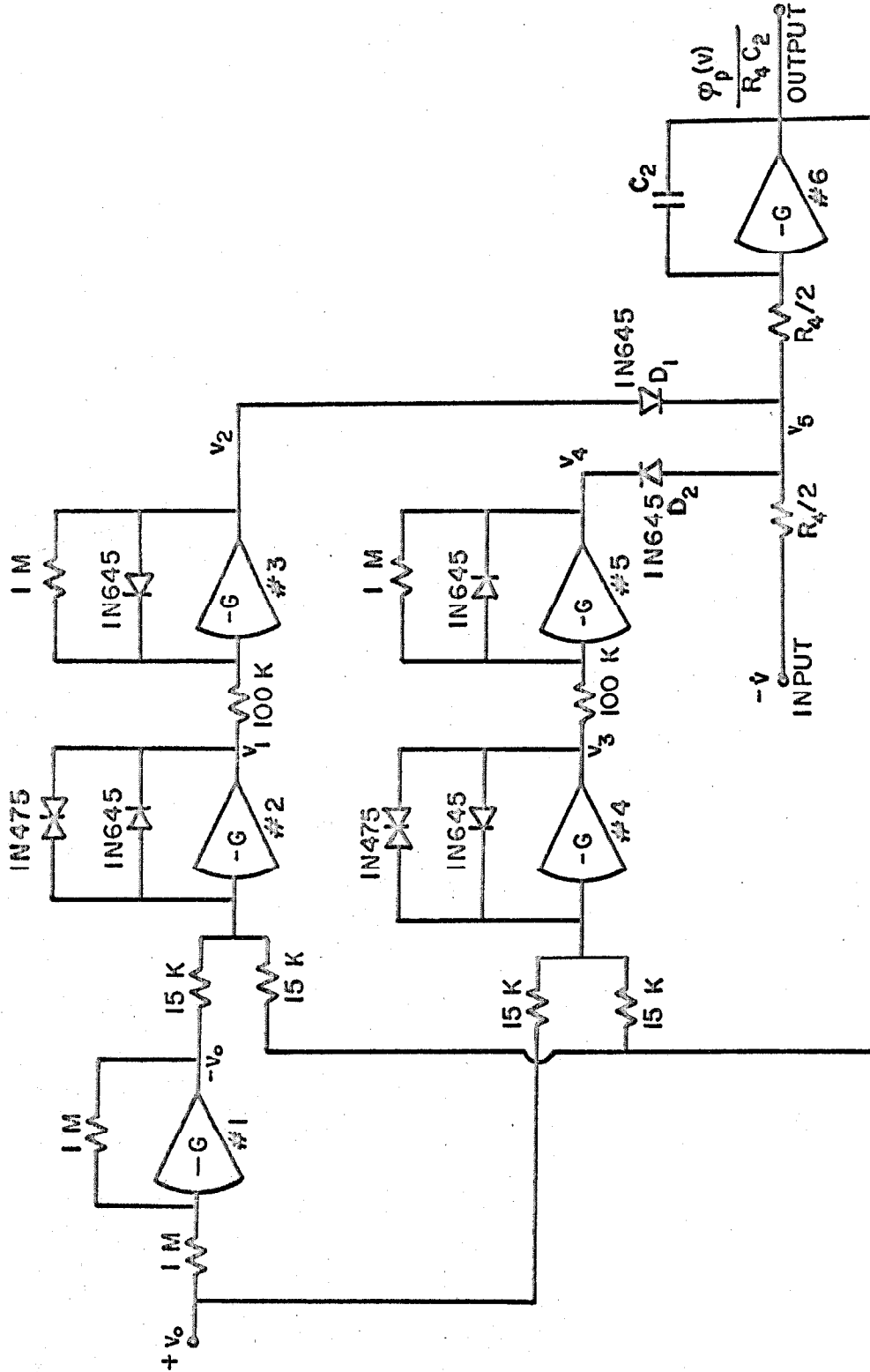
Figure A.5. Low Frequency Elasto-Plastic Function Generator.

negative yield level and has negative $\dot{v}$. Since there is always some finite voltage drop across a conducting diode, v_5 is never held exactly at zero during yielding; but tests indicated that with the diodes shown it could be limited to approximately 0.2 volt in a case with essentially zero yield level and with the amplitude of $\dot{v}/2$ at 12 volts.

Since there is no feedback to the summing point of the integrator in this circuit no leakage currents allowing the capacitor C_2 to slowly discharge in low frequency tests are introduced by the nonlinear circuit. Of course the capacitor itself will have some leakage current and some current passes into the input of the amplifier, but these are not peculiar to the nonlinear problem, and they do not preclude testing at quite low frequencies with good components. Experiments showed that the hysteresis loop produced using this low frequency device had no detectable degradation at 0.02 cps.

The high frequency limitation of this device is due to the time required for the output voltage of the flip-flop amplifiers to change. As mentioned in the previous section the maximum rate of change of amplifier output voltage for the amplifiers used is about 2 to 8 volts per microsecond. Since the output of either amplifier #3 or #4 has to change by approximately 60 volts each time yielding is initiated (with the circuit shown), time lags of as much as 30 microseconds are possible. This time lag causes an overshoot which remains as long as the system continues to yield in the given direction, since there is no way to correct the output voltage of the integrator in this system. Thus the exact effective yield level is a function of the rate of change of v

when it reaches yield level. In some experimental cases at about 500 cps the output was found to overshoot the low frequency yield level by as much as one volt. This overshoot could be expected to decrease linearly with frequency, for a given amplitude of v, so that this system might be quite acceptable for work at 10 cps or 50 cps, depending on the accuracy desired.

A. 3. Modification of the Amplitude Distribution Analyzer

Appendix B. 2 points out that the time constant of the Quan-Tech Laboratories Amplitude Distribution Analyzer, Model 317, was very inadequate for the measurements made in this study. It was quite simple, however, to use an external RC filter and voltmeter to measure the mean value of the output from the Schmitt trigger of the analyzer, and thus to achieve the desired time constant. An output terminal which was connected directly to the Schmitt trigger output was added to the analyzer. The point of connection was the collector of the 2N711 transistor labeled Q15 on the schematic diagram accompanying the Model 317 analyzer. Connecting the Schmitt trigger output to an impedance greater than or equal to 100 kilohms resulted in no detectable loading effect on the internal circuitry.

A Hewlett-Packard Electronic Voltmeter, Model 410 C, was used to measure the RC filtered voltage level of the Schmitt trigger output. The input impedance of this voltmeter is 10 megohms for voltage ranges up to 150 millivolts full scale and is 100 megohms for higher

voltage ranges. Thus, using an RC filter with R=100K resulted in not more than about 1% error due to D. C. current passing through the voltmeter.

The capacitor used in the RC filter was an electrolytic of 250 microfarads. Any D. C. current passing through the capacitor in such an RC filter results in the voltmeter reading less than the actual D. C. voltage applied to the filter. It was necessary to use some trial and error to choose an electrolytic capacitor with low enough leakage current to give satisfactory accuracy. With the capacitor which was used, however, the combined leakage currents through the capacitor and the voltmeter resulted in only about 1.5% error in reading a D. C. voltage.

In Section 2.4 it was mentioned that a test case was checked using an external D. C. amplifier to bypass the first stage of the Quan-Tech analyzer. An input terminal was connected directly into the second stage differential amplifier of the analyzer for this purpose.

The first stage of the analyzer is a variable attenuator followed by an A. C. amplifier (with low frequency attenuation as shown in Fig. 20). The output of the first stage has a D. C. bias of about 11.2 volts. When the attenuator controls are set for a 10 volt maximum input to the analyzer, the output from the first stage is the bias voltage plus the input voltage attenuated by a factor of 9.20:1. In order to bypass the first stage it is necessary to use some technique to give the proper bias to the input to the second stage. One possible technique is to use an analog computer amplifier as shown in Fig. A.6. Any deviation of
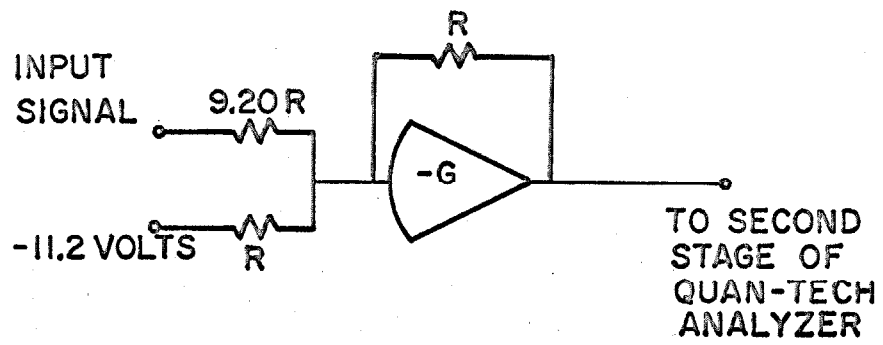
Figure A. 6. D. C. Device to Bypass First Stage of
Quan-Tech Analyzer.

the bias voltage of the input to the second stage of the analyzer from

that of the output from the first stage results in an effective change of

the comparison level being used in the analyzer. In fact, due to the

attenuation of the input signal a 0.1 volt error in bias level results in

an effective change in comparison level of 0.92 volt, for the setup

shown in Fig. A.6. One way of minimizing bias voltage error is to

acquire a bias voltage of 11.2 volts from within the analyzer and use

an analog computer amplifier to reverse its sign to give the necessary

input to the device in Fig. A.6.

B. ACCURACY OF ANALOG COMPUTER
INVESTIGATIONS

B. 1. Mean Squared Value of a Stationary Signal

The statistics of a stationary signal must be estimated in prac-
tice by determining the statistics of the signal over some finite time
interval called a sampling time. Thus one would like to know the effect
of the sampling time on the accuracy of the estimation of various
statistics.

Consider determining the mean squared value σ^2 of a large
number of samples from a particular stationary signal. Let each of
the samples be T seconds long. This large number of evaluations of
σ^2 will give a random set of σ^2 values for which one can determine the
mean value and variance. It can be shown that the mean value of the
set of σ^2 values is in fact the true mean squared value of the stationary
signal[36]. The variance of the set of σ^2 values gives an indication of
the probable error in using one sample value of σ^2 to estimate the
mean squared value of the stationary signal.

J. S. Bendat[37] analyzes the effect of sampling time on the
accuracy of estimation of the autocorrelation function for the particular
case of a signal with an autocorrelation function given by

$$R(t) = e^{-b|t|} \cos \omega_o t . \tag{B.1}$$

The power spectral density of such a signal has a peak at frequency ω_o
and the half-power points are at $\omega_o \pm b$. Since R(0) is the mean squared

value of the signal this analysis applies directly to the estimation of mean squared value. The variance of $R(t)$ for the special case where $t = 0$ can be rewritten from Bendat's more general result as

$$\text{Var}(\sigma^2) \approx \frac{1}{bT} \frac{2b^2 + \omega_o^2}{b^2 + \omega_o^2}$$

or

$$\text{Var}(\sigma^2) \approx \frac{1}{bT} \quad \text{for } \omega_o \gg b .$$

The ratio of the standard deviation of a set of observed values for some quantity to the mean value of the quantity will be referred to as the normalized standard error for the quantity. Thus for the mean squared value of the signal discussed above the normalized standard error is

$$\epsilon(\sigma^2) \approx \frac{1}{\sqrt{bT}} \quad \text{for } \omega_o \gg b . \tag{B.2}$$

J. S. Bendat and A. G. Piersol[38] give a simple expression which can be used to estimate the variance in sample mean squared values for any signal for which the autocorrelation function and mean value are known. The autocorrelation function is not known for the response of the nonlinear systems considered in this study, but it is known for the response of a linear oscillator to white excitation. Using the autocorrelation function for a linear system response with zero mean value results in the same approximation of the normalized standard error as given above by (B.2). For the linear system the half

bandwidth b is equal to $\beta_o \omega_o$ where β_o is the fraction of critical damp-ing and ω_o is the resonant frequency.

Since expression (B. 2) approximates the normalized standard error for both the narrow-band signals considered above it seems appropriate to use it to approximate the error for the response of non-linear oscillators when that response is narrow-band. Since the error decreases as the bandwidth increases the error in experimentally de-termining the mean squared value of a broad-band signal for which (B. 2) does not apply should be considerably less than that for a narrow-band signal.

Since power spectral density curves are not plotted for all values of yield level and excitation for which rms levels are determined one needs some other way of approximating the bandwidth of the response of the bilinear hysteretic systems. One such way is to use expression (2. 9),

$$\sigma_{\dot{x}}^2 = \frac{\pi S_o}{4m^2 \beta_1 \omega_1} \quad ,$$

to determine values of the half bandwidth $b = \beta_1 \omega_1$ from the experimen-tal values of $\sigma_{\dot{x}}$. This assumes that the bandwidth of the nonlinear system response is approximately the same as that for a linear sys-tem with the same level of response.

Using the suggested approximation of b one finds that the highest levels of $\sigma_{\dot{x}}$ in Figs. 10 and 12 of Chapter II give the minimum value of b as about 6 rad/sec. From Figs. 9 and 11, however, one notes meas-urements of σ_x at higher yield levels. Since such high yield levels

give a response with its peak near frequency ω_o one can approximate

the bandwidth for this case from the value of σ_x by using expression

(2.7). The result is that for the highest points in Figs. 9 and 11 the

half bandwidth was approximately 2 rad/sec.

The nominal averaging time of the random noise voltmeter used

to determine rms values was 100 seconds. Using T = 100 and the values

of b determined above, expression (B.2) predicts a normalized stan-

dard error in mean squared value of about 7% for the highest point in

both Figs. 9 and 11 and less than 4% for all other experimental points.

This corresponds to 3.5% and 2% errors, respectively, in rms values.

For a narrow-band response the bandwidth of the displacement and

the velocity are approximately the same. Thus the above error analysis

applies to measurements of both displacement and velocity response.

B.2. Probability Distribution of a Stationary Signal

Consider the problem of estimating P=Prob. (x > X) for some

stationary signal x(t) by analyzing a sample of length T seconds. The

mean of a large set of such sample values of P will be the true value of

P for the stationary signal. To determine the expected error in esti

mating P for the stationary signal by a sample P one would like to know

the variance of a large set of sample P values. This variance, however,

cannot be very precisely determined from present knowledge of the

statistics of continuous random processes.

Bendat and Piersol[39] give a discussion of the error involved

in estimating a stationary probability density from a sample of length

T seconds. The probability density p for a sample must be determined by dividing $\text{Prob}(X-W/2 < x < X+W/2)$ by W. For the special case of signal with a uniform power spectrum over a bandwidth of B cps and zero power spectral density elsewhere Bendat and Piersol use a heuristic argument to obtain a "reasonable approximation" of the normalized standard error as

$$\epsilon(p) \approx A_1 / \sqrt{BTWp}$$

where A_1 is an undetermined constant. This estimate would appear to also apply to $\epsilon(P)$ if Wp is replaced by P in the radical giving

$$\epsilon(P) \approx A_1 / \sqrt{BTP} . \qquad (B.3)$$

If the probability P of a discrete set of points is estimated by the probability of a sample containing r of the discrete points, the normalized standard error can be shown to be

$$\epsilon(P) = 1/\sqrt{rP} .$$

Further, a continuous signal of length T seconds which is completely contained within a bandwidth of B cps can be completely reproduced from knowledge of its value at 2BT discrete points[40]. This suggests that one possible choice for A_1 in expression (B.3) is

$$A_1 = 1/\sqrt{2} .$$

Expression (B.3) may serve to indicate the general dependence of $\epsilon(P)$ on bandwidth, sampling time, and probability but it is not particularly helpful for actually predicting values of $\epsilon(P)$. One normally is interested in estimating $\epsilon(P)$ for a signal which does not have a uniform power spectrum over its entire bandwidth and it is not clear

how expression (B. 3) should be modified to apply to any such situation. This problem is in addition to the uncertainty about the proper choice of A_1 in expression (B. 3).

As mentioned in Chapter II the Quan-Tech amplitude distribution analyzer used in this study contains a Schmitt trigger device which gives zero output when the input signal is less than the chosen comparison level and gives a constant output of 6. 3 volts when the input signal is greater than the comparison level. The probability P is then determined by using a low pass filter and a voltmeter to measure the mean value of the Schmitt trigger output.

One can make a crude estimate of the average error due to the finite sampling time used to evaluate P for a stationary analog system response by observing the range of variation of the voltmeter reading as time passes. The sample being analyzed is constantly changing since the stationary signal is going on continuously so one sees directly from the voltmeter the effect of choosing many different samples all of the same length. Another method of estimating the error in P is to plot probability distribution curves such as those in Figs. 22-24. Since an error due to sample length would be random in nature it would normally lead to scatter of the experimental points away from a smooth curve.

The Quan-Tech distribution analyzer contains an RC low pass filter with a time constant of RC = 0.125. Attempting to use this system to determine values of P of about 0. 002 resulted in variations of the voltmeter reading which were larger than the supposed mean value

being sought. Thus it was necessary to slightly modify the Quan-Tech instrument to allow use of an external RC filter. The filter used had RC = 25. Using this filter, observation of the variation of the voltmeter reading and the scatter of the plotted curves indicated that the error in determining a value of P near 0.002 probably did not exceed 10%. Observations also indicated that the error in measuring P decreased rapidly as P increased, as would be expected on the basis of expression (B. 3).

B. 3.   Power Spectral Density Determination Using a Filter with

Finite Bandwidth

In Section 2.3 the mean squared value of the output from a symmetric narrow-band filter was written in a series as

$$\sigma_{out}^2 = S_{in}(\omega_c) \int_{-\infty}^{\infty} |H_F(i\omega)|^2 \, d\omega$$

$$+ \frac{1}{2} \frac{d^2 S_{in}}{d\omega^2}(\omega_c) \int_{-\infty}^{\infty} (\omega-\omega_c)^2 |H_F(i\omega)|^2 d\omega + \ldots \qquad (B. 4)$$

where $S_{in}(\omega)$ is the power spectral density of the input to the filter, ω_c is the center frequency of the pass band and $H_F(i\omega)$ is the transfer function of the filter. The power spectral density $S_{in}(\omega_c)$ was estimated, in this study, by measuring σ_{out} and neglecting all but the first term in the above expression. The error in this estimation will be greatest when the second derivative of $S_{in}(\omega)$ is large, such as near the peak of a narrow band $S_{in}(\omega)$.

In order to learn something of the magnitude of the error in estimating power spectral density near a peak consider the effect of the second term in the above series for a special case. Let

$$S_{in}(\omega) = \frac{S_o}{m^2\left[\left(\omega_1^2 - \omega^2\right)^2 + (2\beta_1\omega_1\omega)^2\right]} \,. \qquad (B.\,5)$$

This is the power spectral density of the displacement response of a linear system described by

$$\ddot{x} + 2\beta_1\omega_1\dot{x} + \omega_1^2 x = \frac{1}{m}N(t) \qquad (B.\,6)$$

where $N(t)$ has a white power spectral density of magnitude S_o. When the center frequency of the filter is set at ω_1 expression (B. 5) gives

$$S_{in}(\omega_c) = \frac{S_o}{4m^2\beta_1^2\omega_1^4}$$

and differentiation of (B. 5) gives

$$\frac{d^2 S_{in}}{d\omega^2}(\omega_c) = \frac{-S_o}{2m^2\beta_1^4\omega_1^6}(1-3\beta_1^2) \quad.$$

For $\beta_1 << 1$ the last expression can be written as

$$\frac{d^2 S_{in}}{d\omega^2}(\omega_c) = S_{in}(\omega_c)\left(\frac{-2}{\beta_1^2\omega_1^2}\right) \quad. \qquad (B.\,7)$$

For the nominal 2 cps band filter of the Radiometer Wave Analyzer, Model FRA2, used in this study the integrals in expression (B. 4) are

$$\int_{-\infty}^{\infty} |H_F(i\omega)|^2 d\omega = 28.4 \text{ rad/sec}$$

and

$$\int_{-\infty}^{\infty} (\omega-\omega_c)^2 |H_F(i\omega)|^2 d\omega = 4600 \text{ (rad/sec)}^3 .$$

Substituting these values and expression (B. 7) into (B. 4) and neglecting all but the first two terms of (B. 4) gives

$$\sigma_{out}^2 = S_{in}(\omega_c)\left(28.4 - \frac{4600}{\beta_1^2 \omega_1^2}\right).$$

(B. 8)

This is a second order approximation to the mean squared output from the filter when the center frequency of the pass band is set at the resonant frequency of a lightly damped system described by expression (B. 6).

Note from expression (B. 8) that the magnitude of the second term relative to the first depends only on the product $\beta_1\omega_1$. It was noted in Section B. 1 that this product is the half bandwidth of the linear system. That is, $2\beta_1\omega_1$ is the width of the frequency range over which the response power spectral density is above the half-power level.

By assuming that the geometry near the peak of a power spectral density curve for a nonlinear system is similar to that of a linear system, one can use expression (B. 8) to approximate the error in determining the spectral density of the nonlinear system. To do this one would say that an equivalent $\beta_1\omega_1$ for use in (B. 8) for the nonlinear system was one-half the bandwidth between the half-power points of the nonlinear system power spectral density.

The sharpest peak plotted for a spectral density curve in Chapter 2 is that of curve G in Fig. 17. Noting that this is a plot of $\sqrt{S_x}$, the bandwidth between half-power points of S_x is about 58 cps. Thus an equivalent value for $\beta_1 \omega_1$ for use in expression (B. 8), according to the above assumptions, is $58\pi = 182$. Using this value predicts an error of about 0.5% in determining the peak value of S_x, or about 0.25% error in determining the peak value of $\sqrt{S_x}$ plotted.

B. 4. Summary of Overall Accuracy

The accuracy with which the analog computer circuit represented the differential equation of the bilinear hysteretic system was discussed somewhat in Appendix A. 1. The nominal accuracy of each of the resistors and capacitors used in the circuit was 1%. These component errors could combine to give 2% to 4% maximum errors in m, ω_o and β_o as predicted from the nominal values of the components. Experimental measurement of linear system response to harmonic excitation was used, however, to determine m, ω_o and β_o each with an accuracy of about 1%.

Two particular sources of inaccuracy in the elasto-plastic function were mentioned in A. 1. The leakage current through the feedback transistors resulted in an effect similar to that of viscous damping, particularly at low frequencies. At resonance, however, the damping contribution due to this leakage was seen to be like approximately 0.01% of critical viscous damping. At low frequencies the leakage current apparently affected the system transfer function by about 0.025% at

5 cps, and by about 2.5% at 0.5 cps. It, thus, seems that the inaccuracy due to the leakage currents was negligible compared to the overall system accuracy.

The second source of error in the elasto-plastic function was the overshoot at initiation of yield at high frequencies, resulting in the inclusion of too much area in the hysteresis loop. Analysis of a periodic test case and an approximate application of the results to the system with random excitation indicated that the additional area due to the overshoot was probably less than 0.5% of the area of the ideal hysteresis loop for the worst cases in the study. It, thus, appears that the response of the analog computer circuit as used for the excitation used should check that of an ideal bilinear system within about 2%.

The remaining sources of error are various types of possible error in measuring the response of the analog computer circuit. Sections 1, 2 and 3 of this appendix discuss some limitations on the accuracy of the equipment used. In addition to these limitations there is a limitation to the accuracy with which one can read the meters of the various pieces of equipment.

In Section B.1 it was shown that the equipment used was capable of determining the rms response values shown in Figs. 9-12 with an expected error of about 3.5% for the highest point in both Figs. 9 and 11 and less than 2% for all other points in the figures. Since the accuracy with which the dial of the voltmeter can be read is about 1% it seems that the error in measuring the rms values should not have

exceeded about 3% except when the yield level was very high. Allowing

for a possible 2% error in the functioning of the analog computer

circuit this predicts less than 5% deviation between the rms values

presented and those for an ideal bilinear system, except that for the

previously mentioned instances of a very high yield level the error

may have been as much as 6.5%.

In determining power spectral density it is possible to have an

error due to inaccurate determination of the rms output from the

narrow band filter, and another error due to the variation of the spec-

tral density over the finite bandwidth of the filter. This latter error

is most serious near a sharp peak in the spectral density curve. It

was shown in Section B.3, however, that the error due to the finite

bandwidth of the filter was only about 0.25% for the sharpest peak

plotted in Chapter 2.

The error due to the sampling time used in determining the

rms output from the narrow band filter can be estimated by using ex-

pression (B.2). Since the filter had a bandwidth which was narrow

compared to the bandwidth of the signals for which the power spectral

density was determined one can assume that the power spectral density

of the filter output was like the curve of $\left| H_F(i\omega) \right|^2$ plotted in Fig. 13 of

Chapter II. From this curve one obtains a bandwidth between half-

power points of about 4 cps. This gives a value of $b = 4\pi$ for use in

expression (B.2). The sampling time T was 100 seconds, and the re-

sulting expected error in the rms output level of the filter is about 1.5%.

The total error in measuring the $\sqrt{S_x}$ values, due to filter bandwidth, finite sampling time and human error in meter reading probably did not exceed 3%. With a 2% possible inaccuracy in the analog computer circuit this predicts an error bound of about 5% for the square root of power spectral density values reported in Chapter II.

Some of the points on the probability distribution curves have the least accuracy of all the results obtained from the analog computer investigations. As explained in Section B.2 the error in determining a probability value of $P = 0.002$ was probably near 10%. Using expression (B.3) to approximate the dependence of the error on the level of P being determined predicts an error of about 2% in determining a value of $P = 0.05$. Thus the overall accuracy of the probability values, including the errors of the analog circuit, probably varies from about 3% for large values of P to about 12% for $P = 0.002$.

C. SIMPLIFICATION OF EQUIVALENT FREQUENCY EXPRESSION

Expression (3.17) can be rewritten as

$$\left(\frac{\omega_{eq}}{\omega_o}\right)^2 = \frac{2}{\lambda^2} T_1 + \frac{2\alpha}{\lambda^2} T_2 + \frac{2(1-\alpha)}{\pi\lambda^2} T_3 - \frac{4(1-\alpha)}{\pi\lambda^2} T_4 \qquad (C.1)$$

where

$$T_1 = \int_0^1 z^3 e^{-z^2/\lambda} dz$$

$$T_2 = \int_1^\infty z^3 e^{-z^2/\lambda} dz$$

$$T_3 = \int_1^\infty \cos^{-1}(1 - \frac{2}{z}) z^3 e^{-z^2/\lambda} dz$$

$$T_4 = \int_1^\infty (z^2 - 2z)\sqrt{z-1}\, e^{-z^2/\lambda} dz \ .$$

Performing the integration indicated gives

$$T_1 = -\frac{\lambda}{2} (z^2 + \lambda) e^{-z^2/\lambda} \Big|_0^1$$

$$= \frac{\lambda^2}{2} - \frac{\lambda}{2} (1 + \lambda) e^{-1/\lambda} \ .$$

Similarly

$$T_2 = \frac{\lambda}{2} (1 + \lambda) e^{-1/\lambda} \ .$$

Integrating T_3 by parts gives

$$T_3 = \pi\frac{\lambda}{2}(1+\lambda)e^{-1/\lambda} - \frac{\lambda}{2}\int_1^\infty \left(\frac{z^2+\lambda}{z}e^{-z^2/\lambda}\right)\frac{dz}{\sqrt{z-\Gamma}} \quad .$$

Integrating by parts again, with the integrand divided as shown, yields

$$T_3 = \pi\frac{\lambda}{2}(1+\lambda)e^{-1/\lambda} - \lambda\int_1^\infty \left(\frac{\lambda}{z^2}+\frac{2z^2}{\lambda}-1\right)\sqrt{z-\Gamma}\,e^{-z^2/\lambda}dz \quad .$$

Substituting the new forms of T_1, T_2 and T_3 and the original form of T_4 into (C.1) gives

$$\left(\frac{\omega_{eq}}{\omega_o}\right)^2 = 1 - \frac{2(1-\alpha)}{\pi\lambda^2}\int_1^\infty\left[\frac{\lambda^2}{z^2}+\lambda+4z(z-1)\right]\sqrt{z-\Gamma}\,e^{-z^2/\lambda}\,dz \qquad (C.2)$$

but

$$\int_1^\infty(z-1)^{3/2}ze^{-z^2/\lambda}dz = \frac{3\lambda}{4}\int_1^\infty\sqrt{z-\Gamma}\,e^{-z^2/\lambda}dz$$

and substituting this expression into (C.2) gives

$$\left(\frac{\omega_{eq}}{\omega_o}\right)^2 = 1 - \frac{2(1-\alpha)}{\pi\lambda^2}\int_1^\infty\left(\frac{\lambda^2}{z^2}+4\lambda\right)\sqrt{z-\Gamma}\,e^{-z^2/\lambda}\,dz \quad . \qquad (C.3)$$

Or, integrating by parts,

$$\int_1^\infty\frac{\lambda^2 e^{-z^2/\lambda}}{z^2}\sqrt{z-\Gamma}\,dz = \int_1^\infty\left(\frac{4\lambda^2}{z^3}+\frac{4\lambda}{z}-4\lambda\right)\sqrt{z-\Gamma}\,e^{-z^2/\lambda}dz$$

which gives

$$\left(\frac{\omega_{eq}}{\omega_o}\right)^2 = 1 - \frac{8(1-\alpha)}{\pi}\int_1^\infty\left(\frac{1}{z^3}+\frac{1}{\lambda z}\right)\sqrt{z-\Gamma}\,e^{-z^2/\lambda}dz \quad . \qquad (C.4)$$

The integrand in this expression decreases quite rapidly as z increases making numerical integration of (C. 4) a practical method of obtaining ω_{eq}/ω_o for a given value of λ.

It is possible to expand the integral of (C. 4) in an asymptotic expansion which can be used to determine ω_{eq}/ω_o for large values of λ without numerical integration. To do so define a term

$$T_5 = \int_1^\infty \frac{\sqrt{z-1}}{z^3} \, dz \; .$$

This can be rewritten as

$$T_5 = \int_1^\infty \frac{\sqrt{z-1}\, e^{-z^2/\lambda}}{z^3} \left[\sum_{i=0}^\infty \frac{1}{i!}\left(\frac{z^2}{\lambda}\right)^i \right] dz$$

or, reversing the order of summation and integration,

$$T_5 = \sum_{i=0}^\infty \frac{1}{i!\,\lambda^i} \int_1^\infty z^{(2i-3)}\sqrt{z-1}\, e^{-z^2/\lambda} dz \; .$$

Separating the first two terms of the series gives

$$T_5 = \int_1^\infty \left(\frac{1}{z^3} + \frac{1}{\lambda z}\right) \sqrt{z-1}\, e^{-z^2/\lambda} dz$$

$$+ \sum_{i=2}^\infty \frac{1}{i!\,\lambda^i} \int_1^\infty z^{(2i-3)}\sqrt{z-1}\, e^{-z^2/\lambda} dz \; . \tag{C. 5}$$

Note that the first integral on the right hand side of this expression is exactly the integral in expression (C. 4).

The integration in the definition of the term T_5 can be performed exactly by noting that

$$T_5 = -\int_1^\infty (z-1)^{3/2} \frac{dz}{z^3} + \int_1^\infty \frac{\sqrt{z-1}}{z^2} \, dz \ .$$

Integrating by parts on the first integral and collecting terms gives

$$T_5 = \frac{1}{4} \int_1^\infty \frac{\sqrt{z-1}}{z^2} \, dz \ .$$

This expression can, in turn, be integrated by parts to yield

$$T_5 = \frac{1}{8} \int_1^\infty \frac{dz}{z\sqrt{z-1}} \ .$$

But the integrand of this expression is the exact differential of $2\tan^{-1}\sqrt{z-1}$. Thus

$$T_5 = \frac{\pi}{8} \ . \tag{C.6}$$

Expressions (C. 4), (C. 5) and (C. 6) can now be combined to give

$$\left(\frac{w_{eq}}{w_o}\right)^2 = \alpha + \frac{8(1-\alpha)}{\pi} \sum_{i=2}^\infty \frac{1}{i! \, \lambda^i} \int_1^\infty z^{(2i-3)} \sqrt{z-1} \, e^{-z^2/\lambda} dz \ . \tag{C.7}$$

A term $\sqrt{1+y}$ can be expanded in a power series about the origin to give

$$\sqrt{1+y} = \sum_{j=0}^\infty \frac{\Gamma\left(\frac{3}{2}\right)}{\Gamma\left(\frac{3}{2}-j\right)} \frac{y^j}{j!}$$

where Γ denotes the gamma function. The gamma function has the property that $\Gamma(a+1) = a\Gamma(a)$, so that

$$\frac{\Gamma\left(\frac{3}{2}\right)}{\Gamma\left(\frac{3}{2}-j\right)} = \left(\frac{3}{2}-j\right)\left(\frac{5}{2}-j\right) \cdots \left(-\frac{1}{2}\right)\left(\frac{1}{2}\right) \text{ for } j \geq 1.$$

Writing

$$\sqrt{z-1} = \sqrt{z}\sqrt{1-\frac{1}{z}}$$

the power series expansion can be used to give

$$\sqrt{z-1} = \sum_{j=0}^{\infty} \frac{\Gamma\left(\frac{3}{2}\right)}{\Gamma\left(\frac{3}{2}-j\right)} \frac{(-1)^j}{j! z^{(j-1/2)}} \quad .$$

Substituting this expression into (C.7) and rearranging the order of the operations gives

$$\left(\frac{\omega_{eq}}{\omega_o}\right)^2 = \alpha + \frac{8(1-\alpha)}{\pi} \sum_{j=0}^{\infty} \frac{(-1)^j}{j!} \frac{\Gamma\left(\frac{3}{2}\right)}{\Gamma\left(\frac{3}{2}-j\right)} \sum_{i=2}^{\infty} K_i \tag{C.8}$$

where

$$K_i = \frac{1}{i! \lambda^i} \int_1^{\infty} z^{(2i-j-5/2)} e^{-z^2/\lambda} dz \quad . \tag{C.9}$$

For $\lambda \gg 1$ the terms K_i can be approximated as

$$K_i \approx \frac{1}{i! \lambda^i} \left[\int_0^{\infty} z^{(2i-j-5/2)} e^{-z^2/\lambda} dz - \int_0^1 z^{(2i-j-5/2)} dz \right] . \tag{C.10}$$

The second integral in this expression gives

$$\int_0^1 z^{(2i-j-5/2)} dz = \frac{1}{2i-j-3/2} \text{ for } 2i-j-3/2 > 0. \tag{C.11}$$

The condition $2i-j-3/2>0$ is satisfied for $j = 0, 1, 2$ for all values of i included in (C. 8). The first integral in (C. 10) is included in the definite integral tables of W. Grobner and N. Hofreiter. Application of their result[41] gives

$$\int_0^\infty z^{(2i-j-5/2)} e^{-z^2/\lambda} dz = \frac{1}{2} \lambda^{(i-j/2-3/4)} \Gamma\left(i - \frac{j}{2} - \frac{3}{4}\right)$$

$$\text{for } 2i-j-3/2>0 \ . \qquad (C. 12)$$

Thus for $2i-j-3/2>0$ and $\lambda \gg 1$ expression (C. 10) gives

$$K_i \approx \frac{\lambda^{(-j/2-3/4)}}{2\, i!} \Gamma\left(i - \frac{j}{2} - \frac{3}{4}\right) - \frac{1}{\left(2i - j - \frac{3}{2}\right) i! \, \lambda^i} \ . \qquad (C. 13)$$

The magnitude of K_i for $2i-j-3/2<0$ can be bounded as follows:

$$K_i < \frac{1}{i! \, \lambda^i} \int_1^\infty z^{(2i-j-5/2)} dz$$

which gives

$$K_i < \frac{-1}{i! \, \lambda^i \left(2i-j-\frac{3}{2}\right)} \quad \text{for } 2i-j-3/2<0 \ . \qquad (C. 14)$$

Using expressions (C. 13) and (C. 14) to determine K_i and neglecting terms of order λ^{-2} in expression (C. 8) gives

$$\left(\frac{\omega_{eq}}{\omega_o}\right)^2 \approx \alpha + \frac{8(1-\alpha)}{\pi} \left[\frac{\lambda^{-3/4}}{2} \sum_{i=2}^\infty \frac{\Gamma(i-3/4)}{i!} \right.$$

$$- \frac{\lambda^{-5/4}}{4} \sum_{i=2}^\infty \frac{\Gamma(i-5/4)}{i!}$$

$$\left. - \frac{\lambda^{-7/4}}{16} \sum_{i=2}^\infty \frac{\Gamma(i-7/4)}{i!} \right] \quad \text{for } \lambda \gg 1. \qquad (C. 15)$$

L. B. W. Jolley gives a summation for a series very similar to those in expression (C. 15), namely[42]

$$1 + \frac{a}{b} + \frac{a(a+1)}{b(b+1)} + \frac{a(a+1)(a+2)}{b(b+1)(b+2)} + \cdots = \frac{b-1}{b-a-1}$$

$$\text{for } b-1 > a > 0. \qquad (C.16)$$

Factoring a term of $\frac{1}{2}\Gamma\left(\frac{5}{4}\right)$ from each term of the first summation in (C. 15) gives the form used by Jolley with $b = 3$ and $a = 5/4$. Thus

$$\sum_{i=2}^{\infty} \frac{\Gamma(i-3/4)}{i!} = \frac{4}{3}\Gamma\left(\frac{5}{4}\right) = \frac{1}{3}\Gamma\left(\frac{1}{4}\right).$$

Application of (C. 16) to the other summations in (C. 15) yields

$$\sum_{i=2}^{\infty} \frac{\Gamma(i-5/4)}{i!} = \frac{4}{5}\Gamma\left(\frac{3}{4}\right)$$

and

$$\frac{\Gamma(i-7/4)}{i!} = \frac{4}{7}\Gamma\left(\frac{1}{4}\right).$$

Substitution of these values for the summations in (C. 15) gives

$$\left(\frac{\omega_{eq}}{\omega_o}\right)^2 \approx \alpha + \frac{8(1-\alpha)}{\pi}\left[\frac{1}{6}\Gamma\left(\frac{1}{4}\right)\lambda^{-3/4} - \frac{1}{5}\Gamma\left(\frac{3}{4}\right)\lambda^{-5/4}\right.$$

$$\left. - \frac{1}{28}\Gamma\left(\frac{1}{4}\right)\lambda^{-7/4}\right] \quad \text{for } \lambda \gg 1. \qquad (C.17)$$

The values of the gamma functions in (C. 17) are[29]

$$\Gamma\left(\frac{1}{4}\right) = 3.6256$$

and

$$\Gamma\left(\frac{3}{4}\right) = 1.2254.$$